AN ANALYSIS OF HYDRAULIC MONITORING EQUIPMENT FOR INFLOW AND OUTFLOW STRUCTURES IN URBAN SCMS

By

Stephanie Elyse Rindosh

Thesis
Submitted to Department of Civil and Environmental Engineering
College of Engineering
Villanova University
in partial fulfillment of the requirements
for the degree of

MASTER OF SCIENCE

In

Civil Engineering

April, 2016

Villanova, Pennsylvania

STATEMENT OF DISCLOSURE

This publication "An Analysis of Hydraulic Monitoring Equipment for Inflow and Outflow Structures in Urban SCMs" was made possible by EPA grant number 83555601. Its contents are solely the responsibility of the grantee and do not necessarily represent the official views of the EPA. Further, the EPA does not endorse the purchase of any commercial products or services mentioned in the publication.

STATEMENT BY AUTHOR

This thesis has been submitted in partial fulfillment of requirements for an advanced degree at the Villanova University.

Brief quotations from this thesis are allowable without special permission, provided that accurate acknowledgment of source is made. Requests for permission for extended quotation from or reproduction of this manuscript in whole or in part may be granted by the head of the major department or the Associate Dean for Graduate Studies and Research of the College of Engineering when in his or her judgment the proposed use of the material is in the interests of scholarship. In all other instances, however, permission must be obtained from the author.

ACKNOWLEDGEMENTS

This research would not be possible without the guidance of my two advisors Dr. Robert Traver and Dr. Bridget Wadzuk. For two brilliant people, they are humble professors that offer the best advisement, continuous support, and keep positive spirits with their unique sense of humor. They are truly a dynamic team and it is an honor working for them. Thank you for always answering the 4 AM frantic emails without judging my state of mind.

Thank you to the EPA STAR grant, who provided funding for this research and exposed me to the one of a kind Philadelphia's Green City, Clean Waters. Also thank you to two other Villanova professors that are PIs on the grant, Dr. Garrett Clayton and Dr. Andrea Welker. They offer extensive knowledge and advisement that developed successful research for the grant.

Tremendous gratitude to Philadelphia Water Department's Chris Bergerson, Stephen White, and fellow co-ops for not only assisting with instrumentation, SRTs, and making this research possible, but also for showing me the way to the streets of Philadelphia and allowing me to take naps on the Philadelphia sidewalks during long field days.

Thank you to Dr. Kimberly DiGiovanni, a former post-doc on this project, as well as Cara Albright, a Ph. D. student. The two of you were the support columns to all my research and made field days more enjoyable through the freezing winter months and scorching hot summer days. I am also grateful for Dr. Ryan Lee who is a current post-doc on this project for offering me crash courses in statistics and assisting me with extensive analyses.

Thank you to George Pappas and Linda DeAngelis for everything you contribute to the VUSP. Last, thank you to all former and current VUSP graduate and undergraduate students, who not only offered me their muscular strength when I needed it, but also offered me emotional support and uplifted my spirits to overcome any battles I faced in the field or laboratory.

TABLE OF CONTENTS

LIST OF TABLES

LIST OF FIGURES

NOMENCLATURE

A	Drainage Area (acre) /Area (orifice equation)
$A(h)$	Area as a function of depth (ft)
c	Rational Method Discharge Coefficient
C_d	Coefficient of Discharge for Orifice Equation
H	Head Measurement (ft)
i	Rainfall Intensity (in/hr)
Q	Flow rate (cfs)
k_{sat}	Saturated hydraulic conductivity
V_{mean}	Mean velocity (ft/s)
ADV	Acoustic Doppler Velocimeter
CSO	Combined Sewer Overflow
CSS	Combined Sewer System
CWA	Clean Water Act
DCL	Direct Connect Logger
DV	Doppler Velocity
EPA	Environmental Protection Agency
GCCW	Green City, Clean Waters
GI	Green Infrastructure
GIFMET	Green Infrastructure Flow Measurement Evaluation Tool
LTCP	Long Term Control Plans
NPDES	National Pollutant Discharge Elimination System
ORD	Orifice Restricting Device

PWD	Philadelphia Water Department
RMSE	Root Mean Square Error
SCM	Stormwater Control Measure

ABSTRACT

Accurately monitoring stormwater control measurements (SCMs) in the urban environment is extremely difficult because conditions are variable, space is limited, there is the potential for vandalism, and the normal flow of urban life cannot be interrupted. Outside of seasonal variability, monitoring equipment is subjected to harsh conditions with trash, sedimentation, debris, and vandalism that may disrupt the performance of monitoring equipment and the SCM. An investigation is conducted to analyze the differences in accuracy between ideal laboratory settings and urban field conditions. The purpose of this research is to select the most appropriate monitoring equipment for urban SCMs and analyze the accuracy of sensors. The focus is on the inflow and outflow structures of two different urban SCMs (i.e. Philadelphia Zoo rain garden and Morris Leeds tree trench) that are a part of Philadelphia Water Department's Green City, Clean Waters program.

Presently, the accuracy and reliability of monitoring equipment is determined with laboratory experiments, and ultimately the goal is to implement the best suited equipment in the field that will produce the best results for monitoring flow. Laboratory experiments included apparatuses that resemble field conditions and tested existing equipment supplied by manufacturers. An H-flume was selected to monitor inflow for a rain garden's surface channel and produced sufficient laboratory results with a 2.9% average root mean square error (RMSE) compared to the manufacturer's calibration. An acoustic Doppler velocimeter (ADV) sensor was selected and evaluated for a tree trench's 8 in (20.3 cm) subsurface pipe, but was determined to be inadequate due to numerous difficulties including improper datalogging methods, exposure to excessive sedimentation at the SCM site, poor communication between datalogging team, hydrologic studies, and manufacturer service. This research also required thinking outside the

box for typical flow measurement devices in order to develop a new approach for measuring outflow of a rain garden's unique outlet structure, a domed riser. A custom designed "organ orifice" was developed and calibrated under laboratory conditions, which stemmed a linear regression model for the specific head-discharge relationship.

Even though the laboratory results provided background about a sensor's capabilities, the critical test is investigating the device's performance in the field. Two Stimulated Runoff Tests (SRTs) were conducted at the Philadelphia Zoo rain garden site and generated simulated storm events that equated to approximately 2086 CF (59.1 m^3) for SRT 1 and 2341.5 CF (66.3 m^3) for SRT 2. SRT 1 showed that the H-flume capably measured inflow rates with a 6% difference compared to the portable water meter. This test also indicated that there was a construction error with the outflow structure, therefore the organ orifice's evaluation was inconclusive for Test 1. The outflow structure was fixed so that the organ orifice device could be assessed according to the rain garden's performance during SRT 2. The organ orifice's performance was restricted during part of the test due to the rock bed's water levels preventing free outflow. Thus it was only assessed when operating properly under its intended design and resulted in a 4.3% difference when compared to an estimated rock bed storage. During SRT 2, the rain garden's ponding depth caused submergence that resulted in deficient inflow measurements that recorded flow rates substantially higher than the water meter's output. It was determined that during this specific storm simulation, the H-flume could adequately record flows up to 44% submergence. This research analyzes the process outlining preliminary research, laboratory experimentation, and field testing in order to acquire reliable inflow and outflow instrumentation within urban SCMs.

CHAPTER 1: INTRODUCTION

1.1 URBAN HYDROLOGY

Drainage systems for stormwater and wastewater existed in early civilizations, such as the Roman Empire and Ancient Greece. Among ancient cities, drainage features included pipes through buildings, gutters, collector channels, and in some cases storm waters were used to flush out public sewers (Delleur 2003). Today urban sewer systems have evolved to support millions of people who live in urban environments. These water management systems were developed over centuries to reduce the impacts of flooding, and improve public health and sanitation. Many older cities constructed combined sewer systems, which provided drainage for both rainwater and wastewater. Over the years, rapid urbanization and increased impervious areas have reduced groundwater recharge, caused combined sewer systems to overflow and contributed pollutants to local waterways, and ultimately altered the natural hydrology of these areas.

1.1.1 Combined Sewer Overflows (CSOs)

Originally, combined sewer systems (CSSs) discharged water into local waterways. Today, CSSs are designed to carry both sewage and stormwater in one pipe to a treatment facility. Moderate to intense rainfall events and snowmelt often create excessive runoff into these systems, which causes them to exceed capacity at the treatment facility. The excessive water is contaminated with pathogens, oxygen-demanding pollutants, suspended solids, nutrients, and toxics (EPA et al. 1999). In this event, the contaminated water discharges directly into local bodies of water such as lakes, rivers, estuaries and oceans (EPA et al. 1999) and this is known as a combined sewer overflow (CSO). This discharge disrupts ecological life, affects the stream's stability with erosion, and becomes a detriment to hydrologic conditions (Leopold

1968). In the United States there are approximately 950 communities with CSOs (EPA et al. 1999).

In 1989, the Environmental Protection Agency (EPA) defined CSO events as point source pollution. As a result, this forced CSO communities to comply with the National Pollutant Discharge Elimination System (NPDES) and the Clean Water Act (CWA) requirements. Following this motion, in 1994 the EPA required municipalities to develop a CSO Control Policy (EPA et al. 1999). This mandated local governments to address the issues of CSOs with a long term plan and also provide new sustainable infrastructure for the growth of urban communities.

1.1.2 Urbanization

Since 2007, the world has more people living in urban environments than in rural environments (UN 2014). The continuing growth of population and urban development is predicted to add 2.5 billion people to existing cities by 2050 (UN 2014). Rapid urban expansion threatens a watershed's natural hydrology and alters flows to receiving waters. As urbanization increases, more impervious surfaces are replacing pervious areas which destroys vegetation, native soils, and any potential for infiltration. Impervious areas discharge runoff at a high rate that increases flood peaks during storm events (Leopold 1968), which generate more CSO events in combined sewer communities. Urbanization, in conjunction with CSO events, can lead to dangerous impacts on stream morphology, receiving water body's ecological life, localized flooding, and reduction of groundwater recharge (Booth and Jackson 1997). As urban growth continues, sustainable stormwater infrastructure needs to be implemented to reduce flooding and preserve local waterways.

1.2 STORMWATER CONTROL MEASURES (SCMs)

Figure 1.1 depicts the hydrologic cycle of a natural environment and exhibits how precipitation falls onto an undisturbed watershed producing surface runoff or infiltration. If water infiltrates the soil, then it can evapotranspirate into the atmosphere or contribute to the groundwater baseflow. City development alters this familiar water cycle by installing impervious surfaces (Figure 1.1). Impervious surfaces prevent infiltration, which consequently causes excessive runoff directed into sewer inlets at a higher rate compared to pervious surfaces. As a result, the lag time between peak rainfall and peak runoff decreases for storm events and causes flashy hydrographs with intense peaks (Leopold 1968).

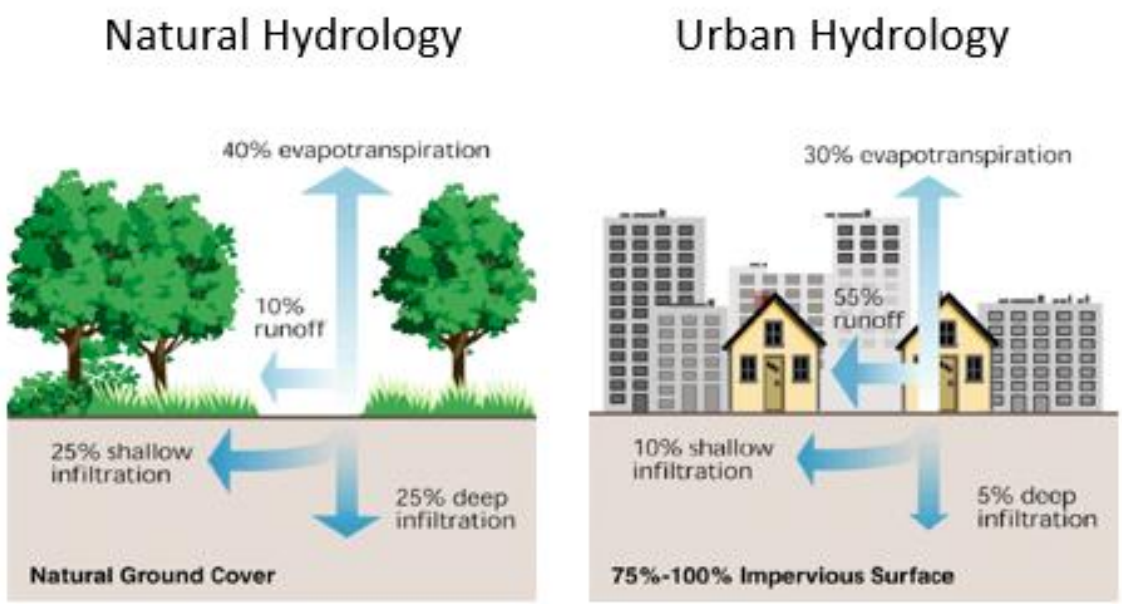

Figure 1.1 Hydrologic cycle comparison between natural and urban hydrology. Adapted from Federal Interagency Stream Restoration Working Group (FISRWG 1998).

Stormwater control measures (SCMs), also known as green infrastructure (GI), are a creative sustainable solution for urban environments. Stormwater control measures are an attractive solution because of their capabilities to address stormwater issues quantitatively and

qualitatively. The quantity reduction is tackled by infiltrating runoff through soil that provides temporary storage and slow release or removal of the stormwater runoff from the surface waters. This approach has other benefits by allowing the water to evaporate and/or transpirate, recharge groundwater, and store water locally to mimic the pre-constructed water cycle for smaller sites. Additionally, runoff rates are decreased which minimizes peak flows in the sewer systems and the burden on downstream treatment facilities.

Stormwater can pollute local waterways with sediments, nutrients, metals, organic compounds, and total suspended solids (EPA et al. 1999). Water quality is addressed by SCMs primarily because of its quantity reduction proficiencies thereby reducing the total pollutant mass reaching the sewer system. Furthermore, soils filter many contaminants and treat the water through physical, chemical, and biological processes. Physically, the soil is a screen that removes large particles from the water as the water seeps into the ground. Though dissolved solids may require further treatment, soils can also absorb contaminants within the water by undergoing chemical processes (e.g. iron fixation and phosphorous adsorption). Lastly, soils have microorganisms that may degrade water contaminated with organic and inorganic substances. The overall stormwater reduction is also beneficial qualitatively for cities with combined sewers that experience CSO events as wastewater disposed into local waterways is reduced.

Starting in 2007, the EPA encouraged local municipalities to utilize green infrastructure (i.e. SCMs) as part of their CSO Long Term Control Plans (LTCPs) (Boornazian and Pollins 2007). Stormwater control measure implementation can minimize CSO discharges since SCMs reduce stormwater volume and runoff rate. Stormwater control measures have countless

financial, social, and environmental benefits, making it an attractive approach for LTCPs from a cost/benefit evaluation (Struck et al. 2012).

1.3 MONITORING SCMs

The implementation of monitoring equipment and collection of good hydrological data is an essential component of any urban stormwater investigation. Monitoring programs have been implemented in cities with SCMs, such as Portland (Portland 2010), Seattle (Tackett 2009), and Philadelphia (PWD 2012). Monitoring individual SCMs provides further understanding of their behavior and assessment of their performance. The data can validate past designs, develop next generation designs, and help evaluate SCMs on larger scales to determine their hydrological influence on multiple watersheds (PWD 2012). Additionally, this data can assist models that influence decision making of current designs.

Over the past few decades, water resources modeling has evolved significantly, specifically with urban drainage systems and SCMs incorporation. However, good models still rely heavily on data for calibration and validation (Silberstein 2006). Data validates a model's capability to represent the physical SCM system, which enables the model's use for decision-making and understanding the tested environment (Harmel et al. 2009; Silberstein 2006; Struck et al. 2012). For example, LTCPs employ hydraulic and hydrological modeling to view SCMs' effects on CSO discharges. A model is only as good as its representation of the processes and the input data, which is why it is necessary to have good field data in order to calibrate parameters for an accurate and reliable model.

Stormwater control measures are still fairly new in design considering the EPA only recently recommended green infrastructure for LTCPs. While SCM benefits have been demonstrated, there are still many unanswered questions about SCM function (e.g. maintenance,

lifespan, large scale watershed benefits), therefore, further research and monitoring of these systems remain necessary. Much has been learned over the past two decades, but SCMs' design life is still unknown, particularly considering climate change that could potentially introduce these systems to more intense storms and droughts (Zahmatkesh et al. 2015). Hydrology is continuously changing in urban environments and the long term effects of SCM systems can potentially impact hydrology on a large scale. Therefore, data is essential to our understanding of SCMs' functionality and their ongoing effects. The reliability and accuracy of this data is dependent on monitoring equipment and its application to a monitoring site.

Instrumenting SCMs is an essential component to acquiring good data. This research is focused on capturing accurate stormwater measurements for quantitative data and does not involve instrumentation for qualitative data. There are many types of SCMs (i.e. rain gardens, green roofs, trenches, swales, etc.) and instrumentation will vary between different sites. Regardless of the site, the basic principles for monitoring are the same. The goal is to accurately measure inflow into the system and outflow of the system. Consequently, it is necessary to do preliminary research of stormwater sites, select appropriate instrumentation, and test the equipment to ensure reliable data that will provide the resolution and response desired from the monitoring effort.

For example, a typical rain garden equipped with monitoring equipment is depicted in Figure 1.2. The goal in this example is to measure the rain garden's inflow and outflow at a high temporal resolution during and after a storm with the ability to detect small changes in the vertical water profile. There is a measuring device capturing the inflow into the rain garden, in this case a V-notch weir. There are also sensors within the rain garden to determine water quantities retained in the system. Typically, this is a shallow well to record ponding depth within

the system and a set of soil moisture meters to measure sub-surface storage. Depending on the design, the site might also have an outflow structure for overflows. Monitoring equipment should be placed in the outflow structure in order to quantify everything entering and leaving the system. The image illustrates an overflow structure with an orifice plate as a monitoring device for the outflow pipe. Lastly, not pictured is a rain gauge which is essential to quantify an SCM's performance for particular storms. This example is specific, but the general components of a monitoring program would be the same, even if less detail is desired.

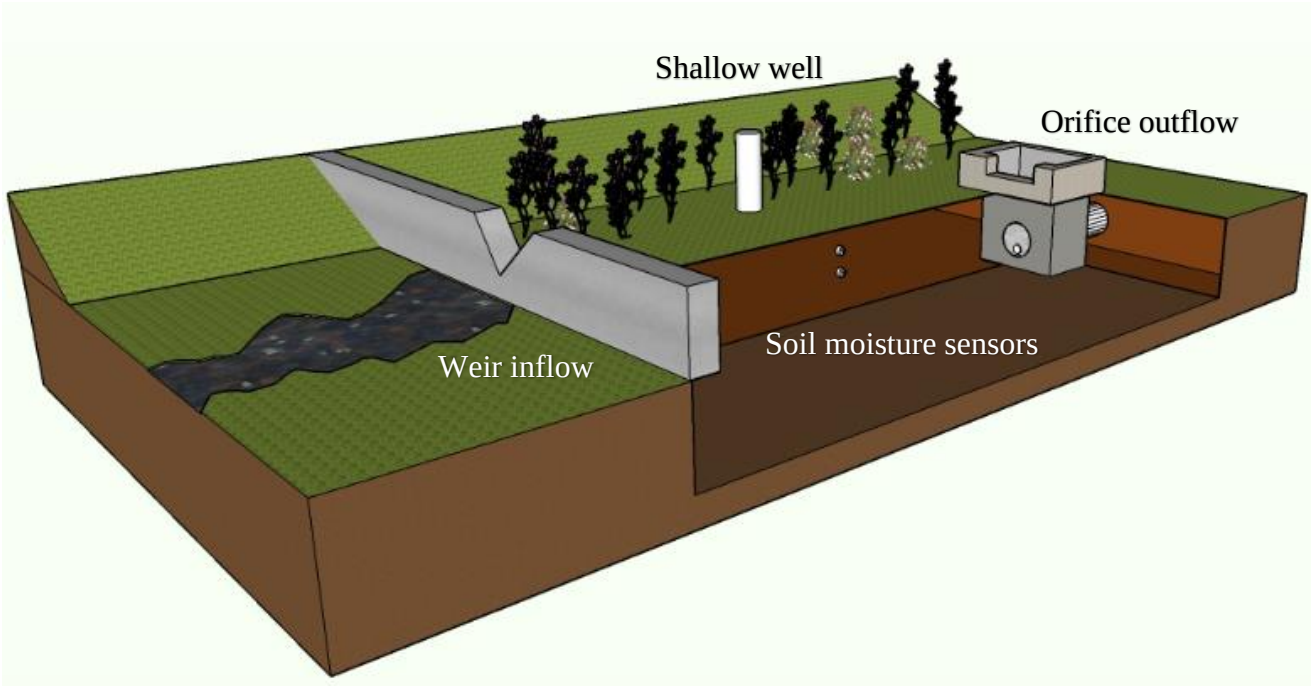

Figure 1.2 Example of instrumented rain garden.

The data collected from SCMs can quantify a variety of components including the site's performance, serviceability, and validation of corresponding models. Instrumentation of these sites is useful only if there is a clear objective of what measurements are desired. This objective influences the selection of monitoring equipment. Additionally, monitoring equipment needs to

be accurate enough based on the study's intended purpose because data's reliability is contingent upon the monitoring equipment's accuracy.

1.4 RESEARCH OBJECTIVE

Monitoring programs need to adequately quantify stormwater entering and leaving SCMs in order to determine their effectiveness. The purpose of this research is to select the most appropriate monitoring equipment for urban SCMs and analyze the accuracy of sensors. The focus is on the inflow and outflow of two different urban SCMs (i.e. rain garden and tree trench) that are a part of Philadelphia Water Department's Green City, Clean Waters program. The accuracy and reliability of monitoring equipment is determined with laboratory experiments. Ultimately, the goal is to implement the best suited equipment in the field that will record the most accurate data. This research involves the analysis of existing equipment supplied by manufacturers, and also requires thinking outside the box for typical flow measurement devices, including the development of new approaches to accurately monitor flow.

Unpredictable precipitation and variability of field conditions impact discharge measurements for SCMs. Accurate sensors are wonderful in laboratory settings, but their accuracy in the field is what really matters. Accurately monitoring SCMs in the urban environment is extremely difficult because conditions are variable. Outside of seasonal variability, monitoring equipment is subjected to harsh conditions with trash, sedimentation, debris, and vandalism that may disrupt the performance of monitoring equipment and the SCM. An investigation is conducted to analyze the differences in accuracy between ideal laboratory settings and field conditions.

CHAPTER 2: LITERATURE REVIEW

2.1 MONITORING SITE & INSTRUMENTATION

The overall goals for stormwater monitoring programs focus on quantifying the reduction of stormwater pollution, including the identification of high risk dischargers, and development of total maximum daily loads (Lee et al. 2007). A large portion of costs for monitoring programs is associated with the purchase of monitoring equipment and therefore, appropriate equipment should be selected based on its suitability for the site and the study. The sensor should be able to accurately operate in the site's climate conditions, be properly installed without affecting the hydraulics or damaging the site, have routine maintenance and fulfill its intention for proper and accurate monitoring (USBR 2001; Maheepala et al. 2001).

Two sites were selected for this research, a rain garden and a tree trench. The focus of instrumentation at each site, if applicable, is the inflow and outflow, ponded depth and interflow between system components.

2.2 FLOW MEASUREMENT

Flow measurement data is one of the most critical parts for SCM monitoring programs and it is often overlooked as a source of error (Quigley et al. 2002). Accurate flow measurement is critical in combined and storm sewer systems in order to analyze peak attenuation, volume reduction, water quality loads, flow-weighted samples, event mean concentration, and the amounts of untreated waters discharging to local waterways (Schenk et al. 2001). Appropriate measurement equipment should be selected according to the goals of the monitoring program for a particular site (Maheepala et al. 2001) and the constraints of the site design and expected flow rates. Flow devices for monitoring rain gardens are dictated by the expected flow rates. Large ranges of flow rates are a factor because it is difficult to find flumes to measure low flow rates

(O'Bannon 2012) in conjunction with high flow rates. Smaller watersheds, like ones in urban sewer environments, tend to have peaky flow rates over a wide range that should be captured by the monitoring equipment (Quigley et al. 2002).

For the present work, monitoring equipment was selected and researched for a surface inlet channel, sub-surface drainage pipe, and outlet overflow. Selection of monitoring equipment requires analyzing the claims made by manufacturers and developing new sensor applications (Schenk et al. 2001).

2.2.1 H-Flume

2.2.1.1 Background

Hydraulic control structures (e.g. weirs or flumes) capably monitor flow rates in small watersheds (Harmel et al. 2009). These measurement devices provide an indirect flow rate measurement by using a physical structure in combination with a depth measurement to derive the flow rate from the energy equation. H-flumes, one type of flume, were originally created by the National Resources Conservation Service to monitor open channel flows (USBR 2001) and are a combination of a flume and triangular weir. This combination is beneficial for flow monitoring because it can measure a high range of flows and its performance is not substantially affected by sedimentation (ASTM D5640), which is especially advantageous in urban environments with peaky flow rates (Quigley et al. 2002) and where sedimentation builds up on the streets and washes off during rain events.

The similarity between an H-flume and a weir is the critical depth's measurement in an open channel. Critical depth is forced at a single point by the weir or H-flume and consequently there is a unique discharge and depth relationship (USBR 2001; Sturm 2010). A stilling well in the H-flume houses a level sensor to minimize any turbulence and natural oscillations on the

water surface (Herschy 1995), such that there is an accurate reading of the critical depth to achieve the most precise flow rate from a rating curve.

Extensive experimentation and development of rating curves for weirs has resulted in their wide use as a flow measurement device (Sturm 2010). However, weirs have their limitations. The range of flows is limited with weirs due to head loss (USBR 2001). Since the flow rate is related to depth, it is necessary to have enough head differential between inflow and ponding water so that a weir is not submerged by the downstream flow. If the head is not available, then the flow rate measurements are limited. H-flumes are not as limited by these conditions and may be more useful for certain sites. Urban environments may not have the necessary head with surface runoff from the streets. Head can also reduce the capacity of the channel (USBR 2001), which results from the lack of drainage and potential standing water in urban environments.

If large volumes are entering a system, then submergence of these structures is a concern for measuring accurate data. If an SCM site has ponding then backflow can cause submergence of the inflow structure. Weirs can only operate under 15% submergence compared to H-flumes, which can operate under 30% submergence (USBR 2001).

2.2.1.2 Potential Measurement Errors

Overall the greatest source of error with measuring stormwater flow rates is with approach flow conditions if the flow is too turbulent, too low, or unstable (Quigley et al. 2002). Generally, approach flow conditions should be tranquil. Tranquil flow is defined as “fully developed flow in long, straight channels with mild slopes, free of close curves and projections, and waves” (USBR 2001). Thus, flow measurements of open channels require subcritical flow upstream of the H-flume, and typically the Froude value should be less than 0.5 (USBR 2001) to

limit waves. Manufacturers will generally state the minimum required approach channel length with respect to the measuring device in order to achieve a tranquil flow.

Uncertainty in measurements can occur and be a source of error, especially if the approach flow conditions are appropriate (Herschy 1995). Uncertainty in measuring depths for an H-flume are due to various reasons, including sensor accuracy, presence or absence of stilling wells, and sedimentation build up (Harmel et al. 2009; Herschy 1995; Sauer and Meyer 1992). The level sensor could be a source of error in the H-flume, including proper installation and routine maintenance (Quigley et al. 2002). The level sensor should be calibrated and maintained regularly to minimize sensor error. As mentioned previously unlike some hydraulic structures, H-flumes tend to be unaffected by upstream turbulence and sediment build-up (Quigley et al. 2002). However, the associated stilling well can have sedimentation buildup that could affect the sensor's measurement accuracy. This can be avoided with proper and routine maintenance. An example of a stilling well and flume setup is illustrated in Figure 2.1.

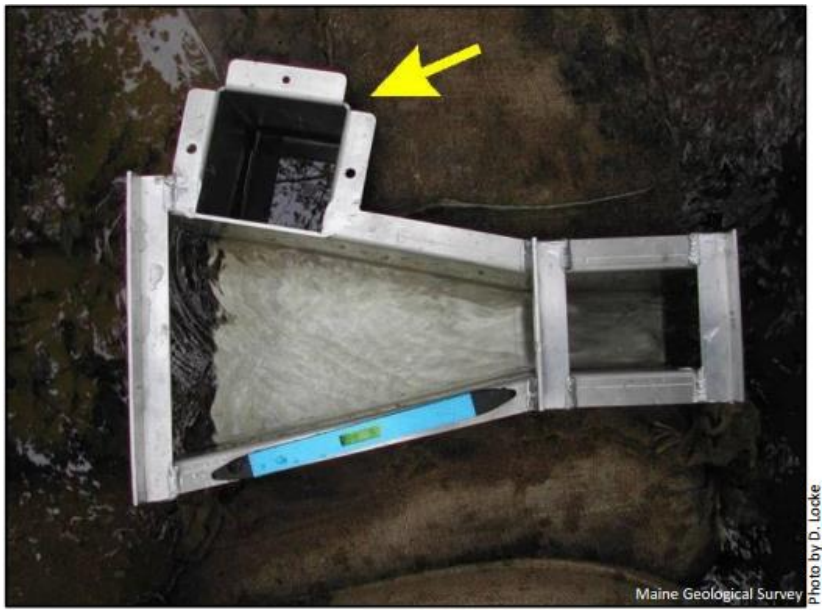

Figure 2.1 Example of stilling well at stage level of USGS 3-inch Modified Parshall flume from Main Geological Survey (Locke 2012).

There can be a stilling well depth response lag if there is a rapid change in velocity and subsequently depth in the flume channel (Herschy 1995). The lag will affect the head measurement and is dependent on the size of the open channel in correspondence with the size of the opening for the stilling well. As most urban watersheds are small, the size of the open channel and opening for the stilling well is a matter of inches, and lag should not be a concern.

2.2.2 Acoustic Doppler Velocity (ADV) Flowmeters

2.2.2.1 Background

There are numerous types of direct flowmeters available such as non-intrusive and intrusive acoustic Doppler velocity (ADV) technology. Intrusive flowmeters protrude the flow and causes distortion to the flow profile, while non-intrusive flowmeters are typically placed outside of the conveyance structure and do not disrupt the flow (Figure 2.2). The figure also depicts the difference between invasive and non-invasive flowmeters, which defines if the flowmeter touches the water.

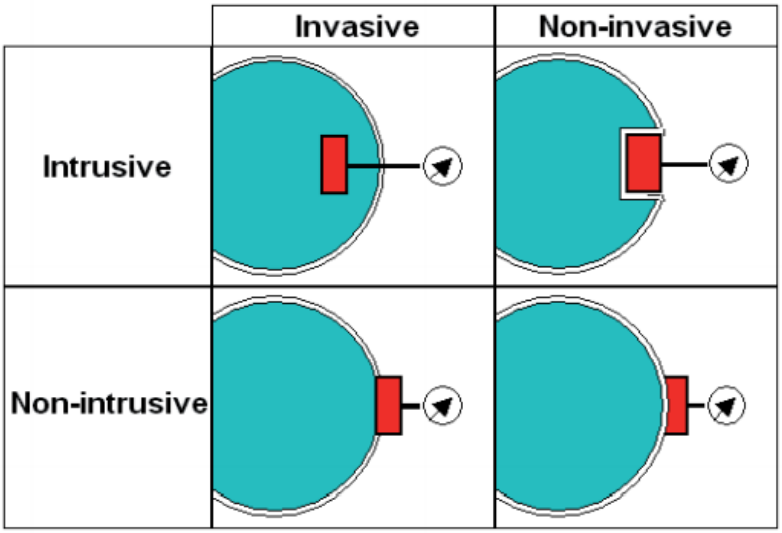

Figure 2.2 Area Velocity Sensor position for Intrusive vs. Nonintrusive from National Measurement System's "An introduction to non-invasive ultrasonic flow metering" (TUNVEL 2010).

Although, non-intrusive flowmeters do not intervene with the flow profile, it is not suitable for urban environments since the desired flow rates are in underground pipes in the stormwater sewer system. A non-intrusive flowmeter would require digging through concrete in order to attach the flowmeter around the pipe, resulting in a more permanent installation. Intrusive flowmeters are not sufficient for small flows since their larger size creates an interference with the flows (Maheepala et al. 2001). ADV sensors are widely used for measuring storm drainage because of their small size, ease of installation and maintenance, versatility, low intrusiveness, and relatively low cost (Bonakdari and Zinatizadeh 2011; McIntyre and Marshall 2008). They are also perfect for research purposes since they are not a permanent installation, thus they can be used temporarily in multiple places and have very low impact on existing site conditions (McIntyre and Marshall 2008).

ADV technology typically determines the flowrate through a pipe with an indirect method of calculating flow (ASTM D 5389):

$$Q = A(h) * V_{mean} \qquad \text{(Equation 1)}$$

where

- Q = flow rate (cfs)
- A(h) = area as a function of depth (ft^2)
- V_{mean} = average velocity (ft/s)

The ADV typically records data by independently recording the level of water with a pressure transducer and simultaneously recording a "one-dimensional velocity measurement for a conical control volume" (Aguilar et al. 2015). The Doppler sensor sends a signal in the opposite direction of the flow and is reflected back by the particles moving with the water. The signal is an ultrasonic signal that detects small particles air bubbles traveling with the direction of flow (McIntyre and Marshall 2008). This is known as the Doppler shift where the Doppler frequency analyzes the echoes of the suspended particles in a conical volume in order to

determine a relative velocity within the conical volume that is representative of the cross section (Bonakdari and Zinatizadeh 2011).

Since ADV sensors emit an ultrasonic wave to detect the particles in the water, noise will develop from the natural transience in the sediment distributions and fluctuation in depth. As a result, the ultrasonic signal is held at a higher frequency than the required time resolution so that it can process the flow data and diminish the noise for output data (ASTM D5389; McIntyre and Marshall 2008).

2.2.2.2 Potential Measurement Errors

There are several potential measurement errors that are associated with ADV flowmeters that could result from any combination of the following: excess sedimentation, orientation of the sensor, approach flow conditions, and sensor accuracy. The position of the ADV sensor at the bottom of the pipe can influence errors because sedimentation and silt can get trapped behind the sensor, especially at low velocities. As a result, the sedimentation disrupts the signal and leads to inaccurate results (Aguilar et al. 2015; McIntyre and Marshall 2008).

Since the velocity measurement is dependent upon the Doppler signal and the magnitude of suspended particles in a conical volume, then measurement errors can also occur if the volume is not representative of the cross sectional velocity (Bonakdari and Zinatizadeh 2011). The strength of signal and magnitude of particles affect the velocity output which is variable per storm. Sedimentation and air bubbles traveling with the flow affect the strength of the signal for the Doppler shift. Errors can occur when the particles are not moving uniformly throughout the pipe and suspended particles will tend to reduce the signal (ASTM D5389). This potential measurement error is attributed to a bias with the sensor that will calculate the average velocity

based off of higher concentrations of suspended sediment near the bed (McIntyre and Marshall 2008).

The sensor calculates the area for flowrate as a function of depth, therefore, the accuracy of the pressure transducer measurements can also affect the overall performance of the sensor. If flows are exceptionally low and there is not enough water depth for the pressure transducer to detect, then no data will be retrieved (McIntyre and Marshall 2008).

2.2.3 Overflow Measuring Device

2.2.3.1 Background

A common overflow device used in SCMs is a riser pipe with a domed lid, which does not lend itself well to traditional flow measurement, such as a weir or ADV. Therefore, this investigation looked into developing a custom measurement device that can capture the wide range of flow rates for a domed riser overflow structure (Figure 5.1, discussed further in Chapter 5). The inspiration for this device came from two different case studies that were based off of orifice measuring devices.

The first case study is a green roof in Auckland, New Zealand that was trying to capture flows from an overflow that ranged from 0.003 gpm (0.0002 L/s) to 15.85 gpm (1 L/s). An orifice restricting device (ORD) was fabricated and had orifices at different levels as seen in Figure 2.3 (Voyde et al. 2010). Calibration of this device was completed with a pressure transducer to measure the level of the water and known flow rates in order to create a corresponding discharge rating curve.

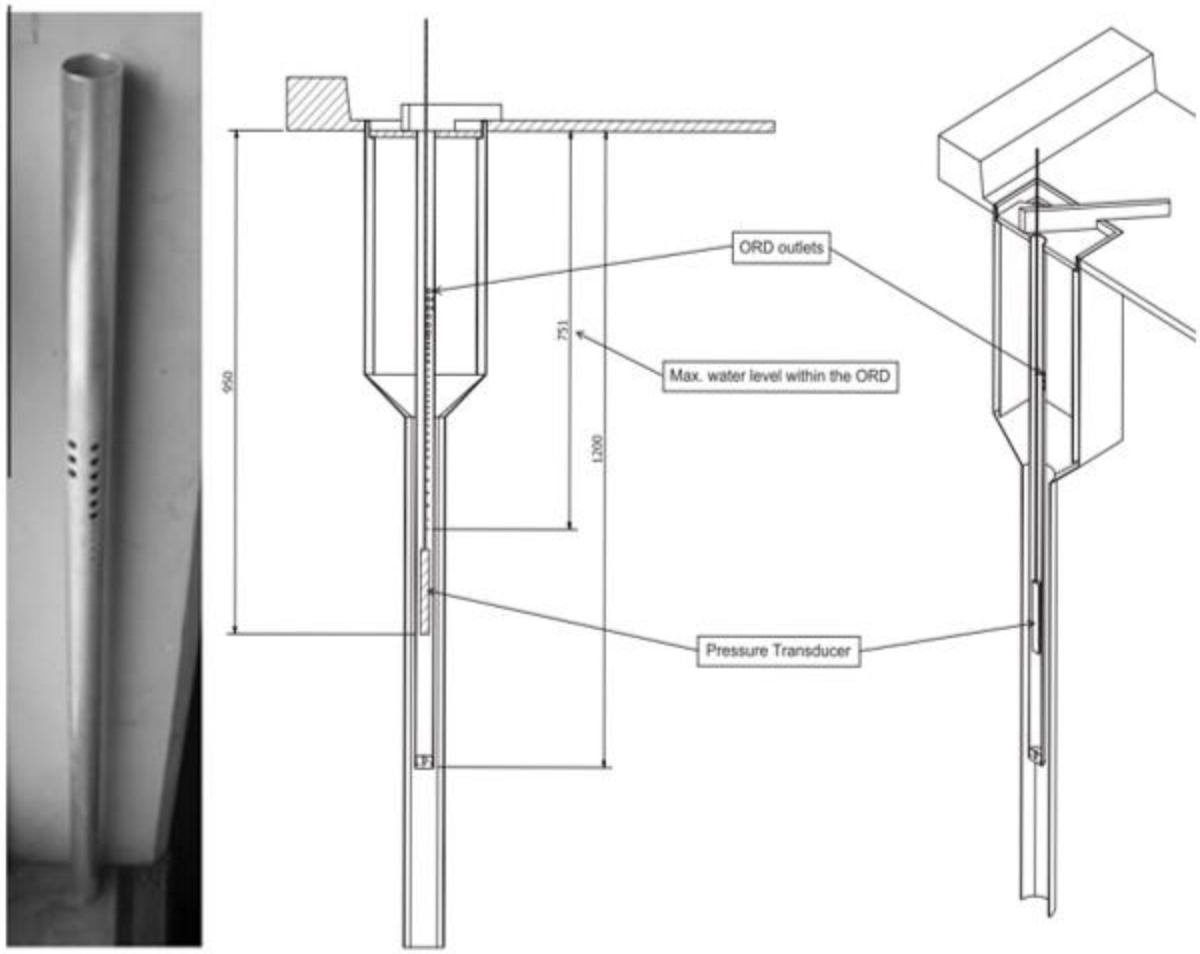

Figure 2.3 Orifice restricted device and installation plans used for overflow of a green roof in Auckland, New Zealand (Voyde et al. 2010).

The ORD has capabilities of measuring a range of flows from the overflow of rooftops and this inspired the first overflow prototype for this study. Similarly the domed riser needed a custom ORD device that could measure overflow, however, it had to measure significantly higher flow rates compared to a green roof.

The second case study is in Kansas City, Missouri where difficulties were encountered trying to capture the extensive range of inflows for monitoring a rain garden. As a result, the study designed and fabricated a compound orifice-controlled device that was comprised of two orifice holes. A small orifice was positioned in a barrel in order to measure low flow rates. The

second orifice was larger and placed above the smaller orifice in order to capture higher flow rates up to 0.17 cfs (4.814 L/s), which was the estimated 100 year storm event (O'Bannon 2012). Theoretically, this produced a two slope line for the rating curve (Figure 2.4). This device is a compact, low cost method for more accurate measurements with low flow rates, while not constricting the flow for higher intensity storms (O'Bannon 2012).

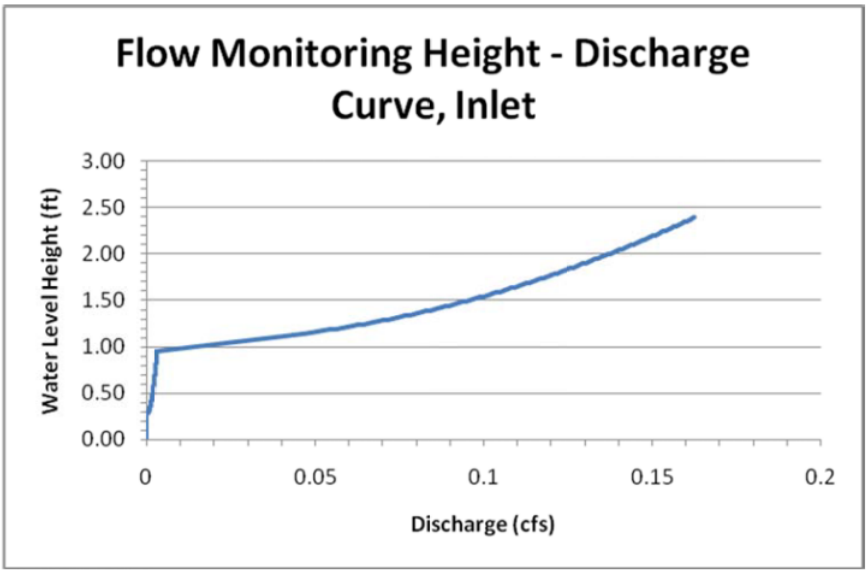

Figure 2.4 University of Missouri-Kansas City's theoretical height-discharge curve for orifice-controlled inlet flow monitoring device (O'Bannon 2012).

A similar compound device is desirable for the domed riser. Although the Kansas City model measures low and high intensity storms, it is not applicable to many urban SCMs with a domed riser overflow. There is less available measuring depth in an urban SCM and higher flow rates need to be captured. Lastly, the two curves have a drastic change in slope where the water transfers to the bigger orifice. This can result in less accurate data in the transitional zone and it is desirable to incorporate a design with smoother transitions.

2.2.3.2 Potential Measurement Errors

Similar to other measurement devices, sedimentation is a concern with the overflow. The case study in Kansas City, Missouri was capturing flows from rooftops and pavement surfaces. As a pretreatment for the rain garden, a screen was incorporated into the inlet in order to prevent debris and sedimentation from entering the barrel (O'Bannon 2012). Another concern for this study was the high flow rates entering the inflow barrel. The expected high flow rates in combination with the barrel structure could cause turbulence leading to inaccurate measurements. As a result, a baffled inlet was installed to address any potential problems (O'Bannon 2012).

2.3 EQUIPMENT TESTING

The Wet-Weather Flow Technologies Pilot Program (a part of the U.S. EPA's Environmental Technology Verification Program) recommended that in order to verify the quality assurance of flow monitoring equipment then testing had to be conducted in both laboratory and field conditions (Schenk et al. 2001).

2.3.1 Laboratory Experiments

Verification of monitoring equipment in a laboratory setting will enforce credibility for the sensor/flow monitoring setup and assist in the overall examination of the site's performance (Schenk et al. 2001). The rating discharge curve obtained for a depth sensor-flume flow meter in a laboratory is often transferred directly to the field. Therefore, laboratory experiments need to be representative of the expected site conditions including structures, size, sensor installation, approach field conditions, and even the approach channel (Rantz 1982). Testing flowmeter equipment in laboratory settings should include a range of flow depths and velocities. The monitoring equipment's flow values should be compared to highly accurate measurements from

a known existing sensor within the laboratory. All flow conditions should be analyzed, especially conditions that are expected in the field including surcharge, submergence, and backflow conditions (Schenk et al. 2001).

2.3.2 Field Validation

Uncertainties exist within the measuring error of monitoring equipment (Dotto et al. 2014; McMillan et al. 2012; Sauer and Meyer 1992). However, additional uncertainties are the sensor's applicability and the measurement's representation for specific site conditions (Bonakdari and Zinatizadeh 2011). Flow measurement errors are often caused by field conditions that deviate from laboratory settings where the rating curve was developed for that particular flow device (Quigley et al. 2002; Rantz 1982).

The Philadelphia Water Department performs Simulated Runoff Tests (SRTs) as part of their Comprehensive Monitoring Plan in order to evaluate individual SCMs (PWD 2012). SRT methods that are conducted in Philadelphia were derived from similar approaches utilized by Oregon's Bureau of Environmental Services in Portland (Portland 2010). Both cities use a Sensus WL-1250 portable water meter tester that connects to a fire hydrant and disperses a controlled flow rate into the SCM. The meter permits a set volume into the SCM, which is a precise method for evaluating the SCM's performance and any flow meters or other monitoring equipment.

Specifically, SRTs in Philadelphia are used to assess the performance of an SCM's infiltration. Infiltration testing validates that the SCM was built correctly and indicates if any soil has been compacted during the construction process (Gulliver et al. 2009). Similarly, the city of Portland evaluates SCMs and analyzes the flow volume and peak flow reduction between pre and post construction (Portland 2010).

SRT methods have also been used in other studies as well as a method of assessing SCM practices. A study in Minnesota was conducted on the performance of SCMs based on a four level assessment: (1) visual inspection, (2) infiltration capacity testing, (3) synthetic runoff test (SRT), and (4) monitoring (Gulliver et al. 2009). The second level suggests infiltration capacity tests (Modified Phillip-Dunne) throughout the SCM basins help understand the variability of K_{sat} values. This is beneficial for understanding an approximate K_{sat} value, however, it is only a rough estimate for the entire SCMs drawdown time (Gulliver et al. 2009). As part of the third level assessment, a SRT (denoted as synthetic runoff test) is used to measure the drain time of the entire rain garden to a given volume. The study concluded that a SRT is a quick and efficient method with little associated costs to evaluate the drainage time of an entire system.

Synthetic Runoff Test was also used in an early study in 1997 to evaluate the water quality and performance of two grass swales located in Taiwan and Virginia. The study utilized a SRT that was dosed with pollutant concentrations and, similar to other tests, the flow was dispersed at a known steady rate. This investigation supplied the water from two storage tanks into the grass swales (Yu et al. 2001).

In literature, SRTs have been used to analyze SCM performance. Simulated Runoff Tests could also be used as a method to validate the operation of monitoring equipment. Verification of in-field tests can provide information on the manufacturer's stated range of equipment capabilities, requirements for maintenance of sensors, reliability of equipment, and response to flow changes (Schenk et al. 2001).

CHAPTER 3: PROJECT BACKGROUND

3.1 PHILADELPHIA WATER DEPARTMENT'S GREEN CITY, CLEAN WATERS

The city of Philadelphia has one of the nation's oldest water infrastructure systems. The city is distinguished by being America's first city to supply clean drinking water to the public (1801) and having the country's first water and wastewater systems (1815). Over the years, the city's sewer systems evolved to approximately 3,000 miles of sewers with 79,000 stormwater inlets and 164 CSO outfalls (PWD 2011). The combination of urbanization, climate change, and aging infrastructure makes the city susceptible to CSOs, flooding, and polluted waterways. Complying with the Clean Water Act, *Green City, Clean Waters* (GCCW) is Philadelphia Water Department's long term control plan to reduce stormwater pollution entering the combined sewer systems. It is a 25 year plan that involves integrating green infrastructure as part of the city's water infrastructure system. The GCCW program is a $2.4 billion investment that is projected to reduce stormwater pollution entering local waterways by 85% (PWD 2011).

As part of the GCCW initiative, a Comprehensive Monitoring Plan was implemented to verify the functions of the sewer systems, SCMs, and local waterways. Monitoring data for specific SCMs will enable performance assessment, including the volume reduction effectiveness and improvements in water quality. The data will be used to quantify green infrastructure's effects on a larger scale to assess the hydraulic and hydrologic influence on CSOs (PWD 2012).

As part of an EPA STAR grant, Villanova University is monitoring, developing, and analyzing several common SCM designs in support of PWD's *Green City, Clean Waters* initiative. This research specifically investigates the two most common designs: a rain garden site (Figure 3.1a) and a tree trench site (Figure 3.1b).

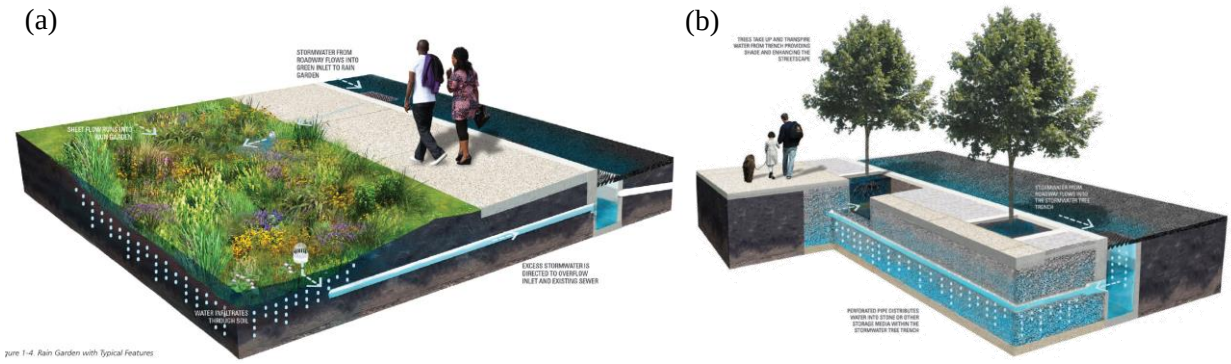

Figure 3.1 Common Philadelphia Water Department designs, (a) rain garden and (b) urban tree trench designs (PWD 2011).

The rain garden captures stormwater by surface runoff entering a trench drain. The anticipated depth measurements for the rain garden range from 0-1.5 ft (0-0.5 m). There is also an overflow pipe at the rain garden that discharges water into a side rock trench. The tree trench captures water in a stormwater inlet and discharges water through a subsurface 8 in (20.3 cm) perforated pipe. There is no overflow structure for this site. These general components of the site affect the selection of monitoring equipment

3.2 CLIMATE

Variation in temperature and precipitation affects soil moisture, vegetation growth, evapotranspiration, and the water table. Therefore, climate dictates the design and performance of SCMs, and also influences the selection of monitoring equipment. For example, temperature can disturb a sensor's accuracy during extreme cold weather and harsh rain events can affect the operating range of some sensors. A sensor's resilience to climate should be investigated prior to the implementation of a stormwater monitoring program. Philadelphia's climate experiences seasonal variation with an average total precipitation of 44 in (111.8 cm) per year (Appendix A, Table A.1). The majority of storms are low volume, low intensity events. It is shown in Figure 3.2 that over 70% of total rainfall events were 1 in (2.54 cm) or less from 1948-2006.

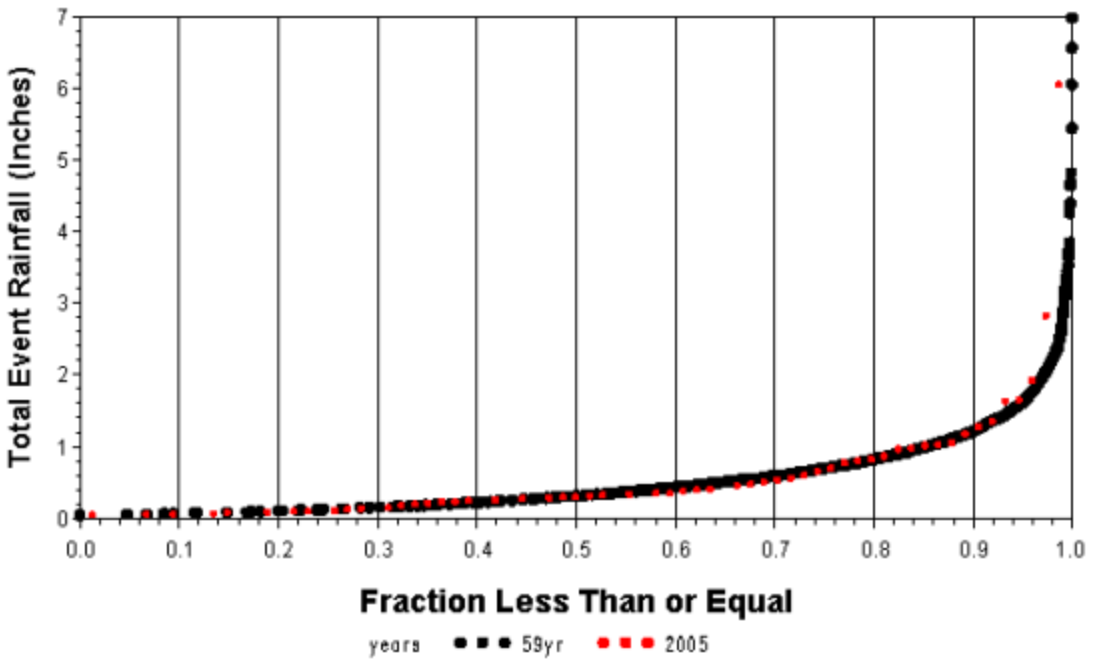

Figure 3.2 Event Rainfall Volume at the Philadelphia International Airport over 59 years (1948-2006) with 6 hours as the minimum inter-event time (PWD 2009). Year 2005 is graphed as a comparison over the 59 year period.

3.3 SITE DESCRIPTION

The Philadelphia Zoo Rain Garden and Morris Leeds Tree Trench sites were selected for this research. The selection of these sites were contingent on sufficient drainage area compared to the site's size, located near public parks or schools, and the underdrain pipe detached from the combined sewer system. Philadelphia sites have a capped underdrain pipe that may be modified with a small drilled hole if an SCM fails causing slow-release orifice flow into the combined sewer system.

Size of a measuring site has an impact on the use and maintenance of sensors by requiring special knowledge of the instrument's operations compared to the site's functionality (Bonakdari and Zinatizadeh 2011). Therefore, prior research was conducted on each site to

determine drainage areas, site ratios, and predicted flow rates. This information assisted with the selection of adequate monitoring equipment.

3.3.1 Philadelphia Zoo Rain Garden

The Philadelphia Zoo Rain Gardens is in west Philadelphia at the Zoo's giraffe parking lot. The rain garden is located on West Girard Avenue between North 38th and 39th Street (Figure 3.3). The rain gardens are a series of SCM systems, consisting of two rain gardens connected by a grass swale. This system receives inflow that would normally be delivered to culverts within the CSS.

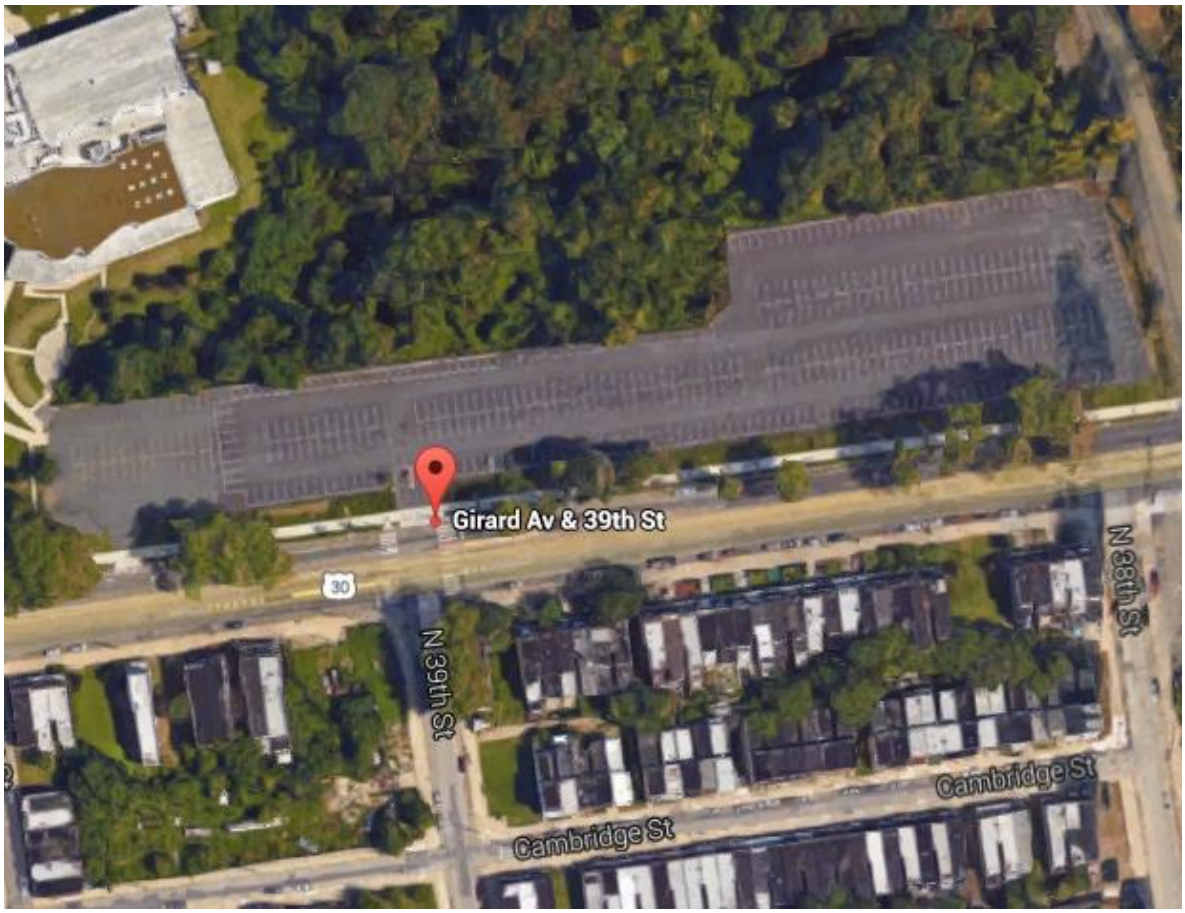

Figure 3.3 Location of the Philadelphia Zoo Rain Gardens on W. Girard Avenue between 38th and 39th Street. (Image taken from Google Maps, 2016)

The rain gardens consist of two inflow surface channels and one outlet structure that acts as an overflow system (Figure 3.4; Appendix B, Figure B1). The outlet structure is in the downstream rain garden and it discharges water directly into a rock bed. Originally the rock bed was designed to be placed underneath the rain garden. However, during construction pipes were discovered beneath the rain garden and as a result the rock bed was installed directly next to the rain garden beneath the parking lot.

Figure 3.4 Rain garden treatment series with location of rock bed (top right blue box) and surface inlet channels (pink). Flow goes from left to right in this picture.

3.3.1.1 Inflow Structures and Drainage Area

Runoff is captured off W. Girard Street and discharged into the rain garden via a surface channel called a trench drain. The trench drain is a common PWD design for a surface inflow channel (Figure 3.5).

Figure 3.5 Inflow channel (trench drain) at the Philadelphia Zoo Rain Garden.

The drainage area of the Philadelphia Zoo Rain Garden was provided by the PWD; the impervious drainage area on Girard Ave for the downstream rain garden is 8,707 ft^2 (808.9 m^2) and the impervious area for the upstream rain garden is 7409 ft^2 (688.3 m^2). The rain gardens also capture water that falls on the surrounding sidewalks and in the bowl of the rain garden. The total drainage area for the entire system (Appendix B, Figure B.2) is 11,130 ft^2 (1,034.0 m^2) and 12,470 ft^2 (1,158.5 m^2) for the upstream and downstream rain gardens, respectively.

3.3.1.2 Peak Flow Rates

An initial analysis used the rational method (Equation 2) to estimate the peak discharge for the surface inflow channels for a 0.5 in. (1.3 cm), 1 in. (2.5 cm), 2-year, 10-year, 25-year, and 50-year storm to aid in selecting proper flow measurement devices. A rational runoff coefficient of 0.875 was used for concrete. The precipitation intensity for each storm event was acquired from the National Weather Service and National Oceanic and Atmospheric Administration (NOAA) for the Philadelphia area. The precipitation intensity was obtained for storm duration of 5 minutes and 15 minutes. The downstream rain garden's flow rates are the primary concern

because it has a larger impervious drainage area. The predicted peak discharge is displayed in Table 3.1 for the downstream rain garden (Appendix B, Table B.1). The rational method for peak discharge is expressed as:

$$Q = ciA; \qquad \text{(Equation 2)}$$

where,

- Q = Peak discharge, cfs
- c = Rational method runoff coefficient
- i = Rainfall intensity, in/hr
- A = Drainage area, acre

Table 3.1 Predicted Peak Discharge for Philadelphia Zoo Downstream Rain Garden Inlet using Equation 2.

Peak Flow Rates	**Storm Depth**		**5 Minute Duration**		**15 Minute Duration**	
Storm Event	0.5 in (1.3 cm)	1 in (2.5 cm)	2 Year	10 Year	2 Year	10 Year
Q (cfs) (m^3/s)	0.09 (0.003)	0.17 (0.005)	0.87 (0.025)	1.13 (0.032)	0.58 (0.016)	0.76 (0.022)

3.3.2 Morris Leeds Tree Trench

The Morris Leeds Tree Trench is a SCM installed in northwest Philadelphia near the Morris Leeds Middle and High School. The tree trench is located on the corner of Lowber Avenue and Sedgwick Street (Figure 3.6). This site is unique because it is primarily underground. Similar to the Zoo rain gardens, this system receives water from the adjacent street Lowber Avenue. However, the water is captured into a stormwater inlet and dispersed into a subsurface trench (Appendix C, Figure C.1), which is temporary storage for the water. There are

also five tree pits spaced along the trench's length (Figure 3.7) that have roots reaching into the rock bed (Figure 3.8).

The subsurface trench is an infiltration trench that allows the water to permeate into the ground or be taken up by the plants. If the system fails, then there is an existing underdrain pipe that leads to the combined sewer system. The pipe is currently capped for this site, however, if it fails then a hole will be drilled into a cap and it will act as an orifice relief.

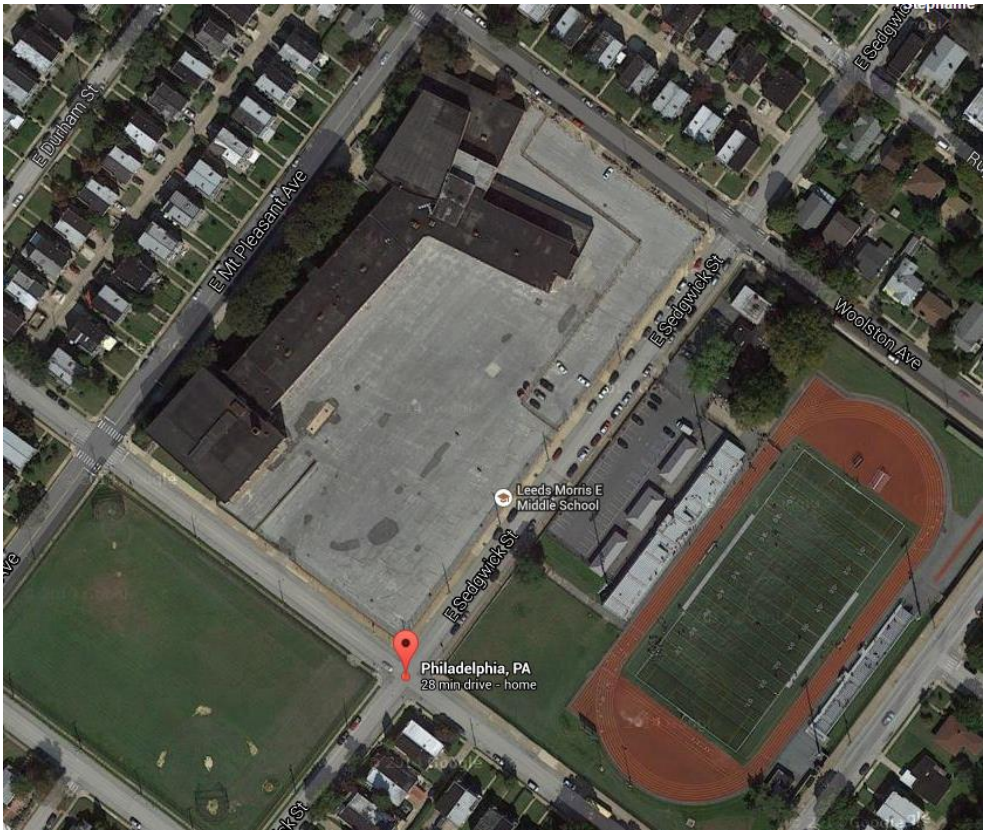

Figure 3.6 Morris Leeds Tree Trench is location on the corner of Lowber Ave. and Sedgwick St. Philadelphia, PA 19150. (Image taken from Google Maps, 2016)

Figure 3.7 Morris Leeds Tree Trench site. (Flow travels right to left in this image).

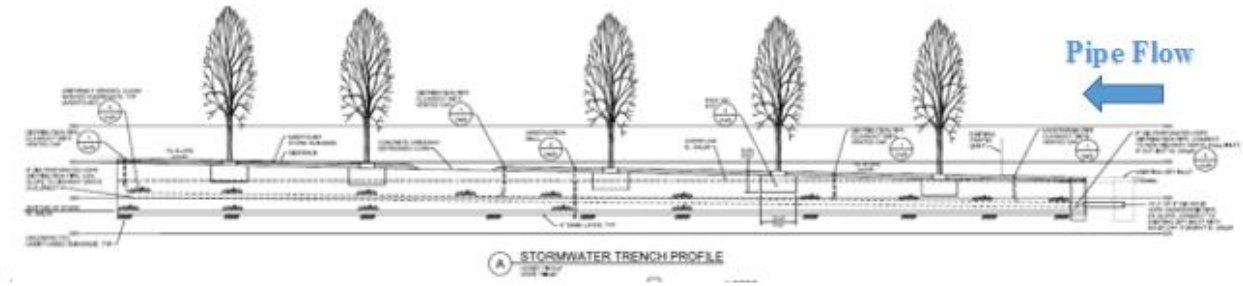

Figure 3.8 Drawing of five tree pits with subsurface pipe through rock bed (drawings provided by PWD).

3.3.2.1 Inflow Structures & Drainage Area

The drainage area is captured from both sides of Lowber Avenue and enters a "green inlet". The green inlet is a Philadelphia Water Department design and is placed upstream of the combined sewer inlet. The green inlet has a filter bag that removes silts and debris from the water according to PWD standards (Figure 3.9a). There are two green inlets across from one another that are connected with a conduit (Figure 3.9b). The green inlets capture the water and distribute it directly into the subsurface trench.

Figure 3.9 Green inlets for stormwater tree trench at the Morris Leeds site: (a) filter bag (left), (b) two green inlets located across the street to capture all runoff from Lowber Ave (right).

The drainage area of Morris Leeds School was determined with AutoCAD 2014. The PWD provided map was scaled in AutoCAD and each drainage area was outlined for the Morris Leeds tree trench site. Two drainage areas were estimated for the site's inlets on Lowber Avenue for the school side and baseball side. The drainage area was specified by PWD as the middle of the street's crown to the sidewalks (Figure 3.10). Table 3.2 displays the drainage area for the tree trench site on Lowber Street.

Figure 3.10 Drainage Area of Morris Leeds Tree Trench

Table 3.2 Approximation of Morris Leeds Drainage Areas

Site	Location	Drainage Area (ft^2) (m^2)
Morris Leeds Tree Trench	Lowber Ave (School Side)	13,800 (1282)
	Lowber Ave (Baseball Field)	12,800 (1189)

3.3.2.2 Peak Flow Analysis

Peak discharge was also calculated for the Morris Leeds site following the same procedures as the Zoo rain gardens (Equation 2; Table 3.3). The only difference in the equation is the value for Morris Leed's drainage area. The two drainage areas were summed together, 26,600 ft^2 (2,471.2 m^2), because both inlets merge to one pipe before water enters the subsurface trench.

Table 3.3 Predicted Peak Discharge for Morris Leeds Tree Trench site using the Equation 2.

Peak Flow Rates	**Storm Depth**		**5 Minute Duration**		**15 Minute Duration**	
Storm Event	0.5 in (1.3 cm)	1 in (2.5 cm)	2 Year	10 Year	2 Year	10 Year
Q (cfs) (m^3/s)	0.27 (0.008)	0.53 (0.015)	2.66 (0.075)	3.45 (0.097)	1.78 (0.050)	2.33 (0.066)

CHAPTER 4: INFLOW MEASURING DEVICES

4.1 SELECTION OF H-FLUME FOR ZOO RAIN GARDEN

Selection of monitoring equipment requires analyzing the claims made by manufacturers and assessing the applicability of sensors to the monitoring site (Schenk et al. 2001). The predicted flow rates from Table 3.1 (§3.3.1.2) assist in the instrument selection for measuring inflow. The selected measuring equipment for the Zoo rain garden is a TRACOM 0.75 ft (0.23 m) H-flume, which can record flow from 0.0006 to 0.957 cfs (1.7 E^{-5} to 0.027 m^3/s). The greatest advantage of the H-flume, and reason for selection, is that it can record the range of low and high flows that are encountered in Philadelphia. The runoff from storm events will be captured and recorded with a CS451 pressure transducer installed in the stilling well of the 0.75 ft (0.23 m) H-flume.

4.1.1 Laboratory Testing

Quantitative flow analysis should be tested on the H-flume in order to determine any expected errors with low and high expected peak flows (Quigley et al. 2002). Laboratory testing for a full range of expected field conditions was conducted to validate the accuracy of the calibration provided by the manufacturer TRACOM. The testing took place in Villanova University's fluids laboratory, utilizing an existing laboratory flume and flow meter. In order to record accurate measurements, the examination of the TRACOM H-flume followed protocol of the United States Department of the Interior Bureau of Reclamation's *Water Measurement Manual* and TRACOM's Installation Instructions. Due to laboratory constraints, minimal adjustments were made to the installation requirements.

4.1.1.1 Installation Requirements

The H-flume lab installation was constructed to simulate the field as closely as possible and in congruence with TRACOM's protocol. The flume is required to have an approach channel straight upstream with a length of at least 5 times the depth of the flume [D=0.75 feet (0.23 m)]. As a result, a 4 ft (1.2 m) long approach channel was constructed. The approach channel followed the dimensions of the upstream section of the H-flume, 0.75 ft (0.23 m) depth and 17 29/32 in (45.5 cm) wide. The channel was leveled on top of a set of 2x4 ft (0.6x1.2 m) wooden blocks. Additionally, the flume was painted with a sand additive to imitate the roughness of concrete in order to reflect field conditions. The H-flume was bolted onto the end of the approach channel and caulked around the edges (Figure 4.1).

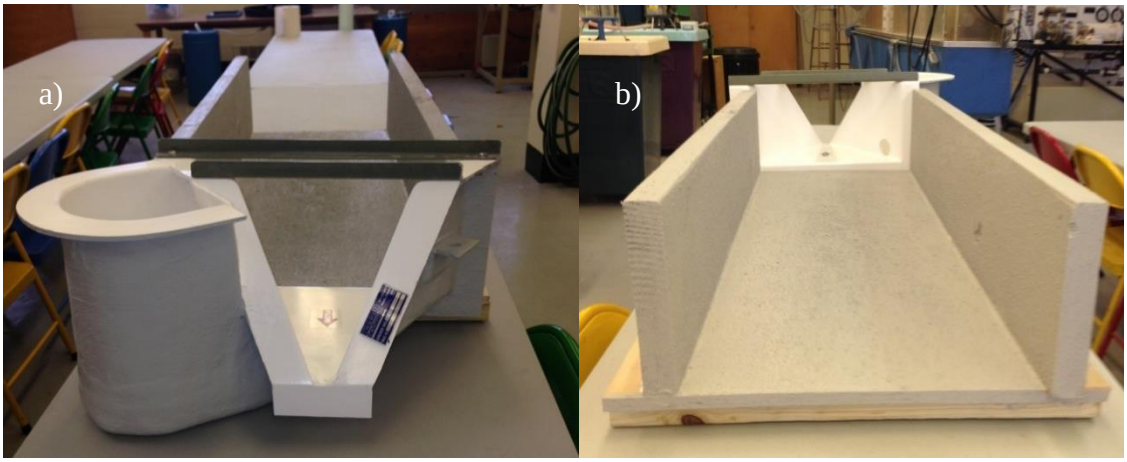

Figure 4.1 H-flume with Constructed Approach Channel (a) Upstream and (b) Downstream Views

The flume was set in a straight section of the open channel in the laboratory's existing flume. Per TRACOM's installation requirements, there were no drops, bends, flow junctions, etc. immediately upstream of the H-flume location. The floor of the flume was set level from front to back and from side to side. According to the manufacturer, TRACOM, "a level installation is critical to the proper operation of the flume" (Kazimer 2014).

The upstream section of the approach channel was connected to a piece of plywood (Figure 4.2). This enclosed the approach channel so that all water was captured and directed into the channel, and not surpassed on the sides. Discharge of the flume was free spilling. However, additional testing was completed to inspect the limit of submergence levels without affecting the free flow discharge.

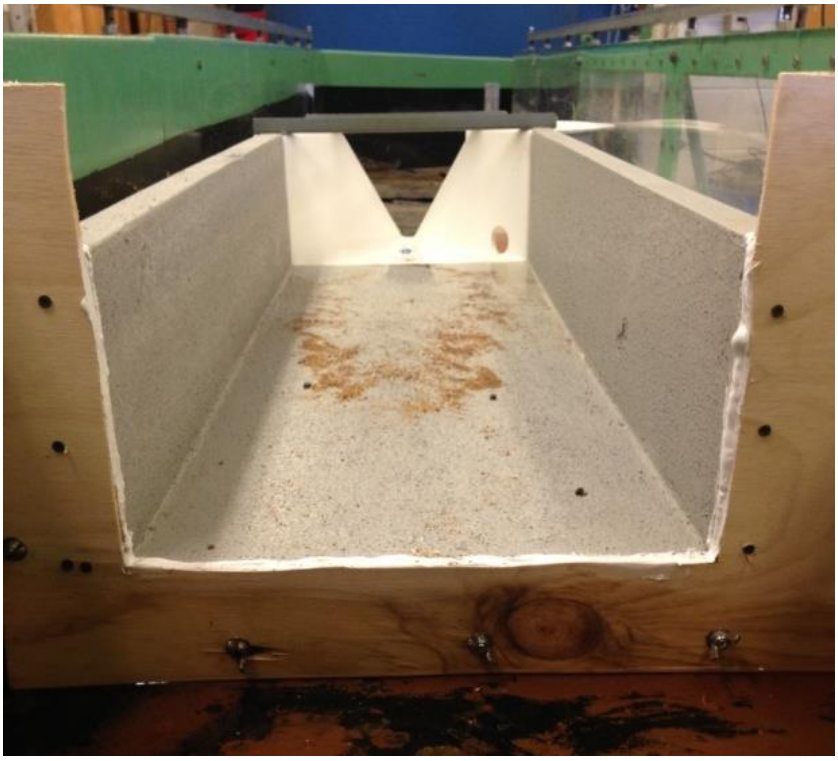

Figure 4.2 H-flume's Installed Approach Channel to Stilling Basin

4.1.1.2 Approach Flow Conditions

According to TRACOM installation instructions, “the approaching flow should be uniformly distributed across the channel, tranquil, and subcritical” (Kazimer 2014). The approaching flow should not be turbulent, surging, unbalanced, or possessing a poorly distributed velocity pattern. The water was discharged upstream into a small box area that imitated a stilling basin to reduce any turbulent flow.

A few tests were conducted with the stilling basin design with a short inflow pipe (Figure 4.3a). However, turbulence existed at the higher flows because the short pipe added water directly to the surface. Consequently, there was a large amount of energy that caused turbulent flows. In order to decrease the turbulence, the pipe was extended which forced the water to hit the bottom of the stilling basin thus reducing the energy (Figure 4.3b).

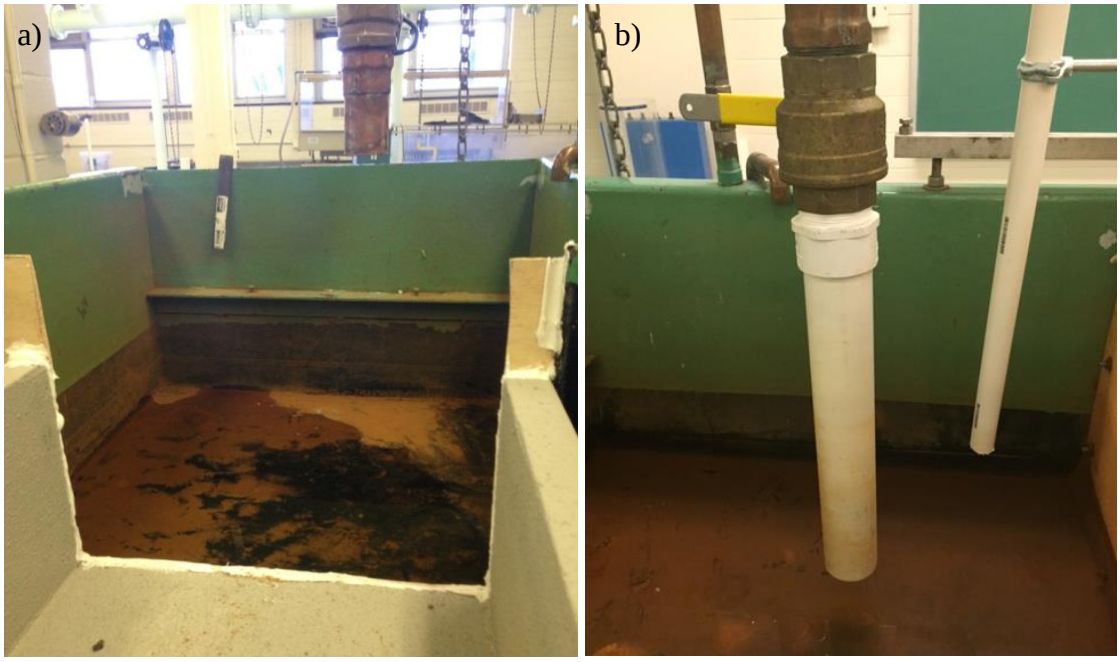

Figure 4.3 Stilling Basin and (a) Initial Discharge Pipe, (b) Modified Extended Discharge Pipe

According to the manufacturer, for a 0.75 ft (0.23 m) H-flume the recommended flow rates are 0.27-430 gpm (1.02-1627.7 L/min) [0.0006 – 0.958 cfs (1.7 E^{-5} to 0.027 m^3/s)]. Villanova's facilities could only achieve a maximum flow rate of 0.7 cfs (0.02 m^3/s). Therefore, testing was restricted to this limit.

4.1.1.3 Methodology

In order to validate the factory's calibration, flow rate measurements and head measurements had to be recorded simultaneously. The laboratory's existing flow meter is a 4 in

(10.2 cm) Toshiba Electromganetic Flowmeter LF434 Series and was used to measure the accuracy of the manufacturer's calibration. Head measurements were taken from the stilling well attached to the H-flume. In order to confirm the depth of the head, two measurements were recorded from different devices. One device is a Sensix ToughSonic3 ultra-sonic water level sensor that was mounted to the side wall of the laboratory's existing flume. The other device is a Campbell Scientific CS451 pressure transducer that was placed within the stilling well.

Testing began with a low, uniformly distributed flow and was slowly increased by subtle increments. The head measurements from the ultrasonic and pressure transducer were recorded with a CR1000 datalogger. Each flow rate was recorded for approximately 3 minutes before adjusting to the next flow rate. The CR1000 documented the head measurement by taking a scan of the water level every 5 seconds and averaging the values over a minute. Once the flow rate reached the upper limit of 0.7 cfs (0.02 m^3/s), the test was conducted again by slowly decreasing the flow rate. Points were plotted from increasing flow rates and from decreasing the flow rates. Both set of points should replicate the curve of the manufacturer's calibration.

Additional tests were also conducted by varying the flow rates sporadically. For example, a flow rate would be set to 0.3 cfs (0.008 m^3/s), then increased to 0.6 cfs (0.017 m^3/s), then decreased to 0.08 cfs (0.002 m^3/s), and so on. This was done to confirm that the H-flume recordings are not influenced by the previous flow recording. Also, since storm events do not typically increase and decrease incrementally, this is more representative of a storm event. Ponding can occur in the rain garden and there might be periods where the flume will be submerged and still measuring flow. Therefore, additional testing was conducted to evaluate the effects of submerging the H-flume. This study was conducted by closing off the drain for the laboratory's existing flume and slowly allowing the H-flume to discharge water as it submerged

itself in water. Flow was held constant and depth measurements were taken in the stilling well. There was an additional reading taken with a ruler to measure the depth of the submergence height (Figure 4.4). The depth of the stilling well was held constant in accordance to the flow rate. This depth changed at approximately 4 in, which indicated when the submergence affected the flume's measuring capabilities. The height of the submergence was documented corresponding to the change in depth of the stilling basin.

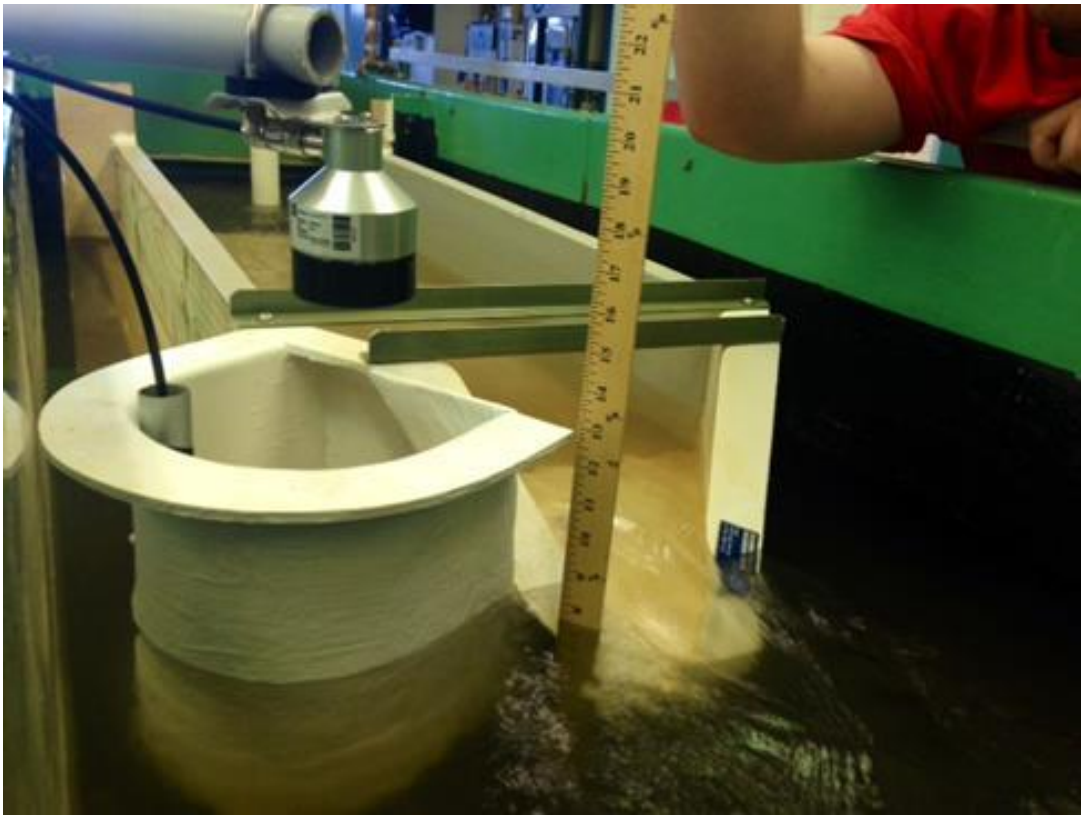

Figure 4.4 Submerged Flume

4.1.2 Laboratory Results and Analysis

Eight laboratory tests were conducted in order to validate TRACOM's calibration. Each test graphed the measurements of the flow rate vs. the corresponding depth recorded. A curve was drawn for the factory's calibration, the pressure transducer, and the ultra-sonic readings. All the graphs displayed similar results to Figure 4.5, where the curve followed the same trend as the

calibrated model. However, the curves of the pressure transducer and ultra-sonic were displaced lower, which could be attributed to any losses in the pipe. The laboratory flowmeter is installed in a pipe on the ceiling and takes 90 degree bends before water is released. It did not make a difference whether the flow rate was increased incrementally or varied sporadically. (See Appendix D, Figure D.1-D.7 for all laboratory tests.)

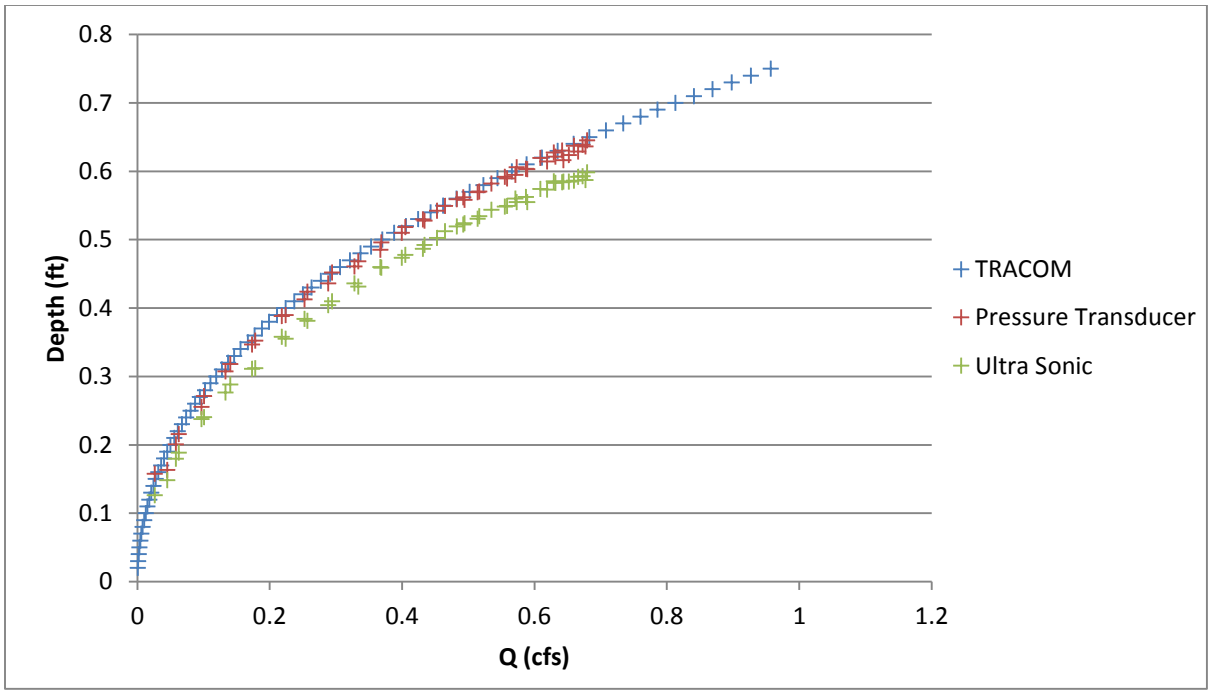

Figure 4.5 H-flume Testing: Increasing Flows Incrementally

An analysis was conducted on the H-flume laboratory results to provide further confidence in the manufacturer's calibration. The root mean square error (RMSE) is used in this analysis to measure the best fit between the laboratory results and the predicted model (i.e. TRACOM's calibration). The manufacturer's calibration included a data table for a head-discharge relationship (Appendix D, Figure D.8), but not a calibrated equation. The data was inputted into Minitab (a statistical software) to generate an equation for the relationship, $Q = 1.7H^{2.179}$, where Q is flow rate (cfs) and H is the head measurement (ft).

The log form of Q and H were computed, in order to create a linear regression of the calibrated data. The linear regression of the equation produced an R^2 value of 99.99% (Appendix D, Figure D.9) comparing to the manufacturer's data table. All data from laboratory tests were also log transformed and the results are compared to the calibrated curve in Figure 4.6. The graph displays that the test data resembles the linear regression and, particularly at larger flow rates, the data delineates the calibrated regression line. The graph indicates that there is a slight discrepancy at lower flow rates (where Log Q is less than -1.2) where there is a larger residual between the test data and manufacturer's calibrated data. This is when the laboratory tests were recording flow measurements lower than 0.06 cfs (0.017 m^3/s).

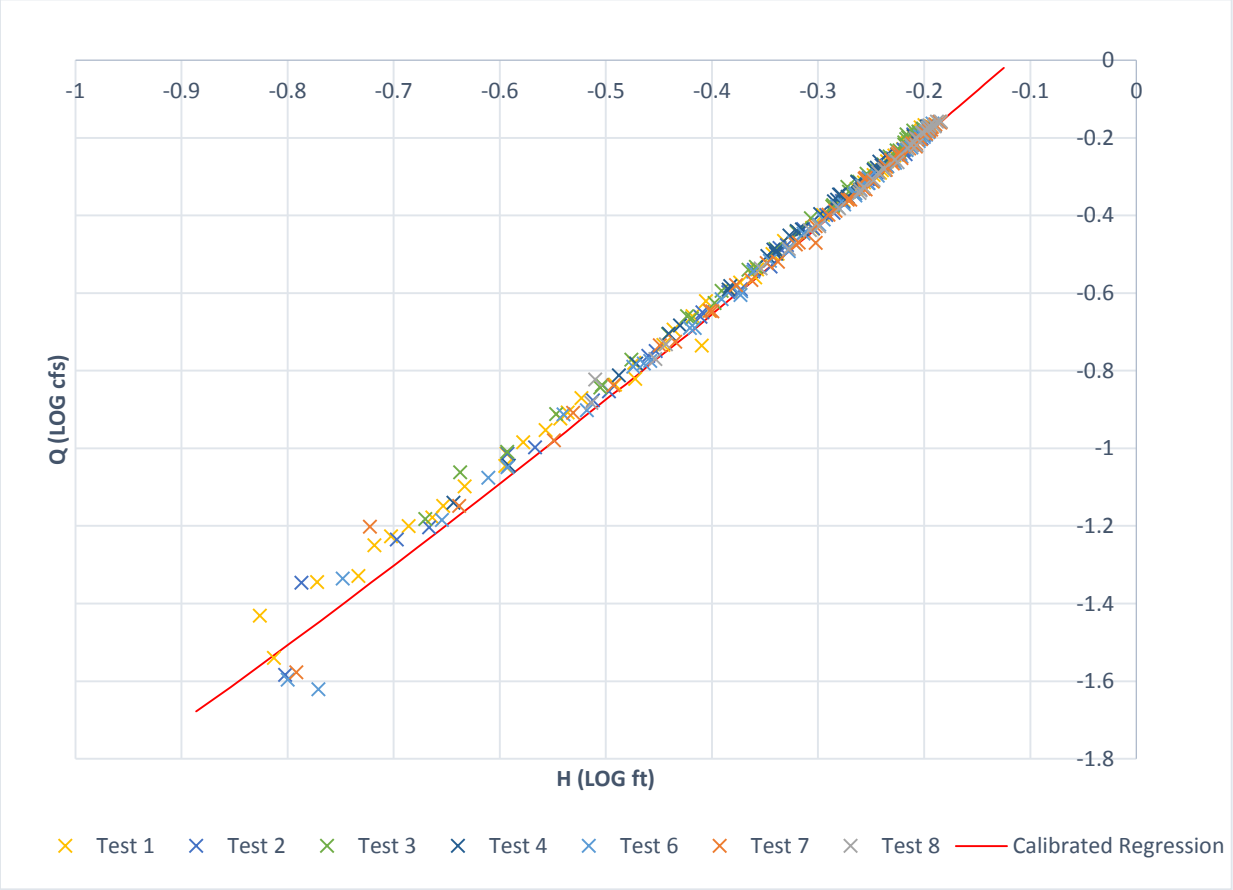

Figure 4.6 H-flume linear regression of manufacturer's calibrated data compared to laboratory tests.

Further analysis assessed the goodness of fit between the calibrated data and each laboratory tests. The RMSE was computed for each laboratory test in addition to the combination of all data sets, the results displayed in Table 4.1. The overall RMSE for combined data sets is 2.9%. Test 1 has the largest RMSE at 3.8% as a result of having the most measurements with flow rates under 0.06 cfs (0.017 m^3/s). The flowmeter for laboratory testing is located on a 4 in pipe upstream of the H-flume system, thus some of the overall error could be attributed to head loss. The RMSE was not influenced by the various laboratory test methods of increasing flow rates incrementally or varying the discharge, implementing further confidence in the manufacturer's calibration. The eight laboratory tests verified the H-flume's calibration and as a result the H-flume was installed in the field following the manufacturer's specifications.

Table 4.1 Root mean square error (RMSE) for laboratory test results.

Test	RMSE
1	3.8%
2	2.8%
3	3.2%
4	2.6%
5	2.4%
6	3.0%
7	2.7%
8	1.7%
All Test Data	2.9%

4.2. Selection of ADV flowmeter for Morris Leeds Tree Trench

The tree trench's inflow structure is an underground 8 in (20.3 cm) pipe that collects water from two green inlets (Figure 4.7) and discharges the water through the 8 in (20.3 cm) subsurface pipe into a perforated pipe in the rock bed (Figure 4.8). The green inlet (Figure 3.9, §3.3.2.1) has a filter bag that captures trash and coarse sediments before discharging water into the subsurface rock bed. An additional component of the green inlet is a trap door always that

remains closed in front of the subsurface pipe. The green inlet design permits water to enter the subsurface pipe via a rectangular opening beneath the trap door creating a sump (Appendix C, Figure C.2). The design is problematic for monitoring equipment involving a hydraulic structure (i.e. V-notch weir within the pipe) because due to the green inlet sump configuration it is not possible to install such a structure. A Thel-mar weir was also considered, but there was fear that it would get flushed into the pipe during a big storm event, or drowned through backwater. Therefore, an acoustic Doppler velocimeter (ADV) flowmeter was the best option because of its low intrusiveness and ease of installation with the green inlet design.

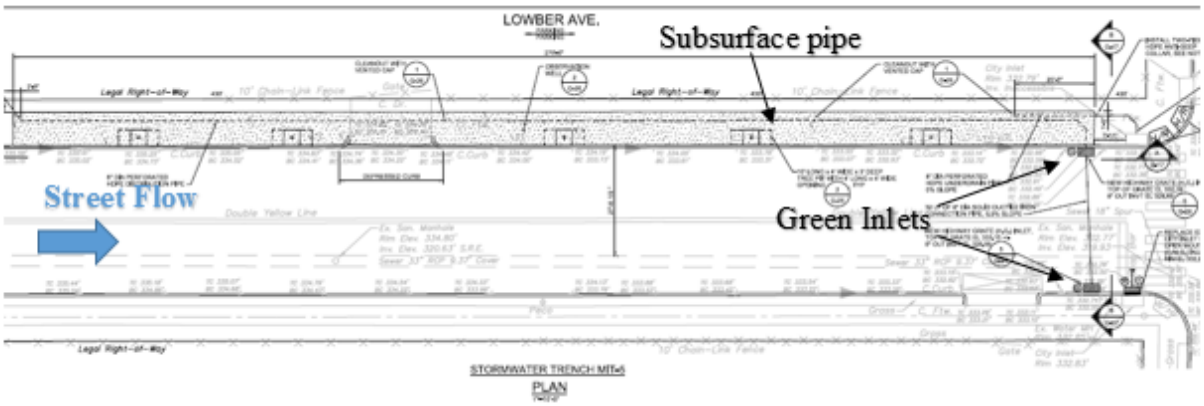

Figure 4.7 Overview of Morris Leeds site, depicts location of green inlets. Engineer drawings provided by PWD.

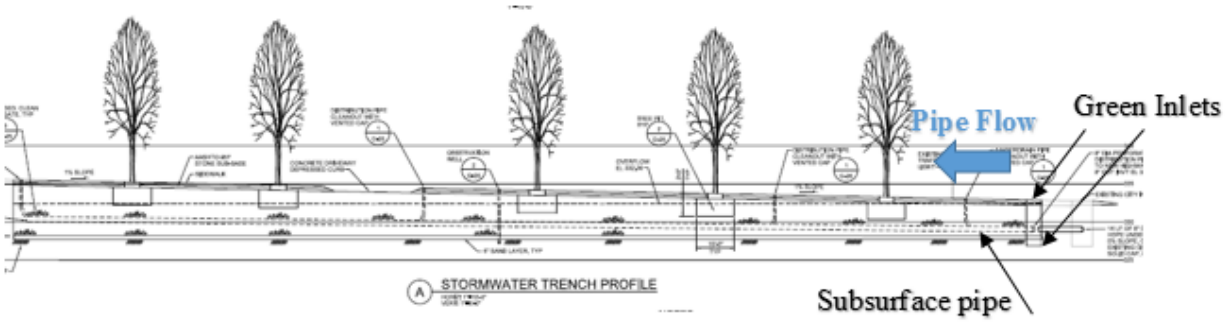

Figure 4.8 Side view of Morris Leeds site, depicts the subsurface pipe that flows through the rock bed beneath the five tree pits. Engineer drawings provided by PWD

The selected ADV sensor was the FloWav PSA-AV, which operates by indirectly measuring flow rates following Equation 1 (§2.2.2.1) by simultaneously taking measurements from a pressure transducer and a continuous acoustic wave Doppler sensor. The Flo-Wav was selected over other ADV sensors because of the manufacturer specifications, and the ability to operate without a proprietary data logger. The stated accuracy for the depth sensor is +/- 1% and the velocity sensor is +/-2%. According to the manufacturer specifications, the pressure transducer measures water depth ranging from 0-15 ft (0-4.57 m) and the Doppler sensor measures velocity ranging from -5 to 20 ft/s (-1.52 to 6.10 m/s).

There are several specifications, identified in literature and discovered through laboratory testing, that the ADV sensor is contingent on for proper operation. Regarding the pressure transducer, levels cannot be measured beneath 0.4 in (10.2 cm), resulting in a deadband. (Deadband refers to the point where the sensor cannot make a reading.) Therefore, depth measurements are recorded as 0 if the water level is lower than 0.4 in (1 cm). The velocity sensor functions under a Doppler shift (discussed via §2.2.2.1) where the Doppler signal analyzes echoes of suspended particles in water. The operation of the velocity sensor requires a minimum water depth of 0.9 in (2.29 cm), which is the sensor's height (Figure 4.9). As stated in the manufacturer's specifications, the velocity sensor needs to be underwater in order to obtain readings. As with all sensors in this class, the depth requirement impacts the measurements for lower flow rates. In previous installations the researchers have artificially created a backwater simulation to enable lower depth readings, but that was not possible at this site.

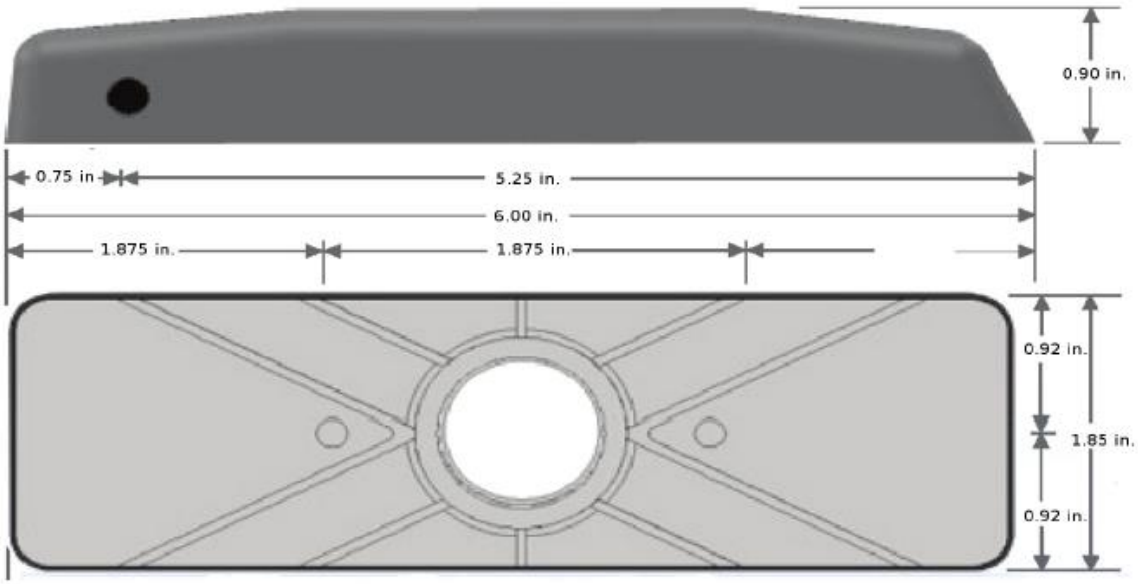

Figure 4.9 Dimensions of the ADV sensor (FloWav 2015).

Three ADV sensors were purchased for the project and in order to expedite data collection, two were immediately installed in the field (in the subsurface pipe downstream of each green inlet) and one was used for laboratory testing (to confirm accuracy and functionality). The intention for application in the field was to be integrated with several other field sensors via a custom datalogging system. A series of laboratory tests were performed to focus on ways to calibrate the ADV sensor for lower range flows, which was unfortunately problematic.

4.2.1 Laboratory Testing

Laboratory testing was conducted to understand how the ADV operates and to verify its accuracy. The testing took place at Villanova University's fluids laboratory utilizing the existing flume and flow meter (Toshiba Electromagnetic Flowmeter LF434 Series) over June 2015 to March 2016. The initial laboratory tests were conducted using an Arduino datalogging system that is similar to what would be used in the field. The Arduino system was not set to adjust the ADV sensor's outputs, but just simply collect and record the raw outputted data.

It was discovered post-laboratory tests and field installation that the ADV sensor has a corresponding datalogger that has numerous settings that creates a unique relationship to accurately record flow. It was also revealed that the sensor has a learning software that records more accurate measurements after approximately 100 readings (Craig Moody, personal communication, April 8, 2016) and utilizes prerecorded readings to acclimate to the hydraulic environment. What was not understood from the manufacturer's literature was that instrument velocity ranges and data table were set within the sensor and not the datalogger. This unfortunately prejudiced the test results.

The tests have been inconclusive about its potential for high accuracy measurement at the limits of its operating range and further investigations are required as part of future work. Current laboratory testing (i.e. April 2016) involve the ADV sensor and the FW-33 DCL (Direct Connect Datalogger manufactured by FloWav) are underway. Initial velocity results are promising, but beyond the scope of this thesis.

The main specification was that in order for the velocity sensor to operate, the sensor had to be completely submerged [0.9 in (2.29 cm); Figure 4.9]. Also, as with all similar sensors, there could not be any blockage with range of the acoustic Doppler signal (usually about 4-10 times the pipe diameter). These constraints were accounted for in the testing. The laboratory tests were conducted under the assumption that the FloWav's outputs would be the same regardless of the datalogging method. A separate Arduino team was involved in developing the custom datalogging system, however, they had minimal background in hydrologic studies. There were difficulties in communication between the Arduino team, manufacturer, and hydrologic studies and as a result misunderstandings contributed to the laboratory tests and initial interpretations of the sensor's functionality. Unfortunately, the base settings on the sensor

were not adjusted to the project flow conditions, which impacted the quality of the testing results.

Therefore, the analysis of this ADV sensor is a qualitative approach on the various tests conducted at an attempt to address the sensor's errors and understand its functionality. The laboratory was important as it did identify the challenge and the lessons learned will drive future testing procedures. Over 25 tests were conducted, but only a sampling are published in this report.

4.2.1.1 Installation

The laboratory set up was constructed to imitate the field conditions at Morris Leeds. A 6 ft (1.83 m) long 8 in (20.3 cm) PVC pipe was bolted to a piece of plywood with flanges and a rubber gasket (Figure 4.10a). The plywood served as a barrier so that water only enters via the 8 in (20.3 cm) pipe. The rubber gasket is placed between the plywood and flanges and prevents leaking. The plywood with the 8 in (20.3 cm) pipe connection was bolted within the flume and sealed with caulk to minimize any leakage. The final set up consisted of water entering the flume upstream of the 8 in (20.3 cm) pipe (Figure 4.10b). The upstream section imitated an inlet where water gathers, raises and then enters the stormwater pipe.

Figure 4.10 ADV sensor laboratory set up; (a) Laboratory set up of the 8 in (20.3 cm) PVC pipe connected to flanges and plywood barrier looking upstream. (b) Laboratory basin looking downstream into the 8 in (20.3 cm) PVC pipe.

The ADV sensor was installed into the 8 in (20.3 cm) PVC pipe with a provided mounting band, similar to the field installation. The ADV sensor's mounting band is a spreader that expands to the diameter of the pipe by tightening the top wing nuts. The sensor gets screwed into the bottom of the mounting band. The ADV sensor and mounting apparatus were placed as far back as possible with one's arm length. It was situated in the pipe's bottom center with the Doppler sensor facing the approaching flow (Figure 4.11).

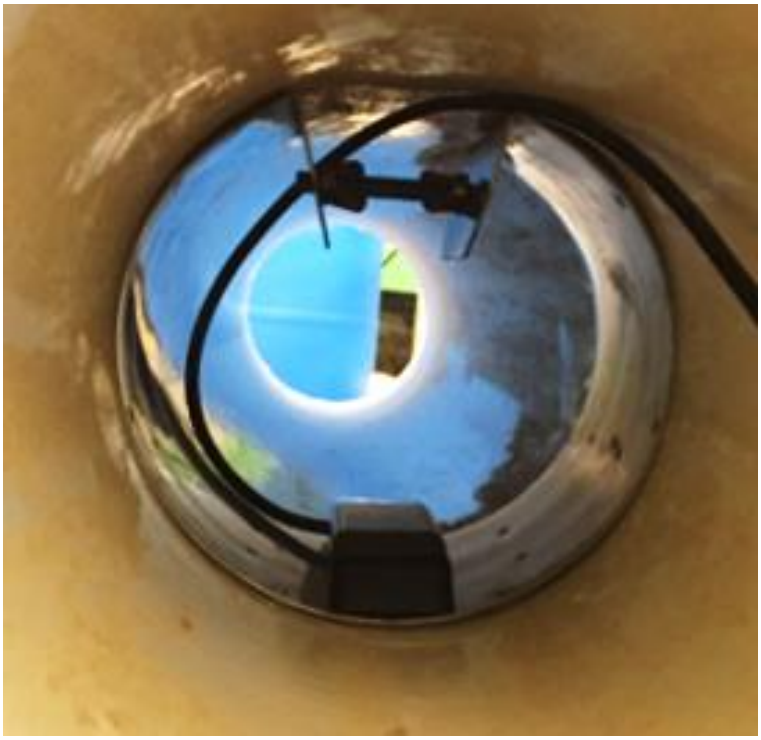

Figure 4.11 ADV sensor installed in 8 in (20.3 cm) PVC pipe testing apparatus with mounting band.

4.2.1.2 Methodology & Results

The initial tests for the ADV sensor were similar to the H-flume (§4.1.1.3). Flow rates were increased and decreased systematically on a 2 min interval, always ensuring that there was at least 1 in (2.5 cm) of water depth. Flow rates were being simultaneously recorded by the existing laboratory flowmeter and ADV sensor. Flow rate readings were taken every 15 seconds and averaged over the span of 1 minute. The results compared the averaged flow rates between the two sensors.

A total of six tests were completed analyzing low flows, constant flows, and a range of flows (e.g. Figure 4.12). The ADV sensor results were inconsistent with the laboratory flowmeter's readings. For some tests the output shows that the ADV sensor followed a similar pattern of increasing and decreasing flows, but the magnitude was higher than the laboratory

flowmeter's recordings. Other tests though outputted constant readings while the flow was varied. No test was able to be replicated, which could be attributed to the learning software within the sensor, which was not known at the time and in hindsight should have been disabled during experimentations.

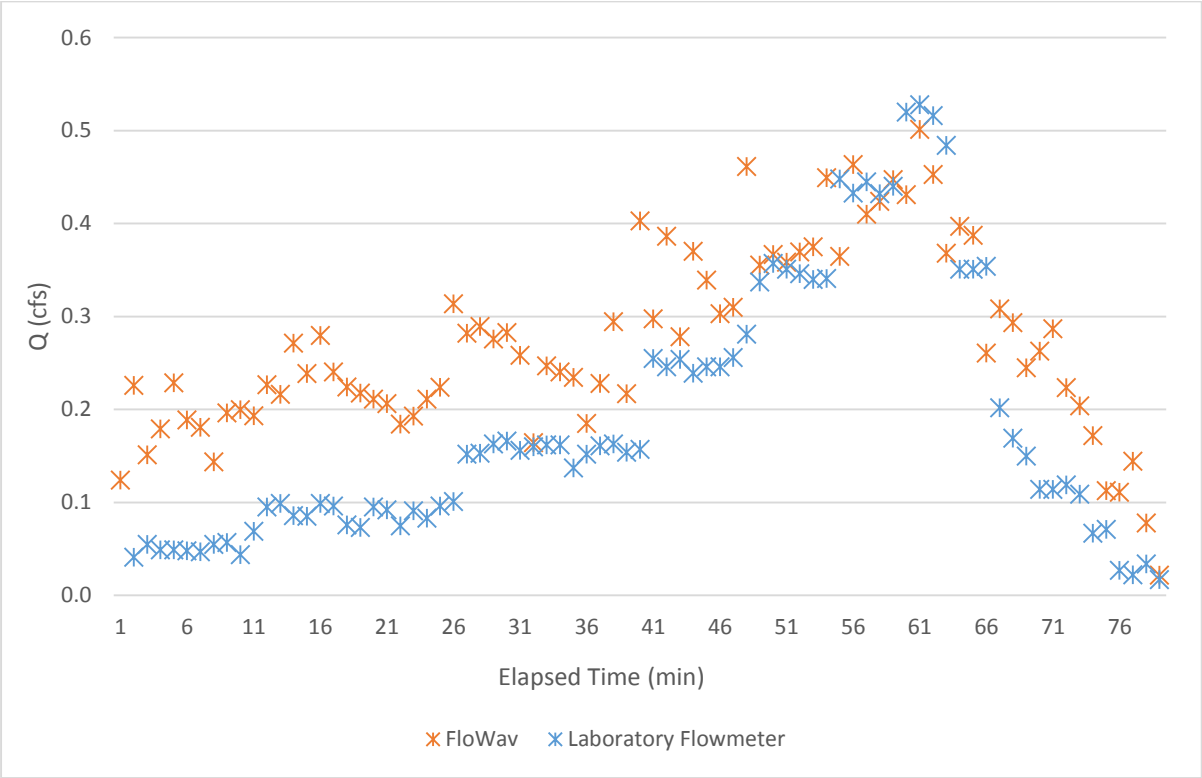

Figure 4.12 An example of the ADV sensor comparison test for full range of flows by incrementally increasing and decreasing flow rates.

4.2.1.3 Troubleshooting Laboratory Problems

All the laboratory tests results produced by the ADV sensor were generally higher than the laboratory flowmeter (e.g. Figure 4.12). Note that for higher flows after multiple readings, the results seem more in line. One study, conducted at Virginia Tech, compared three Acoustic Doppler Velocimeters (ISCO, FloWav, and Nortek) and found that overall FloWav had the highest flow rates as well as the greatest discrepancy of standard deviation for velocity measurements which gave a range that varied between 0.1 (0.03 m/s) and 0.28 ft/s (0.085 m/s)

outside of the actual measurements (Aguilar et al. 2015). The Virginia Tech study found that the flow rates were reasonable and within the specified 2% accuracy. However, that was not the case in this laboratory testing as recorded flow rates were greater than the observed laboratory flowmeter readings by a much greater deviation. For example, at time 2:47 the flowmeter measured a flow rate of 0.101 cfs (0.0029 m^3/s) and the ADV sensor measured 0.31 cfs (0.0089 m^3/s), which is a magnitude three times greater than the actual flow (Figure 4.12). There are instances on the graph where the ADV sensor measurements are accurate, such as at time 3:20 the laboratory flowmeter measures 0.44 cfs (0.0124 m^3/s) and the ADV sensor outputs 0.45 cfs (0.0127 m^3/s) which is within 2% accuracy (Figure 4.12). However, there are far fewer accurate measurements than inaccurate measurements. In fact, 72% of the test results in Figure 4.12 has a percent error of 25% or more. (62% of the test results had an error greater than 50%, and 41% of the test results had a percent error larger than 100%.) Many measurements were several magnitudes higher than laboratory's flowmeter and as a result the average percent error is over 103%. Since the flow rate is indirectly determined by the depth and velocity sensors, troubleshooting the laboratory problems had to address both the depth sensor and the velocity sensor. It was unclear which sensor was outputting faulty results, if it was a combination of either sensors, or whether any internal settings adjusted the sensor's readings.

4.2.1.3.1 Downstream block

The manufacturer instructed that the ADV sensor had to be covered in water [minimum 0.9 in (2.29 cm)] in order to trigger the velocity sensor. Therefore, a 3 in (7.62 cm) block was installed downstream to guarantee that the ADV sensor will always be submerged by a minimum of 3 in (7.62 cm), well above the manufacturer's recommendation (Figure 4.13).

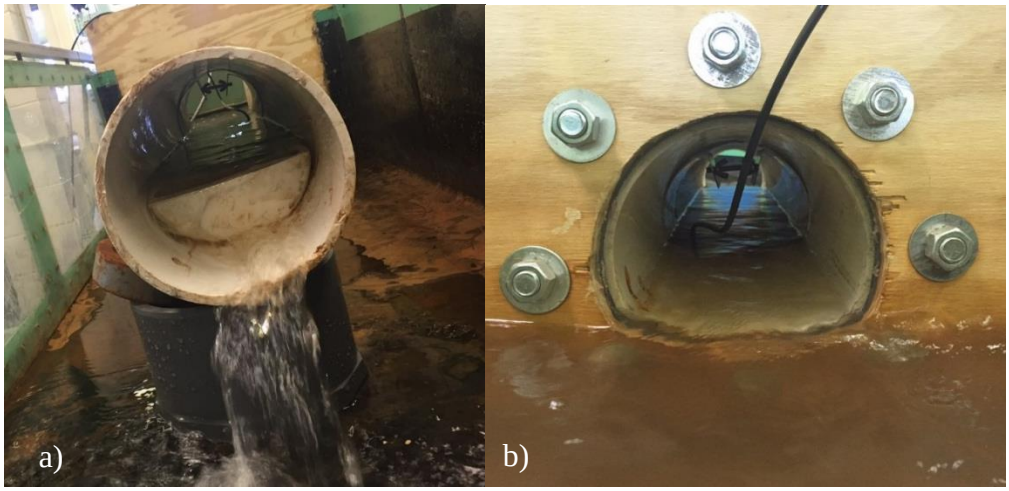

Figure 4.13 Downstream 3 in (7.62 cm) block to create sensor submergenc;. (a) view from downstream of the 3 in (7.62 cm) wedge, (b) view from upstream of the submerged ADV sensor.

As the test was conducted, manual depth measurements were taken with a tape measure to validate the pressure transducer readings. The manual measurements matched the ADV sensor's depth output, and thus concluded that the depth sensor was not the root of the flow rate problem. The flow rate readings with the downstream block (Figure 4.14) showed similar results to previous tests where the ADV sensor tracked the increasing and decreasing flow rates at a higher magnitude.

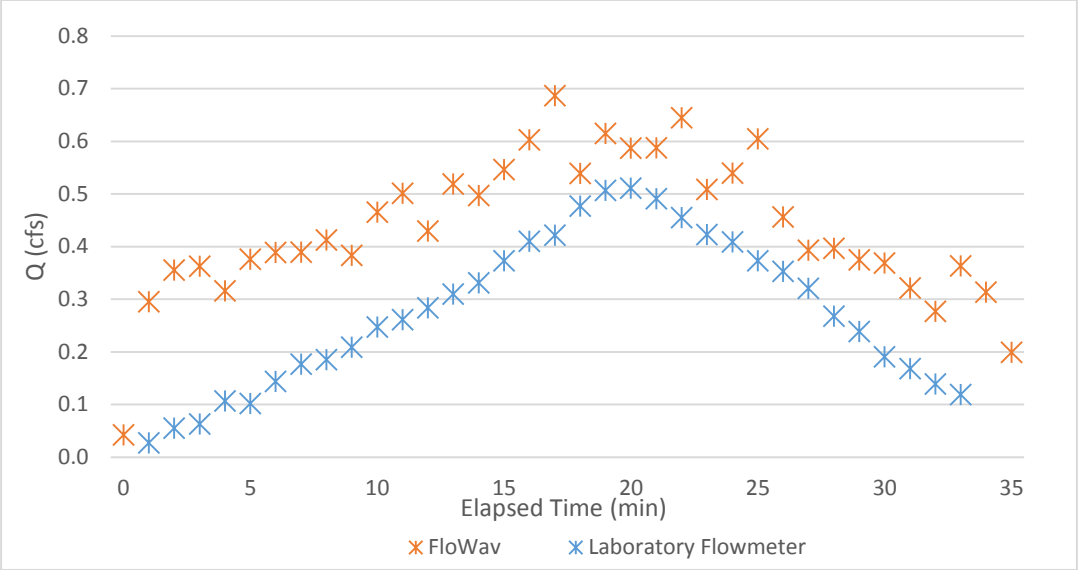

Figure 4.14 Flow rate results of the ADV sensor test with downstream block.

Since the manual measurements confirmed the ADV sensor's depth readings, the inaccurate flow rates were attributed to the Doppler velocity sensor.

4.2.1.3.2 Adjusting Velocity Levels

The inconsistency in the ADV sensor's measurements were perplexing, especially since every test varied from one another. Therefore, the manufacturer was contacted for assistance with evaluating the Doppler sensor. Troubleshooting the velocity sensor was more difficult since it could not be checked with manual measurements. The manufacturer specifies that there are four levels of velocity settings (i.e. in this case): level 2, level 3, level 4, and level 5. On January 11, 2016, a consultant explained the differences between the four levels (Ashley Smart, personal communication, January 11, 2016). Level 2 is used for lower ranges of flow and level 4 is intended for higher ranges with level 3 somewhere in the middle. Level 5 is intended for sewer systems with constant flushes of flow. The consultant also explained that the ADV sensor is a self-learning device and over time adapts to its environment with more accurate readings. For this reason, the consultant stressed the importance of resetting the DV (Doppler Velocity) table

within the datalogging system, which effectively resets the ADV sensor to not be influenced by previously learned data. This information was critical for laboratory testing, as the tests varied from one another, although it was learned after many tests were performed. The Arduino datalogging system did not reset the DV table for the previous laboratory experiments, which explains some of the inaccuracies.

Further consultation with the manufacturer indicated that the ADV sensor begins to adjust its software after approximately 100 readings (Craig Moody, personal communication, April 8, 2016), but the installed field sensors take measurements on a 5 minute interval. Therefore, 100 readings at a 5 minute interval will take 500 minutes (8.3 hours). The learning software capabilities were not discovered until after these laboratory experiments (April 8, 2016), as the team thought this was a function of the datalogger, and not the sensor itself. Tests were conducted for each velocity level (2, 3, 4, and 5). Unfortunately, testing was taking longer than anticipated and over winter break (early January 2016) a power outage caused the existing laboratory flowmeter to break. Therefore, the continued testing had to change flowmeters from the Toshiba Electromagnetic Flowmeter LF434 Series to an IFM (inductive flowmeter). The IFM measures lower flow rates and as a result, the following tests entailed a constant low flow of 8 gpm (30.3 L/min) at each velocity level. Applying a constant flow rate could demonstrate the device's self-learning capabilities (e.g. the time to self-learn and accuracy of each velocity level).

It was necessary to test the IFM flowmeter in order to cover all potential sources of error. Therefore, manual measurements were taken with a 5 gallon (18.9 L) bucket and a stopwatch over seven iterations and compared to the flowmeter's output to confirm the IFM's readings. The manual measurements were taken at lower flow rates since low flows had the greatest

discrepancy and also because the bucket filled up too quickly at high flow rates. The manual measurements and recorded measurements coordinated with one another (Table 4.2), therefore it was concluded that the error's source was not the IFM flowmeter.

Table 4.2 Verification of laboratory flowmeter. Low flows comparison between the laboratory's flowmeter and manual measurements taken with bucket and stopwatch.

Laboratory Flowmeter (gpm)	Manual Bucket Measurement (gpm)	% Error
8.09	8.18	1.13
12.05	11.11	7.79
8.04	8.34	3.76
7.98	7.35	7.86
7.97	7.94	0.42
8.06	7.74	3.93
7.94	7.79	1.86

Additional tests were conducted on the ADV sensor and varied the different velocity levels. Unfortunately, adjusting the velocity levels proved to have no significant impact on the recorded flow rates. At the time there was no knowledge of how to reset the learning system, nor of averaging techiniques that could be employed. The recorded flow rates were not constant, varied significantly within each test, and were all larger than the IFM output (Figure 4.15).

Overall, the experiments and consultations demonstrated that a more advanced analysis and an in-depth knowledge of the sensor intricacies was required to demonstrate that the product can be used for research grade low flow monitoring at the limits of its capabilities. As the results were not performing to the manufacturer's specifications in the laboratory, the equipment was removed from the field. It is unfortunate as that more recent test have provided promising when measuring velocity.

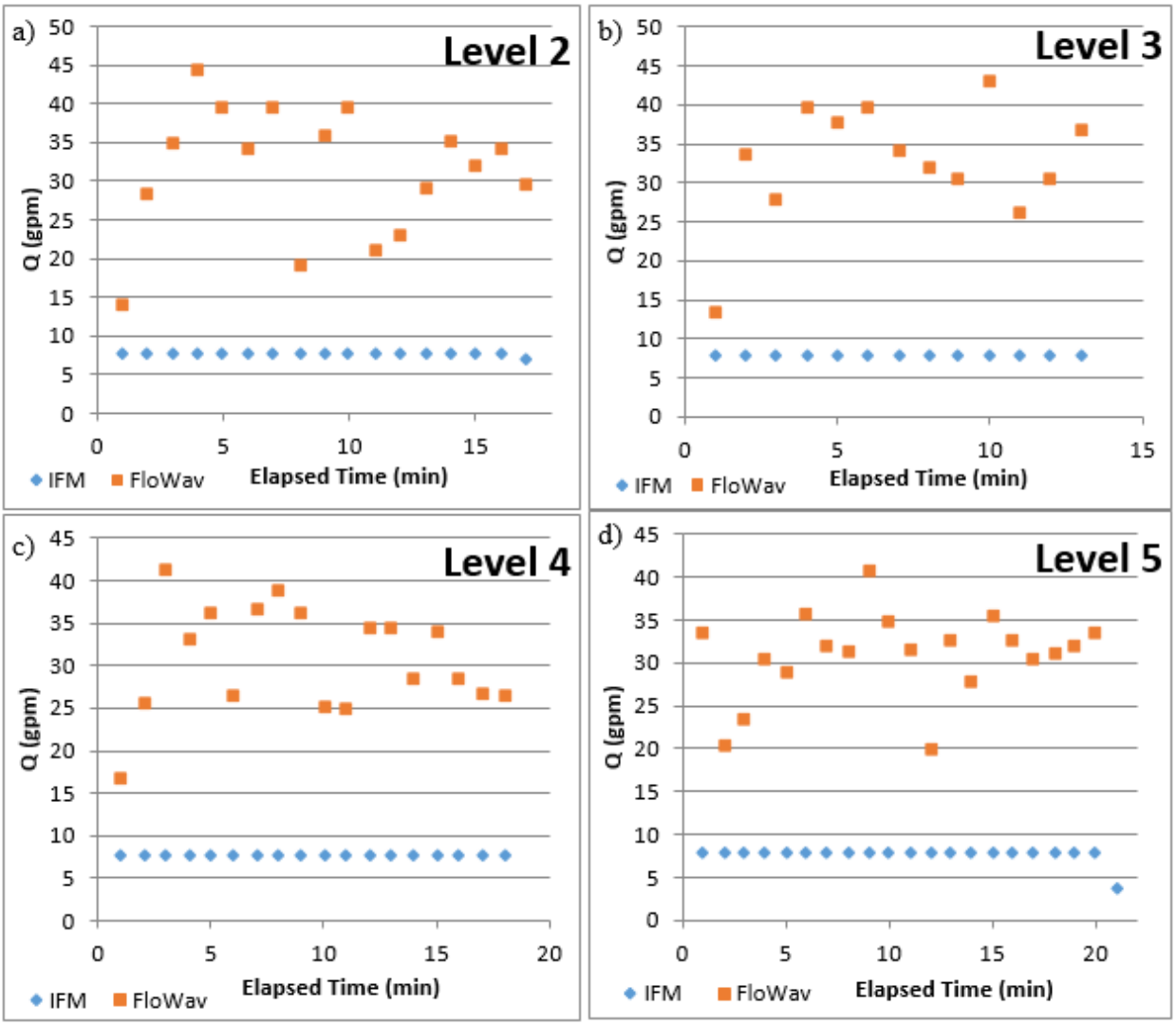

Figure 4.15 Flo-Wav tests with adjusting velocity levels; (a) Level 2, (b) Level 3, (c) Level 4, and (d) Level 5

4.2.2 Field Observations

Field data was collected and evaluated at the same time as the laboratory testing. Figure 4.16 is an example of data series from a storm event on October 28, 2015 to October 29, 2015. The field data appears reasonable in terms of magnitude, but the results have not been verified through modeling and are not confirmed by the laboratory testing. It appears as if a pattern occurs with increasing and decreasing flow rates over three iterations that could be due to rainfall

patterns. The zero results indicate where there was missing data, which could be attributed to no rainfall, or the deadband of the velocity sensor [depths below 0.9 in (2.3 cm)]. This demonstrates the need to merge modeled and measured data for the sensor.

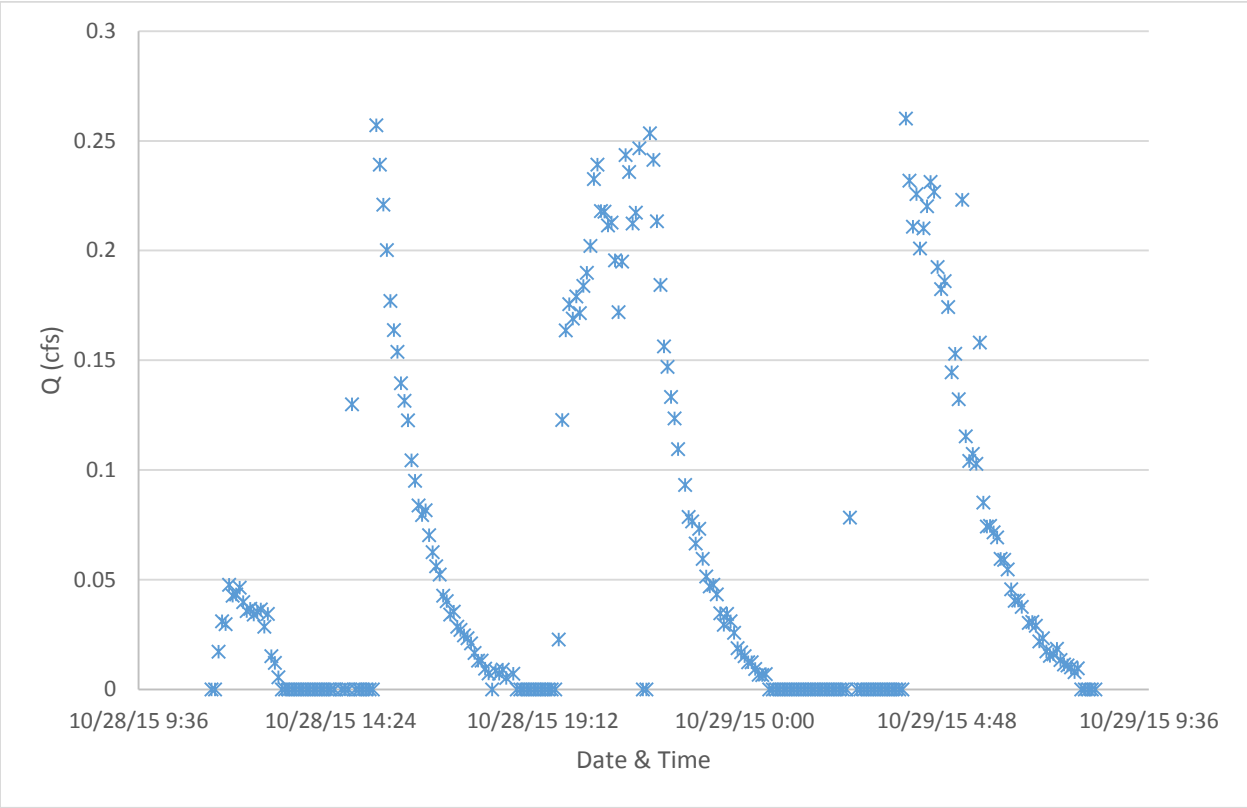

Figure 4.16 Collected field data of ADV sensor from end of October 28, 20150 to October 29, 2015

4.2.2.1. Maintenance

A valuable lesson from the field data was that, it provided observations about the site's functionality. One observation that differed from laboratory testing was that the velocity measurements outputted zero during a storm event. The discovery was made in the December 2015 data collection, approximately 7 months after the ADV sensor has been installed (May 2015). The zero velocity readings differ in this situation than the previous October field data because depth measurements were above the deadband output. The pressure transducer was

recording water level data at 8 in (20.3 cm) of depth indicating a full pipe. The pipe was filling up with water but velocity was being recorded as 0 fps. The recordings suggested one of two things: there could be a blockage downstream in the pipe causing water to fill up with minimal flow that is too minuscule to trigger the ADV sensor, or something was blocking the sensor and disrupting the Doppler signal. The best method of addressing these issues was by a field investigation during maintenance.

The urban environment certainly impacts the site's performance with trash, debris, sedimentation, etc. and this also affects monitoring equipment's performance. Figure 4.17a displays the ADV sensor's condition after being installed in the underground pipe for 9 months. The device had a piece of cloth attached to its wire that was hanging directly in front of the Doppler sensor. Figure 4.17b also displays the amount of sedimentation that was covering the ADV sensor. The debris disrupts the ultrasonic signal causing inaccurate readings of the system.

Figure 4.17 ADV sensor's conditions after nine months of installation; (a) piece of cloth blocking the sensor's signal, (b) covered by a layer of sedimentation sludge.

Maintenance is necessary for an SCM's effective performance and longer lifespan. The tree trench site is maintained once a month where debris and sediment are cleaned out of the filter bags. Additionally, once a year the underground pipe is cleaned out and the debris and sediment is blown out of the pipes (Figure 4.18). Prior to this maintenance, a camera is inserted into a cleanout and pushed through the pipe to capture the sedimentation and debris. Typically the camera reaches the inlet to record everything that was flushed into the system. During this process, the camera was stopped part way through and was unable to reach the inlet. The results indicated that there was a blockage downstream in the pipe.

Figure 4.18 Maintenance of Morris Leeds Tree Trench site with (a) cleaning of underground pipe and (b) the cleaned out filter bag.

The obstruction downstream suggests that the system is clogged and the site's functionality is disrupted. Even small storm events could cause the pipe and inlets to fill up under low flow conditions. The Doppler sensor may not be able to record low flow rates under

full pipe flow because the velocity may be too low for the sensor's accuracy with the associated depth. The custom datalogger system was required to insert the pipe diameter for a register as part of the communication via Arduino to sensor. Therefore, the ADV sensor recognizes the pipe's diameter and may not be capable of recording low velocities that are associated with high depth measurements. The field results suggested that the ADV sensor is unable to perform adequately and further laboratory tests were conducted to simulate this situation.

4.2.3 ADV Sensor Findings

The backup sensor was tested under similar conditions to determine if only one sensor was defective or if inaccurate data was a continuous problem in all the purchased sensors. The laboratory results concluded that all the sensors were problematic. The manufacturer was contacted about the inaccuracies and recommended returning the sensors for a software update. There was a known software error and the sensors required an update. As a result, the ADV sensor was removed from the field and all three sensors were sent back to the manufacturer for software updates. The inability to achieve the required accuracy stresses the importance of testing monitoring equipment in laboratory conditions to confirm the sensor's calibration in the designated research application.

It was discovered in spring 2016 that the ADV sensor has a datalogger counterpart (FW-33 DCL) that operates under specific settings. The updated sensor and its corresponding datalogger were tested to try to understand how the instrument operates. The results displayed in Figure 4.19 show the velocity and depth recordings of ADV sensor's datalogger of an example site on a blue roof in Philadelphia. The system recorded depths at 0.4 in (1.02 cm) and above, illustrating that the sensor needs to be at least halfway submerged in water to acquire depth readings. Velocity readings could not be recorded beneath 0.5 fps (0.152 m/s) due to erroneous

user settings. Even though the sensor was recording depth measurements from 0.4 to 0.75 in (1.02 to 1.91 cm), flow rates could not be calculated due to this user error. However it does demonstrate the importance of understanding the sensor system, and is setting the stage for possible future testing.

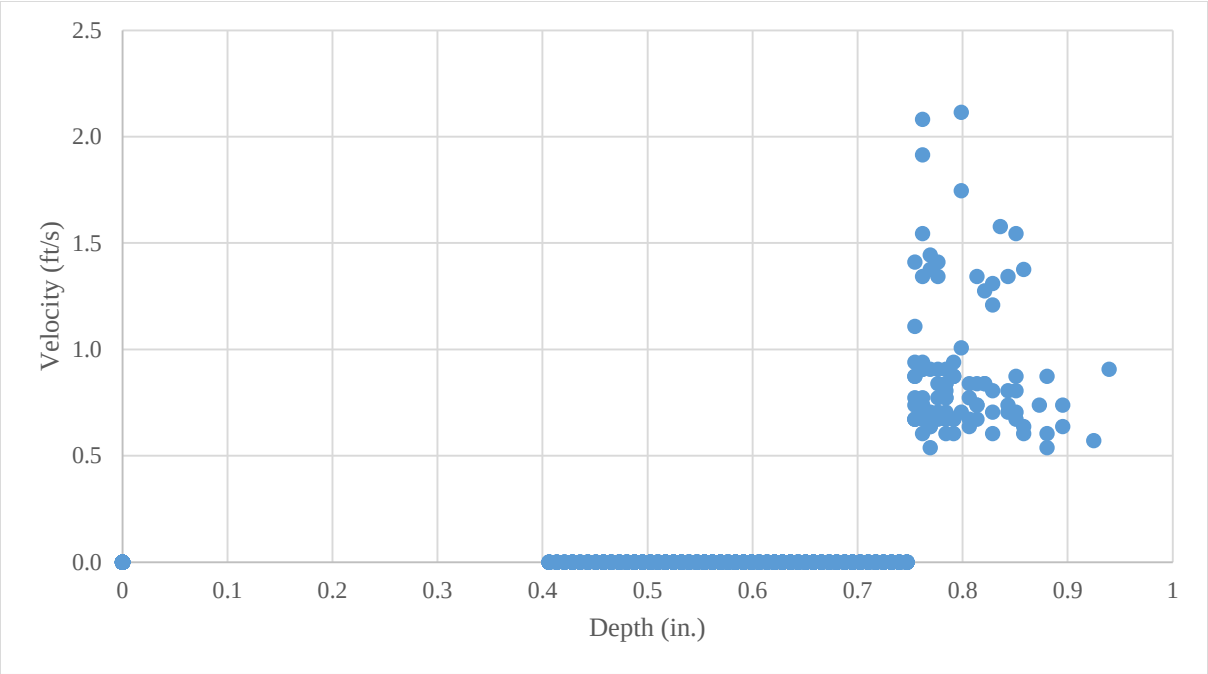

Figure 4.19 Results of Flo-Wav's sensor and corresponding datalogger as an example from a blue roof site in Philadelphia.

Field instrumentation in a street inlet poses challenges with installation, data collection, and battery life. The custom Arduino datalogging system was originally selected because it could eventually be integrated into a larger system with one central downloading location. Ultimately the system could potentially be linked to WiFi causing easy accessibility for data collection. Additionally, the system is substantially cheaper than other datalogging systems and requires less battery power. The current custom Arduino datalogging system (Figure 4.20a) is mounted to the side of the green inlet in a water tight box [~12 in (30.5 cm) x 9 in (22.9 cm) x 4

in (10.2 cm)] (Figure 4.20b). For comparison, the enclosure for the ADV sensor datalogging system (including battery) has a diameter of 4.5 in (11.4 cm) with a 15.4 in (39.1 cm) length (Figure 4.21).

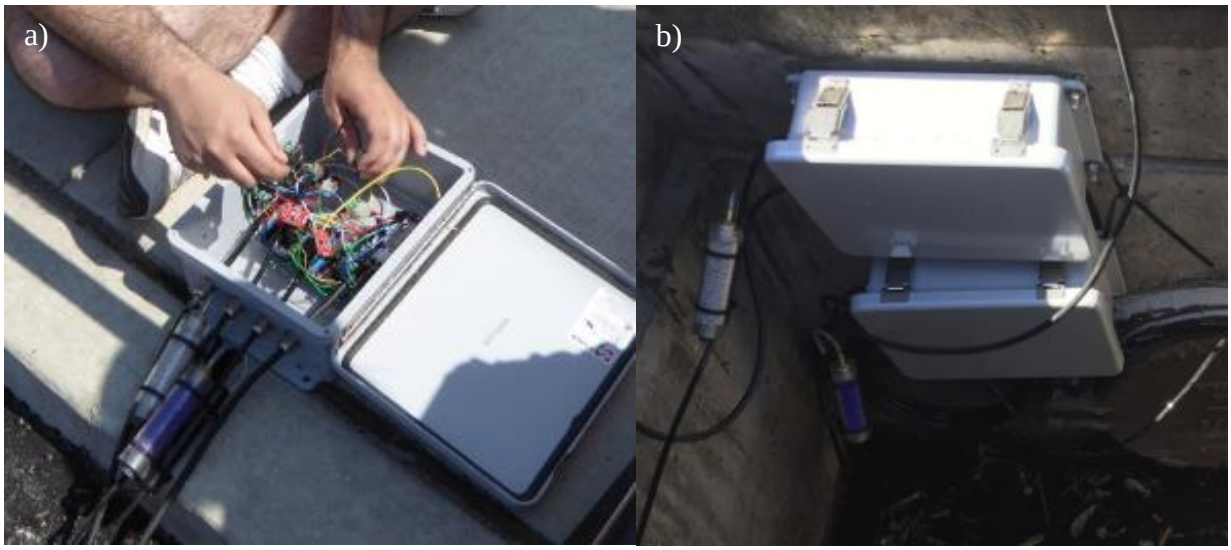

Figure 4.20 Installation of custom Arduino datalogging system; (a) Arduino system inside water tight box (b) Installed water tight box anchored inside the green inlet

Figure 4.21 FloWav FW-33 DCL (direct connect logger) with FloWav sensor attached (FloWav 2016).

If the FW-33 DCL is integrated into the Morris Leeds site, then new methods will need to be determined for mounting and installation with these dimensions. Additionally, the previous system's battery could be changed without opening the green inlet (a battery sack hung by one of the grate openings and one could simply pull the sack out to change the battery). Since the ADV sensor's datalogging system includes the battery in the enclosure, the green inlet will need to be open every time too change the battery. Battery life is also a concern because the battery will need to operate the datalogger and the ADV sensor on a 5 min interval. The battery installed for the ADV sensor's datalogging system is a 6V alkaline lantern battery. From experience at another Philadelphia site with the exact set up (FloWav PSA-AV sensor, 5 min interval recordings, FloWav's datalogger and battery), the battery had to be changed within 6 days. Lastly, data collection is an issue since the datalogger is a separate logging system from the remainder of the site. The ultimate goal was to have a central location to download all the site's data (e.g. weather station, soil moisture sensors, ADV sensor, etc.) with remote access via WiFi, but the FloWav's separate datalogging system prohibits the integration into a central datalogger.

4.2.4. ADV Sensor Summary

Although the accuracy of the field sensors has not yet been demonstrated in this environment, they still provided information about the site's functionality. The ADV sensor was installed in the field for approximately 9 months without any maintenance. Previously, the required maintenance frequency was unknown and sediment buildup was unpredictable. Sedimentation and debris was pushed beyond the filter bag affecting data measurements and the site's performance. Field conditions are very different from laboratory settings with the environmental and urban impacts. Field tests are necessary to understand the site's functionality under these unique conditions. Routine maintenance is necessary for the site, and additionally it

is essential to have more frequent maintenance where there is monitoring equipment to ensure accurate results.

It is also necessary to test monitoring equipment in a laboratory setting to understand how it operates. Further tests on the ADV sensor provided a deeper knowledge of the system's functionality that was not apparent in the literature. The manufacturer's specifications need to be evaluated rigorously at each measuring site's boundary condition or parameter settings (Bonakdari and Zinatizadeh 2011). On the contrary, not understanding how a sensor operates within a specific research application can evoke errors. Therefore, testing the sensor with the associated datalogger and having thorough discussions with the manufacturer is necessary to verify specifications and determine if ultimately the sensor is suitable.

Data processing capabilities play a significant role in data collection, and in laboratory testing. In hindsight, the data learning should have been inactivated during laboratory testing. More recent work is promising in meeting the velocity specifications. If data is only being recorded on a 5 min interval, then it may be a while until the ADV sensor meets the 100 readings quota. As a result, several simulations could be inaccurately recorded, and testing changes may have caused these challenges. Further laboratory investigations can address this ambiguity.

CHAPTER 5: Outflow Structure

5.1 OUTFLOW DESCRIPTION

The outflow structure for the Philadelphia Zoo Rain Garden is a domed riser located in the downstream rain garden (Figure 5.1b) that directs overflow into a rock basin located at the side of the rain garden. The domed riser is a 12 in (30.5 cm) SDR 35 PVC pipe sticking out of the ground with an iron dome on top of it (see Appendix B for specs, Figure B.3). The 12 in (30.5 cm) pipe abruptly reduces to an 8 in (20.3 cm) diameter (Figure 5.1a) and sits overtop an 8 in (20.3 cm) pipe. The 8 in (20.3 cm) pipe leads to the side trench beneath the parking lot (§3.1.1). The domed riser is used as an overflow when there is excessive ponding [i.e. more than 12 in (30.5 cm)]. The water is permitted through the dome and is filtered with a stormwater filter bag before it is discharged into the 8 in (20.3 cm) pipe.

Figure 5.1 Zoo Rain Garden's outflow structure: domed riser. (a) Riser's 12 in (30.5 cm) pipe reducing to 8 in (20.3 cm) pipe. (b) Riser with iron dome top.

The site was surveyed to determine the exact dimensions and elevations of the system. It was determined that the domed riser is approximately 1.25 ft (0.4 m) above the rain garden's lowest elevation point (see Appendix B, Figure B.4 for surveying data). The surveying also examined the elevations at the domed riser's cross section (Figure 5.2). The cross section only

has 12 in (30.5 cm) of ponding locally prior to water entering the overflow system. There is a 3 in (7.6 cm) height discrepancy between the rain garden's low point and domed riser's ground surface elevation because there is more soil atop the domed riser's surface which could be attributed to construction, maintenance, or topsoil being washed downstream. Figure 5.2 shows the ground level, the location of the riser, and the top of the riser. The dark blue area indicates the portion of the pipe that is exposed above the ground surface. Above the dark blue area is the domed casket which is where water will enter the overflow system. The pipe's length above ground is approximately 0.61 ft (0.19 m). Last thing to note are the top elevations at the edge of the rain garden's cross section. Past the domed riser, the rain garden only permits an extra 0.62 ft (0.19 m) of ponding. Past this height, the system overflows onto the sidewalk.

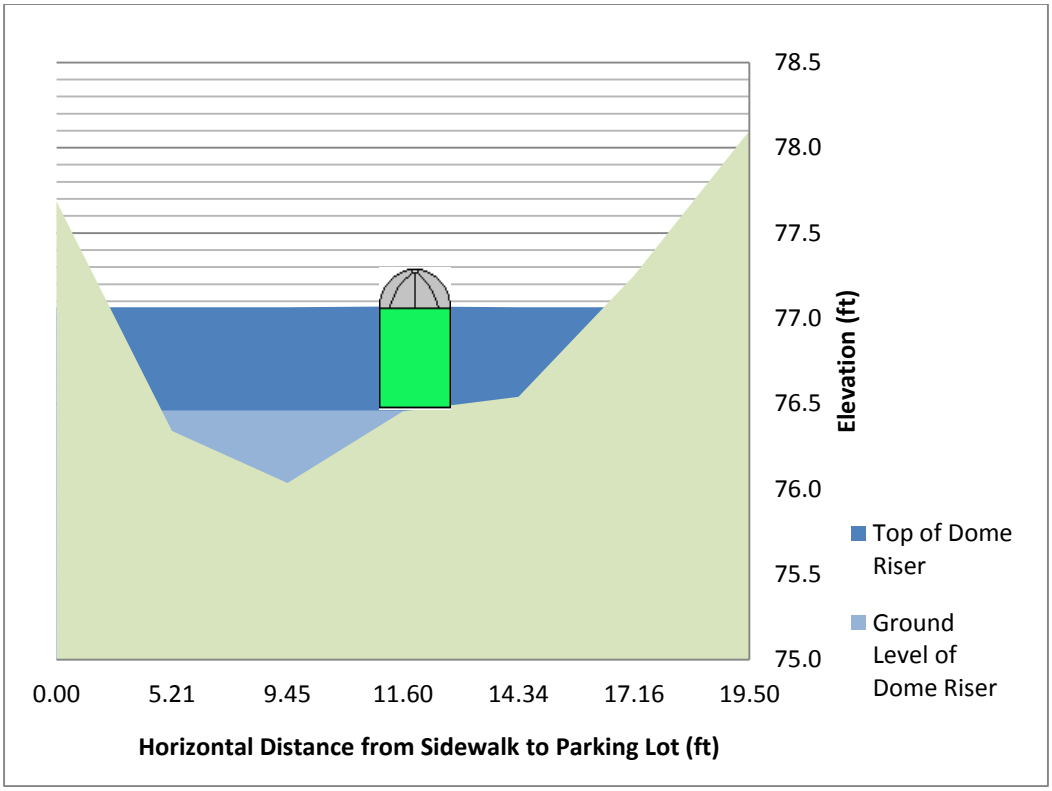

Figure 5.2 Domed riser cross section from surveying analysis. (Note domed riser NTS)

5.2 DOMED RISER LIMITATIONS

One of the difficulties with instrumenting the Zoo rain garden was determining the best method to monitor the overflow. The domed riser is a unique outlet structure with restricting dimensions. The instrument needs to measure a wide range of flows [0-0.5 cfs (0-0.014 m^3/s)]. The selected instrument cannot disrupt existing site conditions and installation cannot permanently alter the site. The initial two options were a flowmeter or a hydraulic structure. A flowmeter was concluded as inadequate for several reasons. It was difficult to find a sufficient flowmeter that complies with all the requirements. Additionally, it was challenging to find a flowmeter that will operate in field conditions with power constrictions. Last, flowmeters are expensive compared to other monitoring techniques like hydraulic structures.

An orifice plate would not be sufficient in this situation. A small orifice hole will record lower ranged flows but will also constrict the flow. There is not enough available head in the system to record the high flows. The smaller orifice can also disrupt the natural flow and cause the system to flood. A larger orifice hole will not adversely disrupt the flow, however, it will not capture the lower flows. Therefore, an orifice plate was determined to be inefficient. Another hydraulic structure for the overflow could be a V-notch weir box that would sit over the domed riser. The V-notch weir box has the same issues as the orifice plate regarding head limitations. One advantage is the V-notch weir box could capture a larger range of flows than the orifice plates. However, a disadvantage is that it is aesthetically unappealing and may not operate properly with trash and excessive sedimentation

There were many monitoring limitations with the overflow structure due to size and the range of flow rates. Existing market items were not appropriate for the design at a reasonable price. This presented an opportunity for innovation with developing a new monitoring device.

5.3 INITIAL PROTOTYPE DESIGNS

A new design was desired for the domed riser. The goals were to implement a device that can measure flow rates up to 0.5 cfs (0.014 m^3/s) and is installed within the domed riser. A rating curve had to be developed with the associated instrument based on laboratory experiments. Inspiration for the final device came from consultations with professors Dr. Robert Traver and Dr. Bridget Wadzuk among two case studies.

5.3.1 Prototype A – Orifice Meter

The first approach was analyzing the use of an orifice meter that was designed in the Auckland, New Zealand study (§Ch 2.2.3.1). The case study self-designed an orifice restricted device (ORD) that measures low flows from a green roof. Calibration of submerged orifices require measurements of depth for the full range of expected flow rates against a standard control, or more precise measuring device (USBR 2001). Based on the hydraulic principle, the orifice equation is:

$$Q = C_d A (2gH)^{0.5} \qquad \text{(Equation 3)}$$

where:

- Q = discharge
- g = acceleration caused by gravity
- H = head differential
- A = the area of the orifice
- C_d = coefficient of discharge (Sturm 2010)

The initial prototype imitated the concept of the ORD. Initially, the design was a graduated cylinder with orifice holes increasing in size at increasing heights. Since the zoo rain garden experiences higher flow rates, modifications had to be made to the original ORD. The self-designed orifice meter was going to be inserted into the domed riser's 8 in (20.3 cm) pipe. When water enters the overflow, water will enter the domed riser's 12 in (30.5 cm) pipe then flow into the orifice meter before it discharged into the 8 in (20.3 cm) pipe. The first design was

an orifice meter with a 4 in (10.2 cm) diameter. The 4 in (10.2 cm) diameter was selected because it provided enough room [~2 in (5.1 cm)] for water to exit the orifice device into the 8 in (20.3 cm) pipe.

The design implemented more orifice holes than the case study to capture higher flow rates. In order to determine the quantity of holes, a theoretical curve was created utilizing Equation 3 with the coefficient of discharge (C_D) equal to 0.6. Orifice holes were added at different heights and evaluated with the theoretical curve. The graph (Figure 5.3) sums the flow rate produced by each orifice opening at each height. The initial theoretical curve had a total of 20 orifice holes with four holes at each level. The first two levels had 0.5 in (1.3 cm) diameter holes and then increased to 0.75 in (1.9 cm) diameter for the next three levels. The theoretical curve determined that the maximum flow rate with 12 in (30.5 cm) of head is approximately 0.5 cfs (0.014 m^3/s) (Figure 5.3).

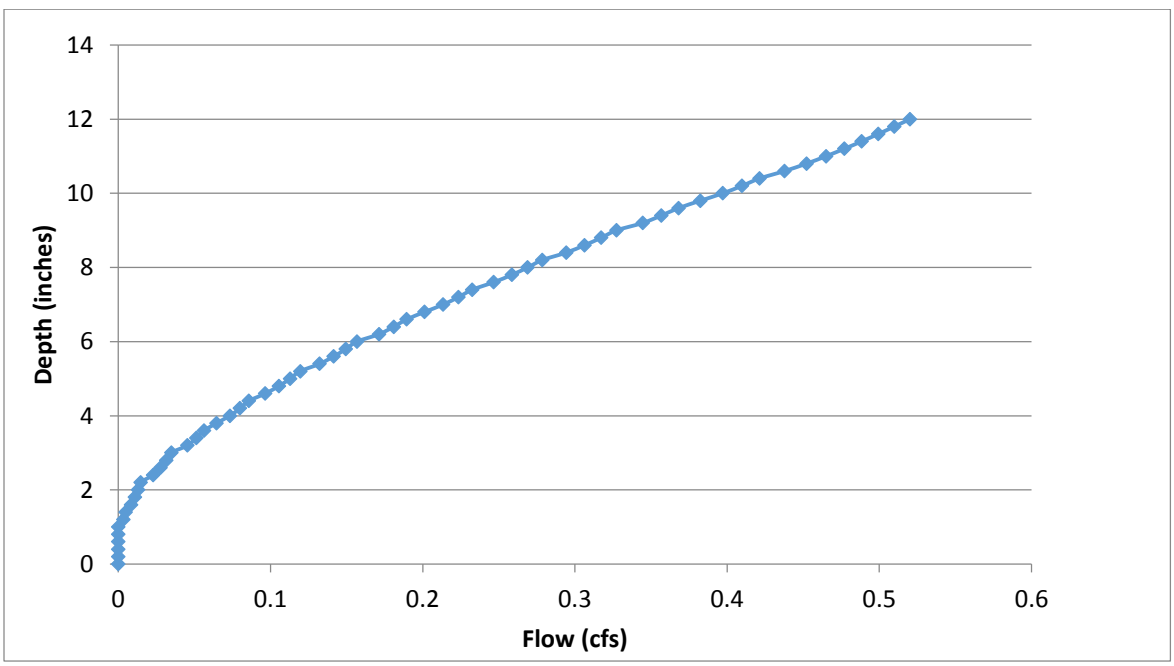

Figure 5.3 Theoretical curve of Prototype A orifice meter based off of ORD design.

The theory was tested by constructing the first orifice meter out of PVC pipe. The orifice holes were measured and drilled according to the theoretical curve design. The different heights between center to center orifice diameters ranged from 0.5-0.75 in (1.3-1.9 cm). As a result, there was overlapping of the orifice holes and the holes had to be staggered.

The prototype was tested in Villanova University's fluids laboratory. The testing apparatus had to imitate the field conditions. In the field the rain garden ponds prior to water entering the domed riser. A 55 gal (208 L) 22.5 in (57.2 m) diameter drum with a 12 in (30.5 cm) diameter hole in the bottom was installed over a trough. Pipes and fittings were connected to the 12 in (30.5 cm) hole that reduce to an 8 in (20.3 cm) pipe. The testing apparatus (Figure 5.4) has a pipe connected to the laboratory's existing flowmeter that extends into the drum. The drum fills up with water, imitating the ponding of the rain garden, then exits through the prototype design.

Figure 5.4 Laboratory testing apparatus for domed riser experiments.

The testing of the first prototype was unsuccessful for several reasons. There was an excessive amount of holes that overlap which allowed additional water to pass through the orifice device. The water levels did not vary over the range of flows because of the excessive openings. The device was intended to operate by measuring the level of water ponding in the middle of the orifice meter. Water would flow into the orifice meter and some water would exit in the upper holes before reaching the ponded pool in the bottom. This was especially inconsistent for lower flows because water would enter by trickling down the sides of the orifice meter. Level readings were also inconsistent for high flow rates because water would enter rapidly and splash up exiting through the higher holes. The higher flow rates also created excessive turbulence within the 4 in diameter. An ultrasonic sensor (SR-50) was used to measure the water levels and readings were extremely inconsistent due to the turbulence (Figure 5.5). A rating curve could not be created due to all of these reasons.

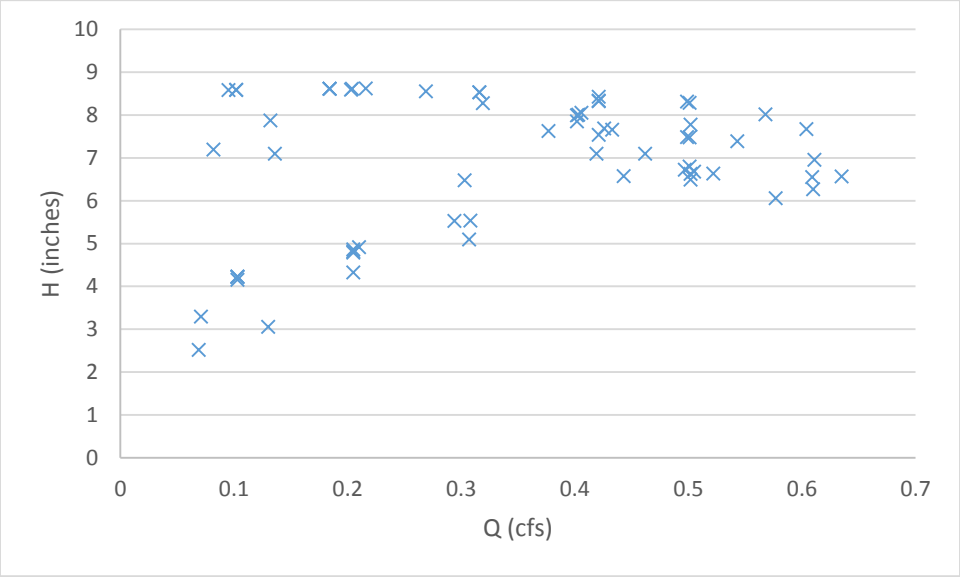

Figure 5.5 Prototype A Test Results

5.3.2 Prototype B – Organ Orifice Meter 1.0

Although the first prototype was not successful, lessons were learned for the next design. The higher flow rates caused too much turbulence, especially within a confined 4 in (10.2 cm) diameter. Also the excessive openings on the side permitted too much water to escape and contributed to inaccurate head measurements. Referring back to the domed riser's structure, the 12 in (30.5 cm) pipe reduces to the 8 in (20.3 cm) pipe. At this connection, there is only a 7.5 in (19.1 cm) opening which lays overtop the 8 in (20.3 cm) pipe. The next design is the organ orifice and incorporates a cap that sits overtop the 7.5 inch (19.1 cm) opening. Directly over the 7.5 in (19.1 cm) opening are three pipes that stand vertical. The three pipes increase in diameter from 1 in (2.5 cm), 2 in (5.1 cm), to 3 in (7.6 cm) and increase in height starting at the bottom surface 0 in (indicated by datum), 3 in (7.6 cm), and 6 in (15.2 cm) (Figure 5.6).

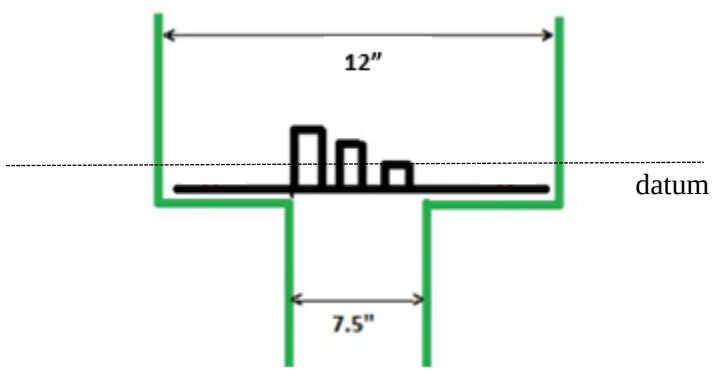

Figure 5.6 Conceptual design (NTS) of organ orifice with different pipe sizes (1 in (2.5 cm) pipe at 0 in, 2 in (5.1 cm) pipe at 3 in (7.6 cm), 3 in (7.6 cm) pipe at 6 in (15.2 cm)

5.3.2.1 Theoretical Approach

In theory the water is supposed to spill into the 12 in (30.5 cm) pipe and then settle at the bottom. The water level increases until it reaches the first pipe opening, which is the smallest opening. Water continues to pour into the first opening until enough head builds up and pours into the second opening. If the head continues to increase then the water will enter the third and

largest pipe. Higher flow rates will utilize all three pipes and lower flow rates will utilize the smaller and lower two pipes.

Figure 5.7 is a theoretical height-discharge curve for the orifice organ device utilizing the orifice equation (Equation 3). The theoretical height-discharge curve utilizes Equation 3 with C_D = 0.6. The theoretical curve has a 1 in (2.5 cm) diameter opening starting at 0 in, 2 in (5.1 cm) diameter pipe opening starting at 3 in (7.6 cm), and a 3 in (7.6 cm) diameter pipe starting at 6 in (15.2 cm). The theoretical graph sums the flow rates from for each new orifice level. The three change in slopes represent each orifice opening at a new height.

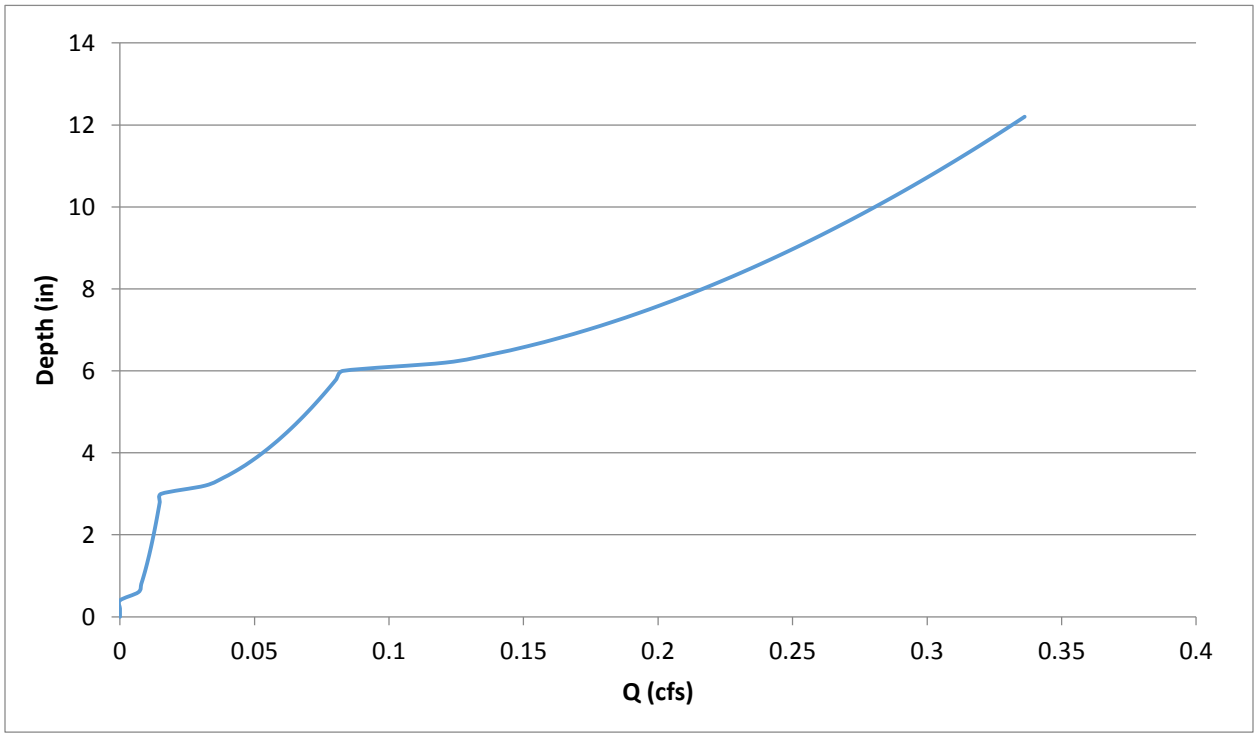

Figure 5.7 Theoretical height-discharge curve for the orifice organ device with discharge coefficient = 0.6.

5.3.2.2 Initial Construction & Installation

The initial prototype was created out of an 8 in (20.3 cm) PVC cap. Three holes were drilled through the bottom that were sized 1 in (2.5 cm), 2 in (5.1 cm), and 3 in (7.6 cm) diameters. The three orifice pipes were also PVC and installed at 0.25 in (0.64 cm), 3.25 in (8.26 cm), and 6.25 in (15.88 cm) from the pipe's bottom surface. The orifice pipes were measured and leveled accurately prior to permanent installation. The orifice pipes were installed into the drilled holes with PVC weld that has a 24 hour curing time.

The organ orifice meter was placed in the drum apparatus for testing. Prototype A's head measurements were noticeably variable when there were turbulent flows. The inaccuracy could be due to the ultra-sonic sensor having a disrupted signal. Therefore, a pressure transducer (CS-451) was used instead of the ultra-sonic sensor. The pressure transducer was placed in a housing tube near the three orifice pipes. Flow measurements and level readings were taken every five seconds then averaged and recorded over a one minute interval. A Campbell Scientific CR1000 datalogger was used for data collection.

5.3.2.3 Testing & Modifications

The overflow prototype's laboratory testing was similar to the H-flume testing (§4.1.1.3). Flow rates were steadily increased and decreased while simultaneously recording head measurements. The collected data produces a rating curve for each prototype. Figure 5.8 displays laboratory tests for low flows transitioning to high flows.

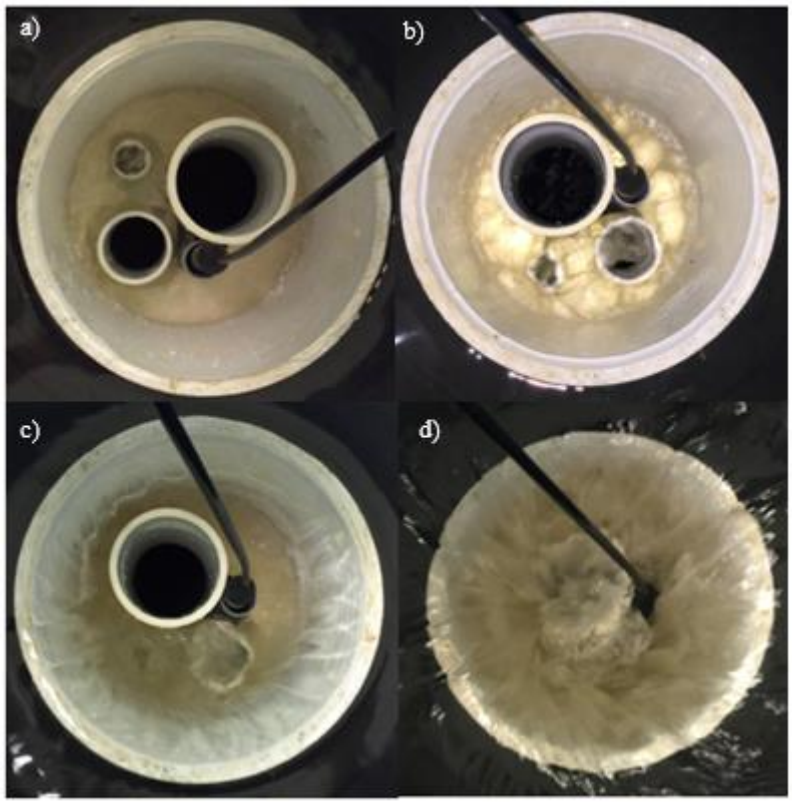

Figure 5.8 Prototype B Laboratory testing low flows (a-b) transitioning to high flows (c-d).

Prototype B produced test results that were inconsistent. Test one evaluated a full range of flows and created a rating curve (Figure 5.9) for the prototype. The test results produced two separate curves and it appears that the curves are distinguished by low and high flows. The results displayed variability in head measurements for flow rates greater than 0.3 cfs (0.008 m^3/s). At approximately 0.3 cfs (0.008 m^3/s), the head measurement decreases and a new curve is produced for the higher flow rates. The variability in the higher flow measurements could be due to turbulence as depicted by Figure 5.8. The head measurements were variable at approximately 6 in (15.2 cm) where the 3 in (7.6 cm) pipe (3rd and highest pipe) was submerged.

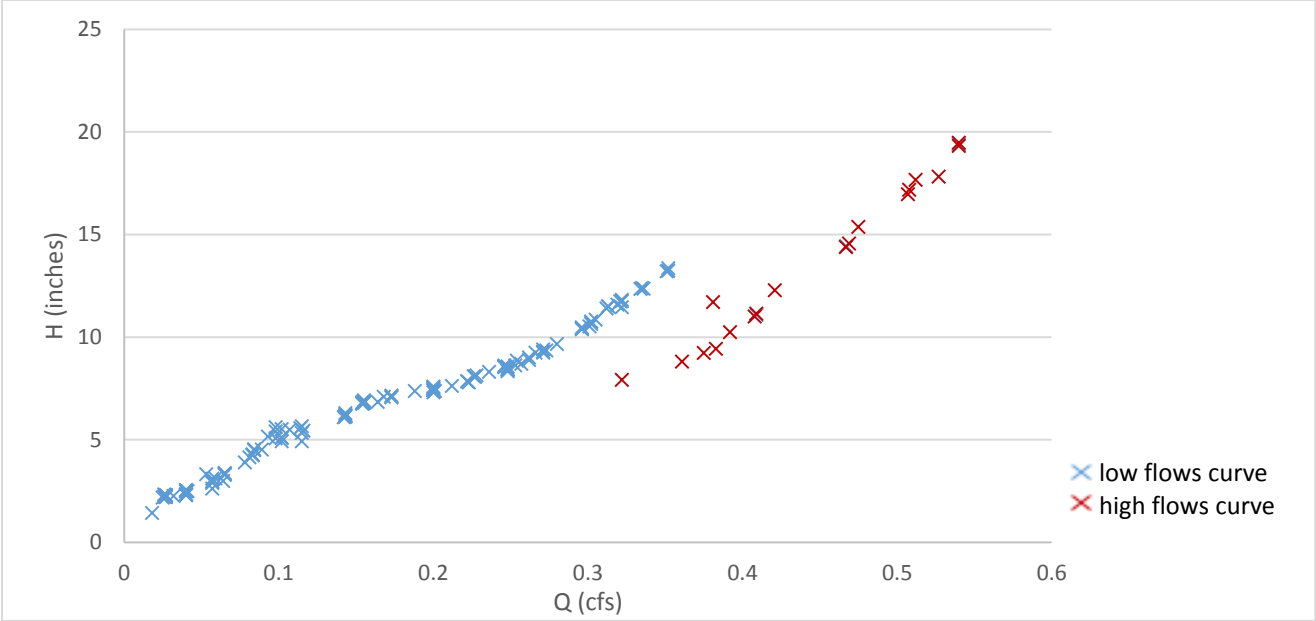

Figure 5.9 Prototype B Test 1 Results

The higher flow rates posed a problem for the construction of an accurate rating curve. However, low flow rates appeared to be consistent. Further laboratory tests were conducted on this prototype to investigate the performance of low flows [0-0.25 cfs (0-0.007 m^3/s)]. If an accurate rating curve was constructed for low flow rates, then modifications would only have to be made to the 3rd pipe for the higher flow rates.

Unfortunately, the low flow rates did not produce a consistent rating curve (Figure 5.10). During testing, multiple head measurements were recorded at a constant flow rate. Flow rates would remain constant for about five minutes. The head measurements for a persistent flow rate would vary by an inch (~2.5 cm), specifically at 0.17 cfs (0.005 m^3/s) and 0.26 cfs (0.007 m^3/s). The results were peculiar because head measurements were significantly changing every minute at a consistent flow rate. The results differed from the first test because the flow rates were adjusted during the first test on a 1-2 minute interval. This test consisted of flow rates being held constant for several minutes.

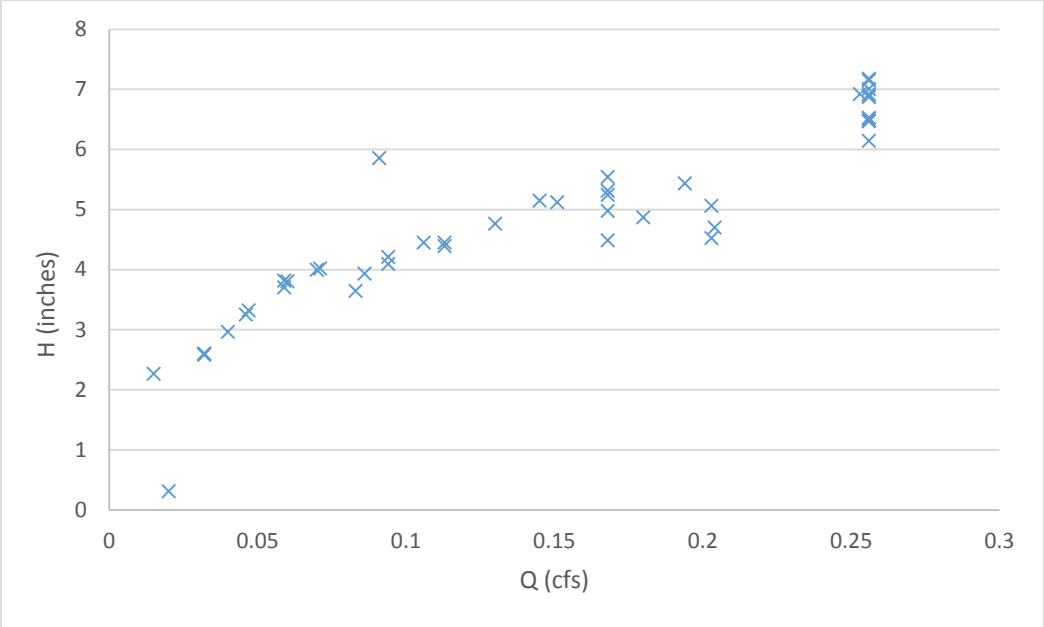

Figure 5.10 Prototype B Organ Orifice Test 2 Results

The term 'low flows' is used for these tests because they are on the low end of the spectrum for the full range of tested flows. The tests are considered low flows with respect to the overflow device. However, some of the 'low flows' could produce turbulence within the device. Turbulence could cause a discrepancy with head measurements, but how variable? Further investigation was directed by observation of prototype B undergoing laboratory experiments. Turbulence was present and water was also inconsistently entering the three pipes. For example, the water level could be at approximately 5 in (12.7 cm) and at this height the water should be in between the second and third orifice pipe. However, water would variably splash and enter the third larger pipe (Figure 5.11) instead of gradually increasing the surface elevation. The water descending from the 12 in (30.5 cm) pipe would arbitrarily pour directly into the largest orifice pipe.

Figure 5.11 Water variably pouring into third orifice pipe.

This phenomenon was unpredictable and occurred at different flow rates. It explains why the rating curve in Figure 5.10 has multiple head measurements for the same flow rates. The orifice pipes and 12 in (30.5 cm) pipe were leveled, therefore, it was not an installation problem. The large diameter from the third orifice pipe interfered with water flowing into the device. Other modifications were made to prevent the water flowing into the system. One idea was to put a cover overtop the third pipe that way water could not flow directly into the opening. As a result, the organ orifice could operate properly where water would fill the bottom and rise into the third orifice hole. To test this theory, an elevated domed cap (known as a mushroom vent cap) was placed on top of the third orifice pipe (Figure 5.12). The cap was elevated ~0.5 inch (1.3 cm) above the opening and was screwed into the side of the third orifice pipe.

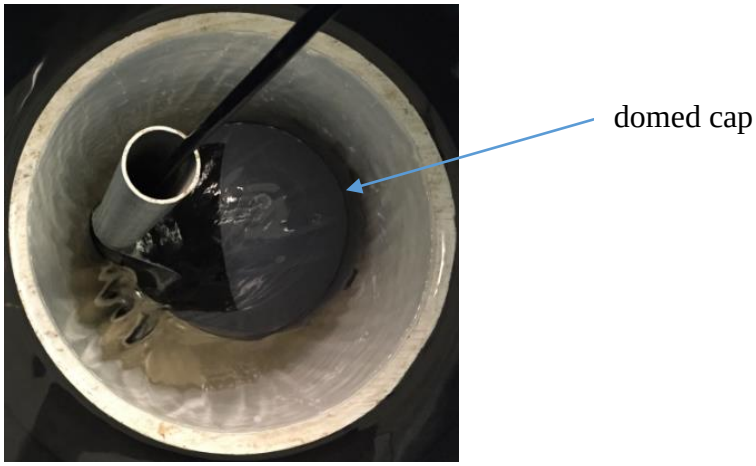

Figure 5.12 Elevated domed cap (mushroom vent cap) covering third orifice pipe

There ended up being several problems with testing the cap over prototype B. The third orifice pipe was covered, but the smaller two orifice pipes were still exposed. Water would enter the system, hit the lid of the cap, and discharge directly into the other two orifice pipes. There was now more losses with low flow events. Furthermore, the cap constricted the flow for higher flow rates. As soon as the water reached the third pipe, the water surface increased drastically. The three inch hole had to be wide open in order to function properly.

Water entering the largest pipe is clearly an issue with calibration. At this point, all testing was completed within a 12 in (30.5 cm) PVC pipe inside the drum. The 12 in (30.5 cm) PVC pipe replicated the domed riser's pipe size, but the testing apparatus was missing the iron dome casket. The dome on top could mitigate the flow entering the 12 in (30.5 cm) pipe. As a result, the flow could be less turbulent and the calibration could change. Therefore, a domed riser was purchased for laboratory experiments and installed in the drum. Prototype B was tested without the mushroom vent cap again in the domed riser apparatus (Figure 5.13). The test results were similar to the earlier results for prototype B. The domed riser mitigated the flow, however, water continued to pour directly into the largest opening resulting to variable head measurements.

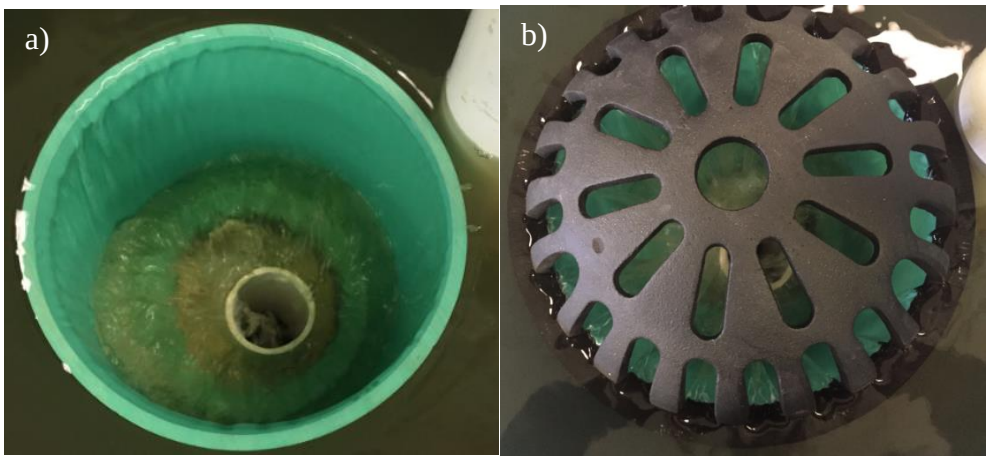

Figure 5.13 Prototype B: Organ Orifice 1.0 tested in domed riser apparatus. (a) Orifice device placed underneath the 7.5 inch (19.1 cm) opening, (b) Testing apparatus with iron domed casket

Evidently there are several problems with prototype B. The dome sitting over the 12 in (30.5 cm) pipe acted as a morning glory spillway. The water descending down 1 foot (0.3 m) into the organ orifice meter caused too much energy which caused turbulence within the system. In order to get consistent head measurements, the water had to lose energy so that turbulence is minimized. Also, the design had to be modified so that water could not arbitrarily enter the 3 in (7.6 cm) orifice pipe.

5.3.3 Prototype C – Organ Orifice 2.0

Prototype C addresses the 3 in (7.6 cm) pipe problem of Prototype B by raising the third orifice pipe to be flush with the 12 in (30.5 cm) pipe. Although this was an apparent solution, the modification was reluctantly changed. Increasing the pipes' heights reduces the overall potential head in the rain garden system. Prototype B allowed an extra 6 inches (15.2 cm) of height for measurements. The extra height allows the capability of measuring higher flow rates for extreme events.

Besides calibration issues, Prototype B's design was not optimal for low flows. The 1 in (2.5 cm) pipe did not have a significant impact on the low flows. Throughout the tests, the water level rapidly increased to the second orifice pipe. The first orifice pipe was submerged quickly with the 1 in (2.5 cm) opening. The quick submergence lead to only a few data points being recorded for the 1 in (2.5 cm) pipe. In order to optimize the design, Prototype C changed the 1 in (2.5 cm) diameter pipe to a 2 in (5.1 cm) diameter pipe. The 2 in (5.1 cm) pipe provides additional orifice area allowing higher flow rates to be captured for the overall system.

The final design for Prototype C was constructed out of a PVC cap. The cap had 3 vertical orifice pipes that had 2 in (5.1 cm), 2 in (5.1 cm), and 3 in (7.6 cm) diameters. The cap elevated the orifice pipes so that the 3 in (7.6 cm) orifice pipe was flush with the riser's 12 in (30.5 cm) pipe (Figure 5.14).

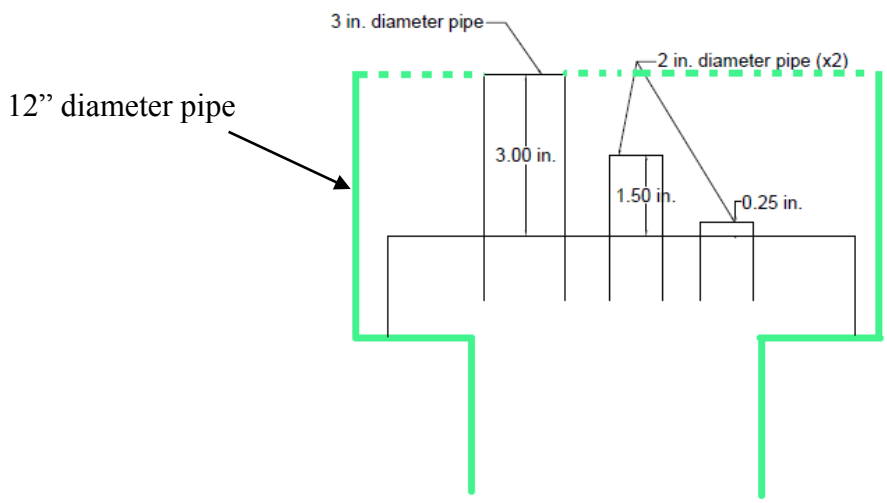

Figure 5.14 Sketch of Prototype C design in domed riser apparatus. (Top dome is not sketched).

5.3.2.1 Calibration Problems

The flush pipes addressed the issue of water entering the third largest pipe. Through observation it was also determined that turbulence was reduced. A rating curve was created for

prototype C by increasing and decreasing flow rates incrementally. Figure 5.15 shows that results were still variable specifically at the second pipe and above the third pipe.

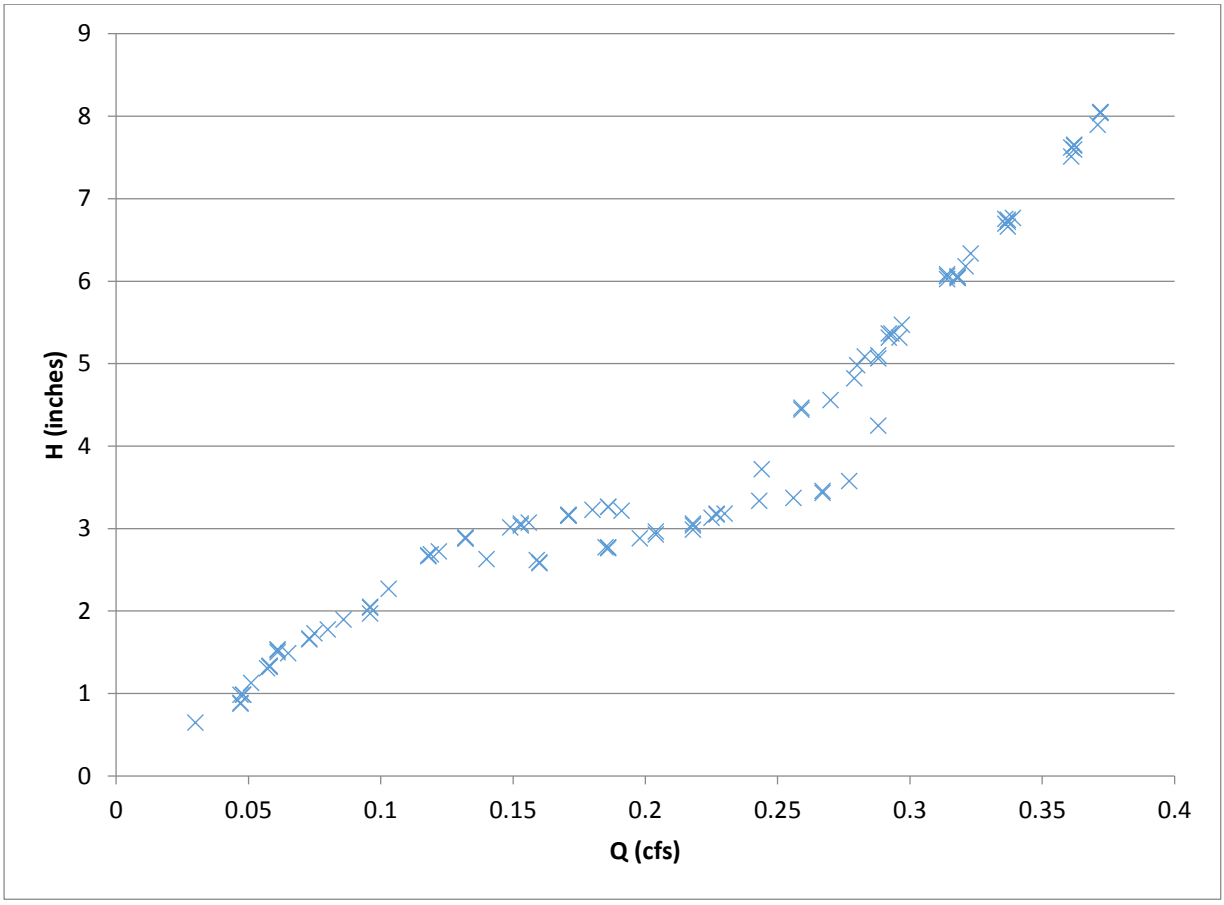

Figure 5.15 Prototype C Test 1: Rating curve developed by increasing and decreasing flows incrementally.

It was unclear why the first test results were variable. At first glance, the inconsistent head measurements were attributed to turbulence in higher flow rates. Figure 5.15 contradicts that theory because flow rates greater than 0.3 cfs (0.008 m^3/s) produced consistent head measurements. The variability was at the locations near the second and third orifice pipe. Further tests were conducted to see what triggers the inconsistency. Prototype C was analyzed for low flows, high flows, strictly increasing flow rates and strictly decreasing flow rates in order to determine when and how the inconsistency occurs.

Figure 5.16 and Figure 5.17 below display the test results for analyzing low and high flows. The objective was to determine which type of flow rates caused inconsistency, where does this occur, and when does this happen. Flow rates were increased and decreased incrementally for each test. The low flows test ranged from 0 – 0.2 cfs (0-0.005 m^3/s) and primarily involved the first two orifice pipes. Figure 5.16 displays that the variability in measurements did not occur prior to the 3 in (7.6 cm) orifice pipe. Once the water level raises to 3 in (7.6 cm), the head measurements were inconsistent. At 3 in (7.6 cm) the flow rate was approximately at 0.18 cfs (0.005 m^3/s).

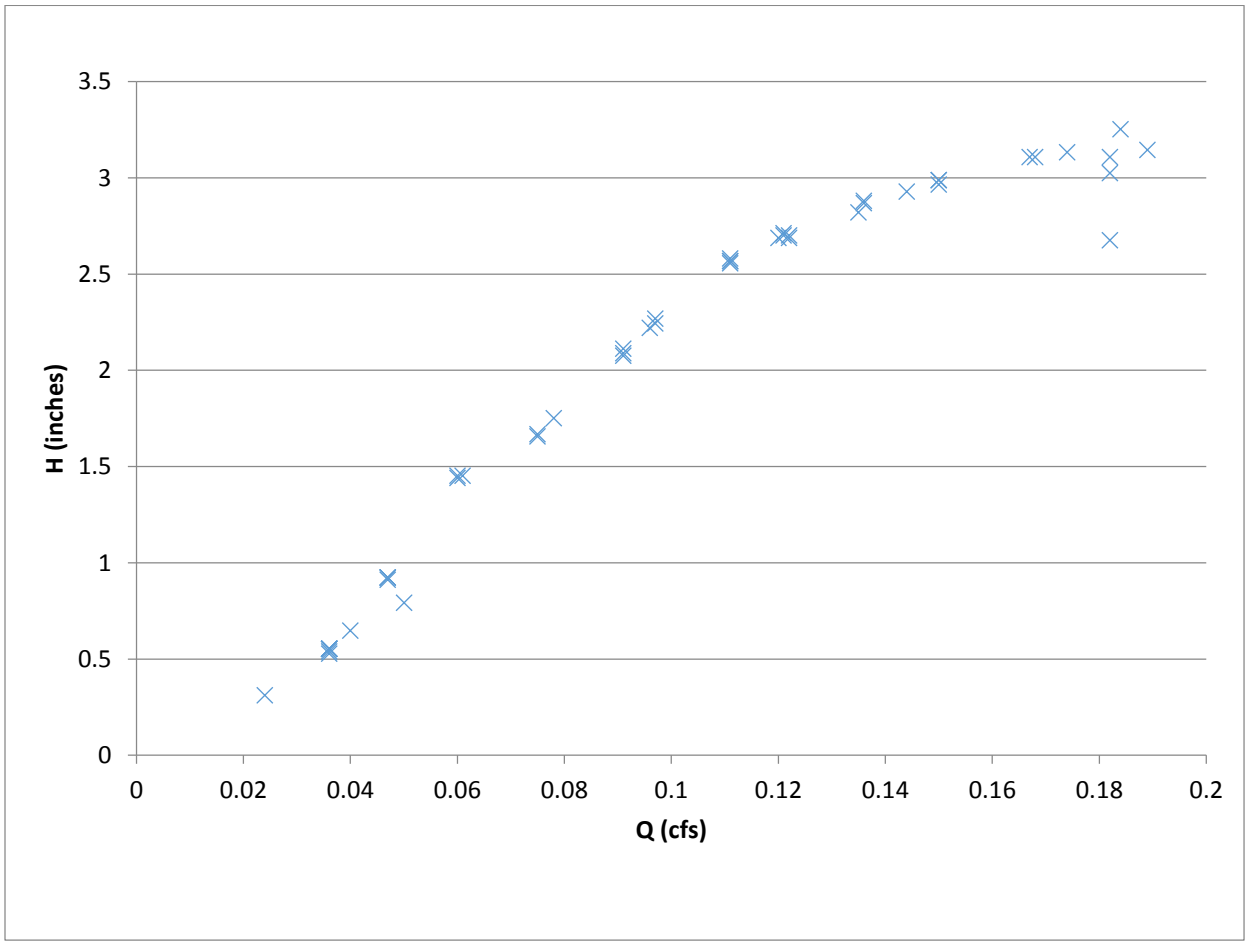

Figure 5.16 Prototype C Test 2: Low flows 0-0.2 cfs (0-0.005 m^3/s).

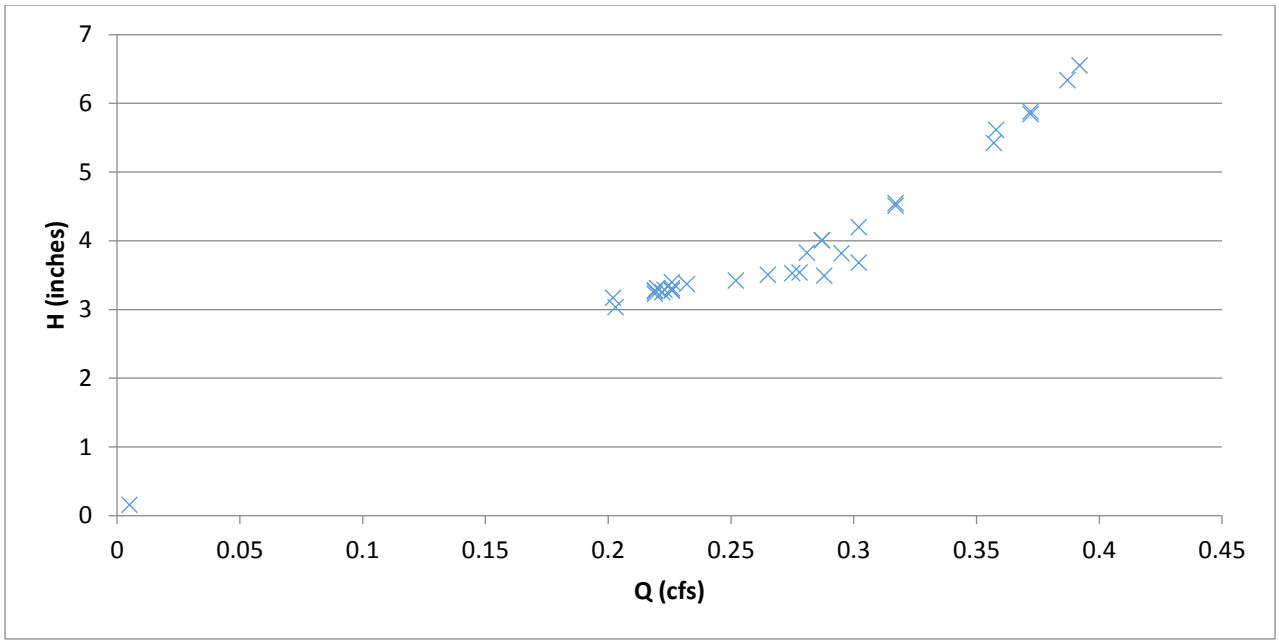

Figure 5.17 Prototype C Test 3: High flow 0.2-0.38 cfs (0.005-0.012 m^3/s).

Figure 5.16 suggests that the third orifice pipe was causing the inconsistency. Therefore, the variability was speculated to be large for the high flow rates test. Test 3 varied flow rates between 0.2 (0.005 m^3/s) and 0.38 cfs (0.012 m^3/s). Figure 5.17 displays that there were inconsistent measurements directly above the third pipe between 3.5 and 4 inches (8.9 and 10.2 cm). The flow rate during this inconsistency is approximately 0.28 cfs (0.012 m^3/s). Surprisingly, the variability was not as extreme as anticipated. Test 1 results (Figure 5.15) display that head measurements ranged between 3.5 and 5 inches (8.9 and 12.7 cm) at 0.28 cfs (0.012 m^3/s) flow rate, which indicated that there was greater variability in Test 1 than Test 3.

Test 3 started immediately with the high flow rates at 0.2 cfs (0.005 m^3/s), which means there was no previous build up from the first two orifice pipes. Consequently, the high flow rates in this test are independent from the low flows. Since Test 3's head measurements are not influenced from the first two orifice pipes, there is less inconsistency. On the contrary, Test 1

includes the full range of low and high flows which suggests that the variability is caused by the whole entire system.

Two more tests were conducted on prototype C to determine if the inconsistency is caused by strictly increasing flow rates or strictly decreasing flow rates. The tests investigated the full spectrum of flows ranging 0 – 0.4 cfs (0-0.011 m^3/s). Test 4, strictly increasing flow rates, and Test 5, strictly decreasing flow rates, are depicted by Figure 5.18 and Figure 5.19 respectively.

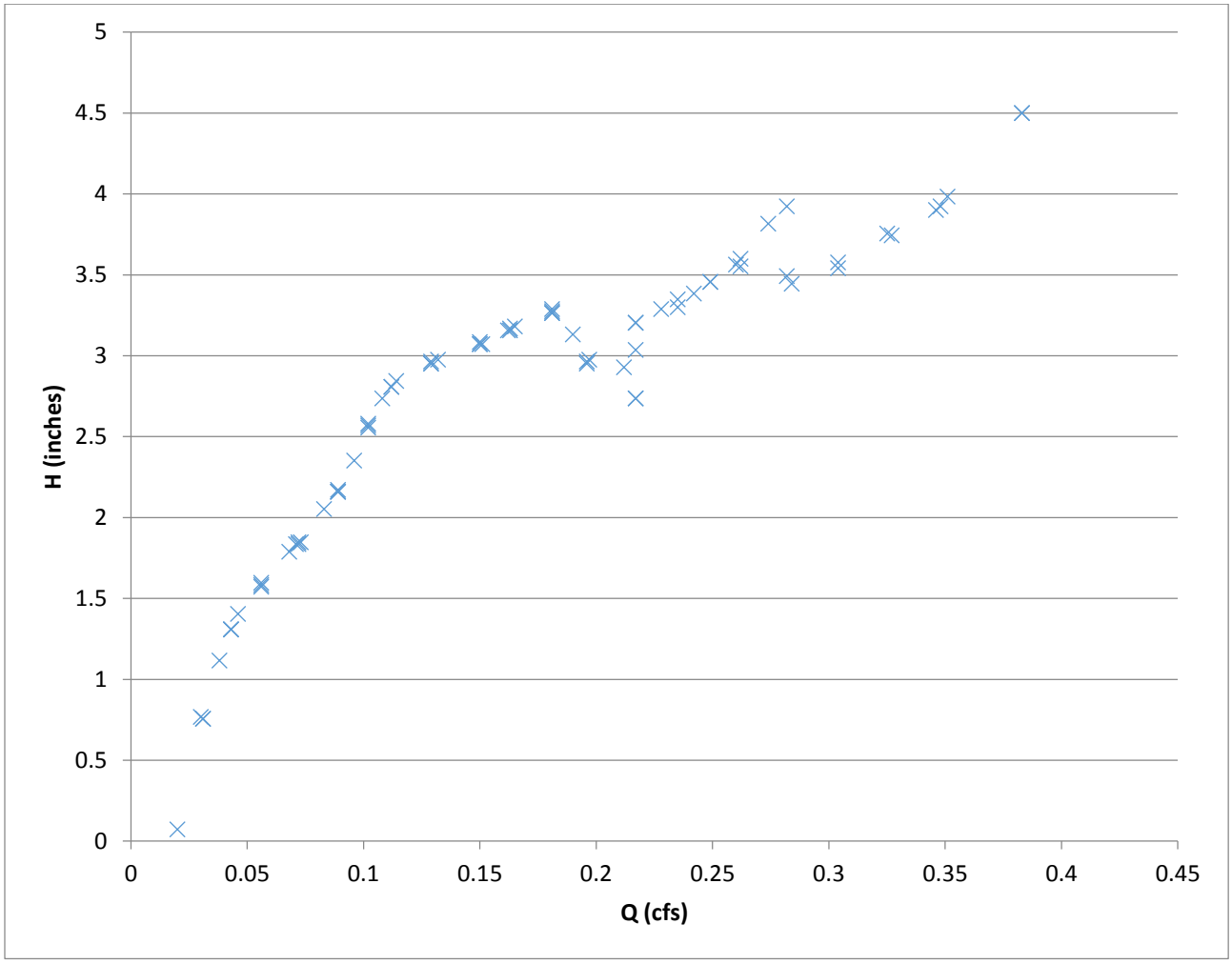

Figure 5.18 Prototype C Test 4: Strictly increasing flow rates

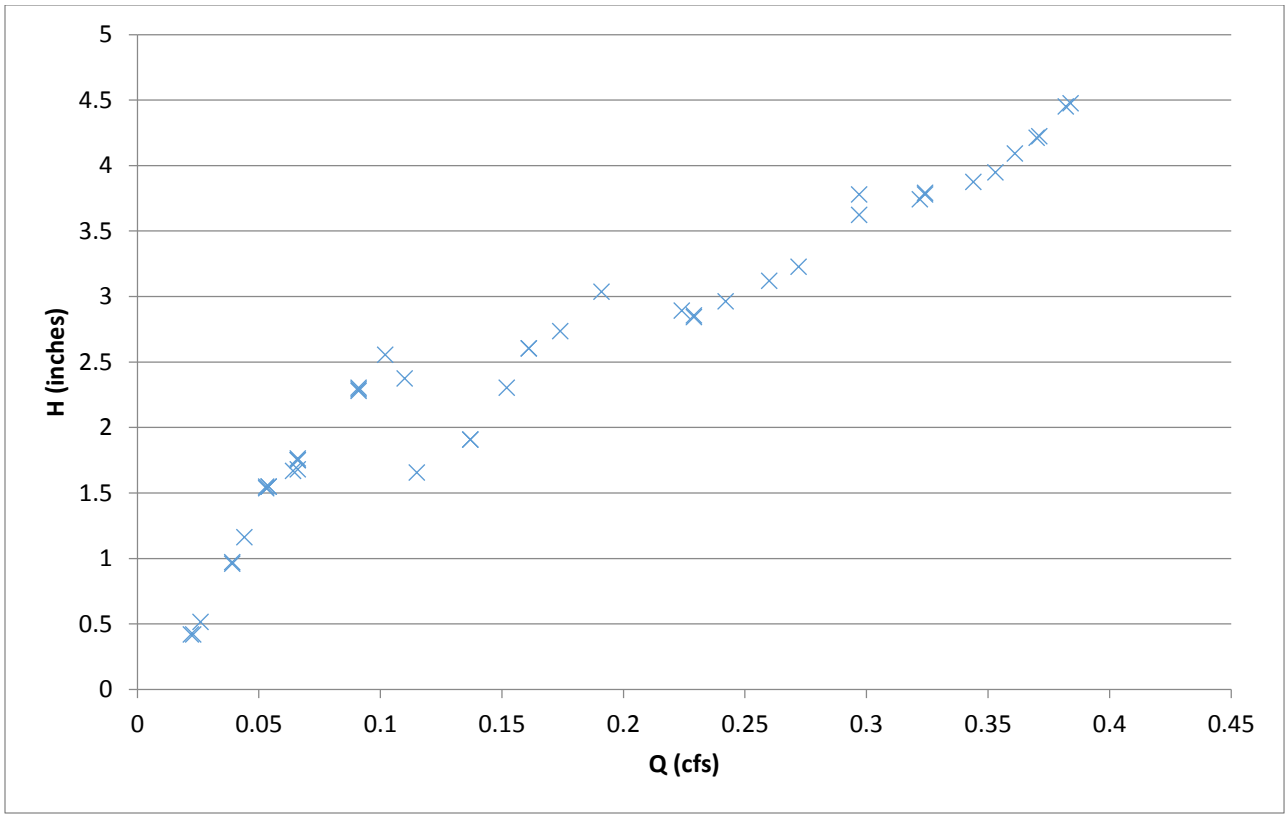

Figure 5.19 Prototype C Test 5: Strictly decreasing flow rates

Tests 4 and 5 show that head measurements were inconsistent regardless of increasing or decreasing the flow. The discrepancy between both tests is the location of inconsistent measurements. Both tests present variability between approximately 0.2 and 0.28 cfs (0.005 and 0.007 m^3/s) and this has been exhibited in all previous tests. Test 5 has an additional variable flow range between 0.1 and 0.15 cfs (0.003 and 0.004 m^3/s). At these flow rates, the water level varies between approximately 1.5 and 2.5 inches (3.8 and 6.4 cm). Surprisingly this level is below the third orifice pipe and above the second orifice pipe. The variability below the third orifice pipe confirms that the whole system was causing the variability and not solely the third orifice pipe. See Appendix E, Figures E.1-E.3 for additional test results.

Another peculiar result from Test 4 and 5 is the overall head measurements were significantly lower than previous tests, specifically with higher flow rates. At 0.37 cfs (0.010

m^3/s) there is about a 4 inch (10.2 cm) difference between Test 1 and 5. Figure 5.20 is a combined plot of all five test results. The largest discrepancy between tests is with larger flow rates. There is also inconsistency with low flows. The variability between tests would develop an inaccurate rating curve, consequently, the current design is not reliable as a measuring device.

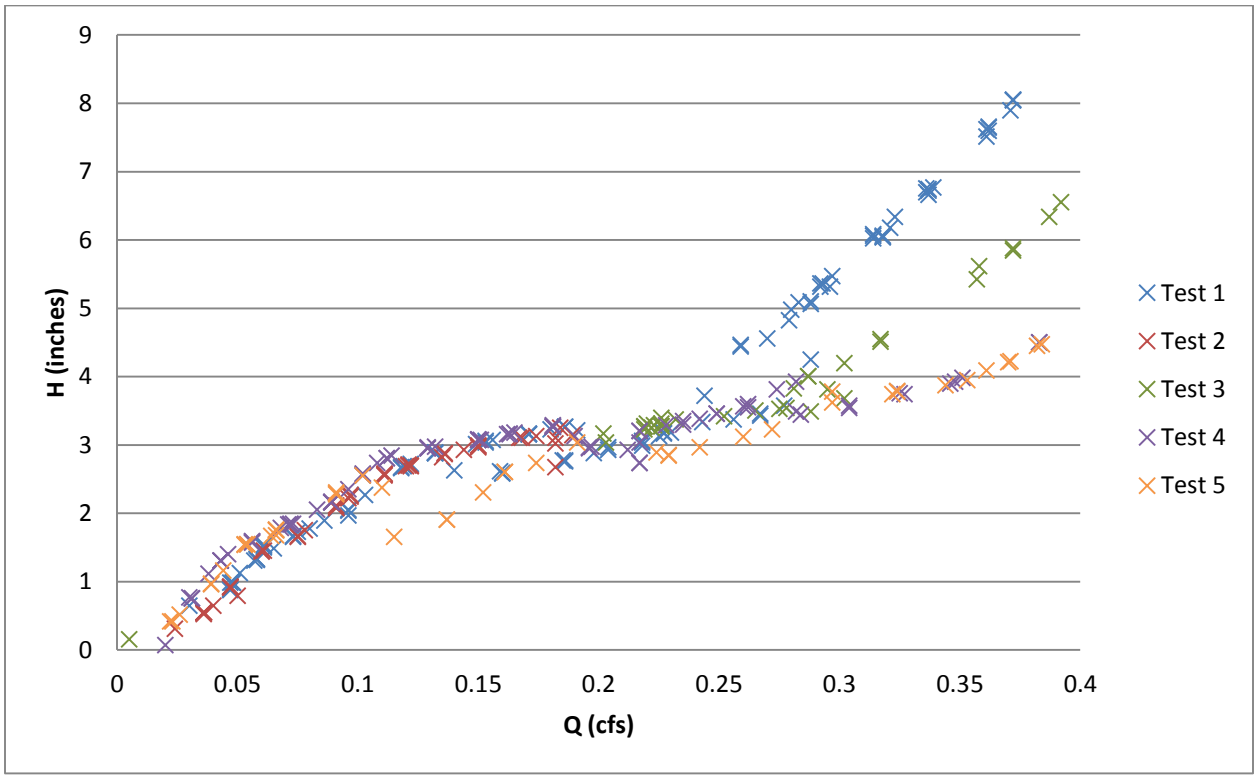

Figure 5.20 Prototype C Test Comparison

Several observations were made during Test 5. When the head measurements varied above the third orifice pipe, there was a suction noise coming from the device. At this occurrence, the water level would rapidly decrease. Test 5 was repeated several times in order to make an observational conclusion for the noise. The occurrence was not always repeatable, but nonetheless it occurred sporadically throughout various tests. The noise occurred when the flow rate was held constant at 0.28 cfs (0.008 m^3/s) for several minutes. At this point, the third orifice pipe increased in head and drastically dropped during the suction noise. Figure 5.21 displays the

transition of the water level dropping. The water would remain leveled at the three inch pipe for several moments. Eventually, the head would increase and water entered the third orifice pipe again.

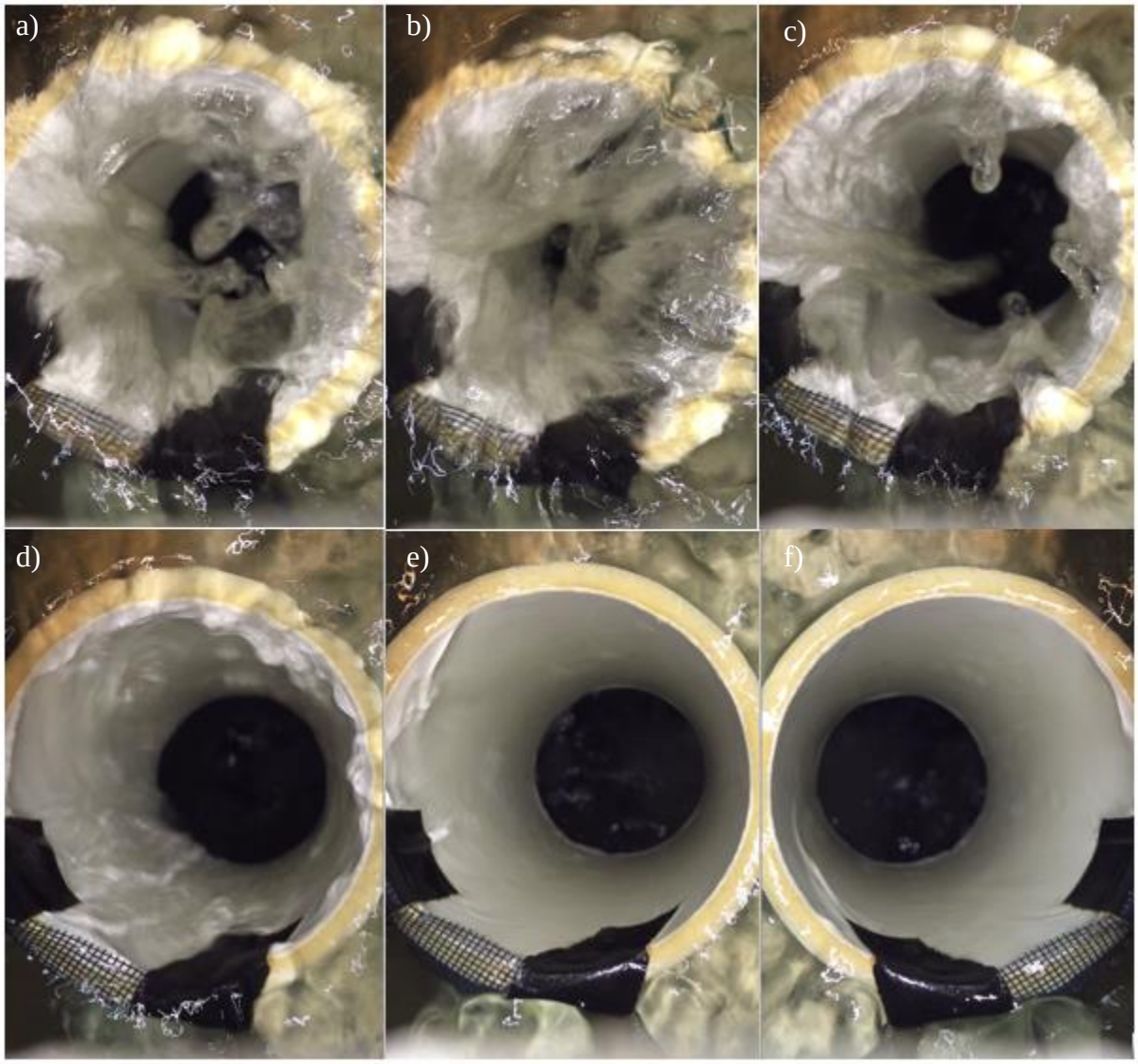

Figure 5.21 Flow transition of head measurements (a-f) in 3 in (7.6 cm) orifice pipe during suction phenomenon.

Vortexes were also detected during observational analysis and could attribute to the suction phenomenon. Similarly, the vortexes were inconsistent and unpredictable. They formed more often in the second orifice pipe, but there were some instances where smaller vortexes

occurred in the third pipe. There were also variations in head measurements without any eye-catching vortexes. Figure 5.22 displays test results where a series of two vortexes were present in the second pipe.

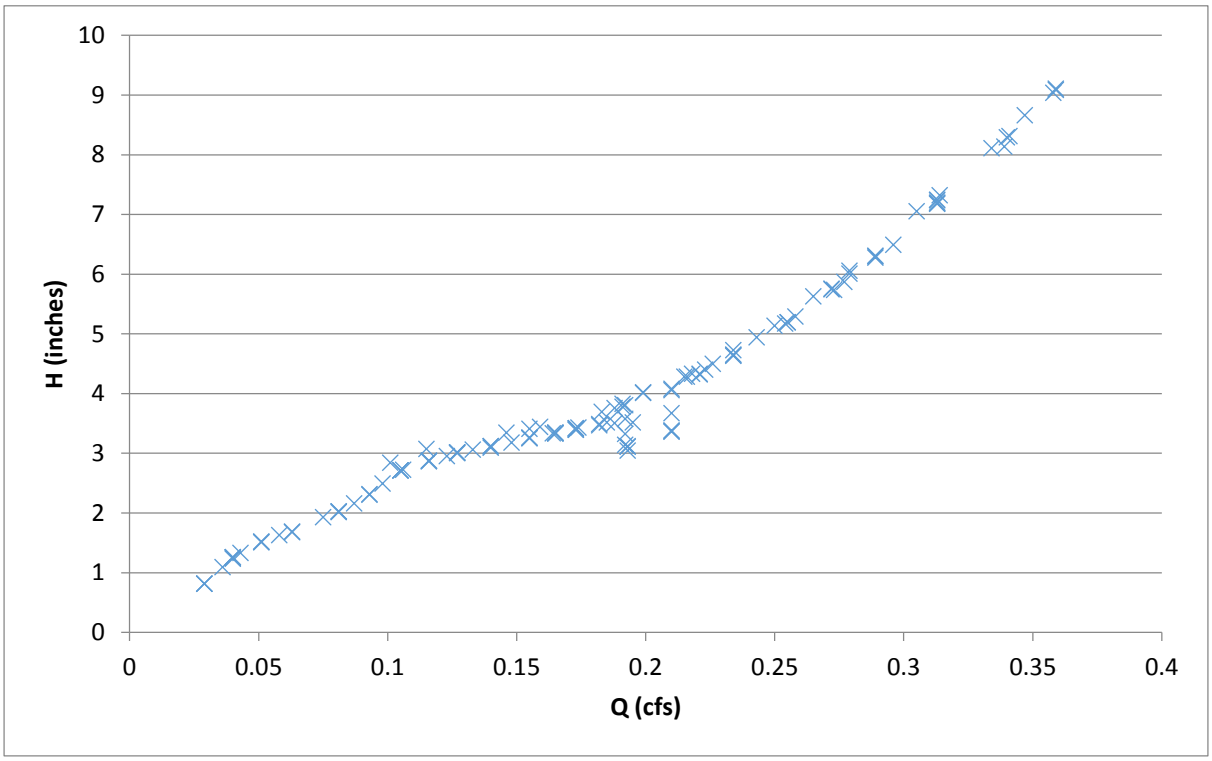

Figure 5.22 Prototype C Test 6: Rating curve with the occurrence of two vortexes

Test 6 was executed by steadily increasing and decreasing flow rates. Figure 5.22 shows the inconsistent head measurements at two locations. The inconsistency indicates where the vortexes occurred during this test. The suction phenomenon was not present during this test and explains why there was an overall increase in head measurements. When a vortex formed the water levels varied which explains the erraticism of all five tests.

5.3.2.2 Case Study

The organ orifice was acting similar to a vortex flow control valve, which is typically a conical shaped structure. Vortex control valves have been used in Chesapeake Bay, Maryland, Ottawa, Canada, and Weedon Bec, UK as stormwater management devices to slow down the

flow going downstream through the outlet of drainage systems (Andoh et al. 2009). These flow constricting devices have two modes of managing flows, pre-initiation and post-initiation. The first stage, pre-initiation, works under low flow conditions where the vortex control valve acts as an orifice. The second stage, post-initiation, occurs under higher flow conditions where the head increases and water begins to circulate allowing an air core to form a vortex. The vortex hydraulically chokes the outlet and prevents excessive amount of water draining the system (Andoh et al. 2009).

The organ orifice followed a similar pattern for the pre-initiation phase. Under lower flow conditions, the first two orifices acted as expected where water passed directly into the outlet. It eventually reached the post-initiation phase and a small vortex formed, however, it was difficult to detect with the eye. Graphically, the data indicated that the flow reached the 'flush flow' point before undergoing the vortex effects. The flush flow point is was studied by (Andoh et al. 2009) and his results are displayed in Figure 5.23. The kick-back in the figure refers to the moment when the vortex flow is fully developed and the flow starts acting like orifice flow again due to the smaller air core (Andoh et al. 2009).

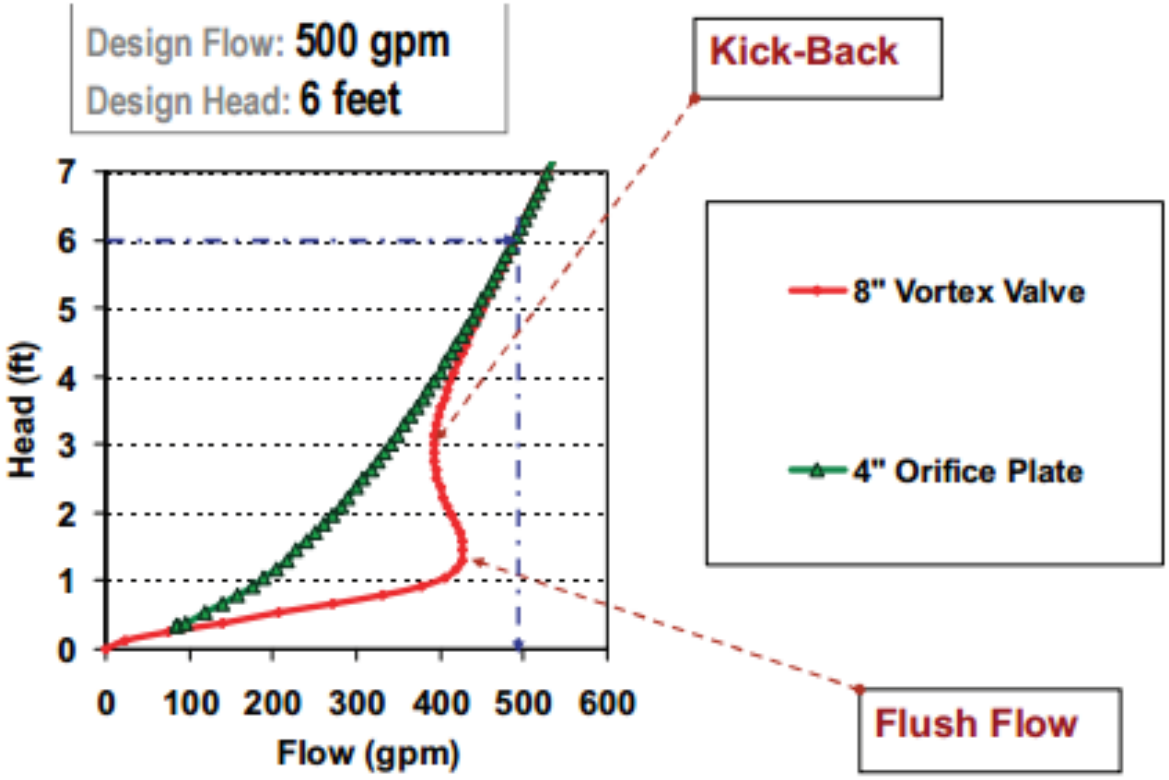

Figure 5.23 Head discharge characteristics for 4 inch Orifice and 8 in (20.3 cm) Vortex Valve taken from The 6th International Water Sensitive Urban Design Conference and Hydropolis #3: "Vortex Flow Controls in Integrated Stormwater Management for Urban Environments" (Andoh et al. 2009)

5.3.2.3 Addressing Vortex Issues

The case study indicates that air core and differential pressures is the potential cause of the vortex. The combination of the high velocities and air core that form the vortex restrict the flow by causing back-pressure that opposes the flow through the valve (Andoh et al. 2009). Interestingly, the organ orifice was having the opposite effect. Figure 5.24 displays a test where there was only the vortex phenomenon present (no suction). The vortex caused the water level to drop and permitted higher flow rates. It is uncertain why this happens. The results could be attributed to differential pressures from the trough underneath the testing apparatus. Irrespective

of the causes, the vortexes were inconsistent and a reliable rating curve could not be established with their presence.

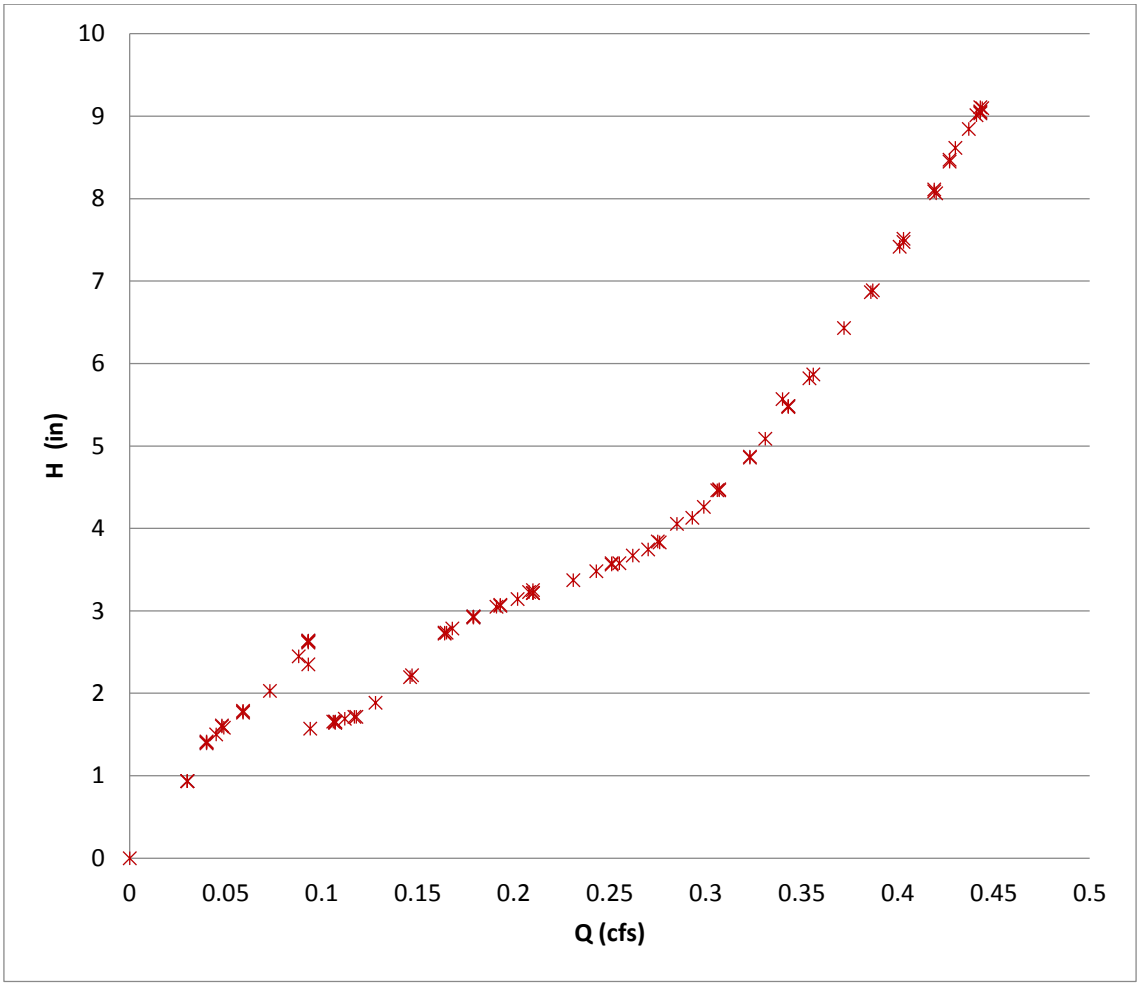

Figure 5.24 Testing in laboratory of organ orifice device undergoing vortex phenomenon.

An air vent tube was used during observational testing to address any pressure differentials. As soon as the suction and vortex occurred in the system, an air vent tube was stuck into the second pipe. The vortex dissipated and water levels raised instantaneously. The vent tube's success could be attributed to the relief of differential pressures or be acting as a baffle for the vortex's air core. Another test was conducted on Prototype C with an air vent tube in the middle of the second orifice pipe. A rating curve was successfully developed with the air vent tube modification (Figure 5.25).

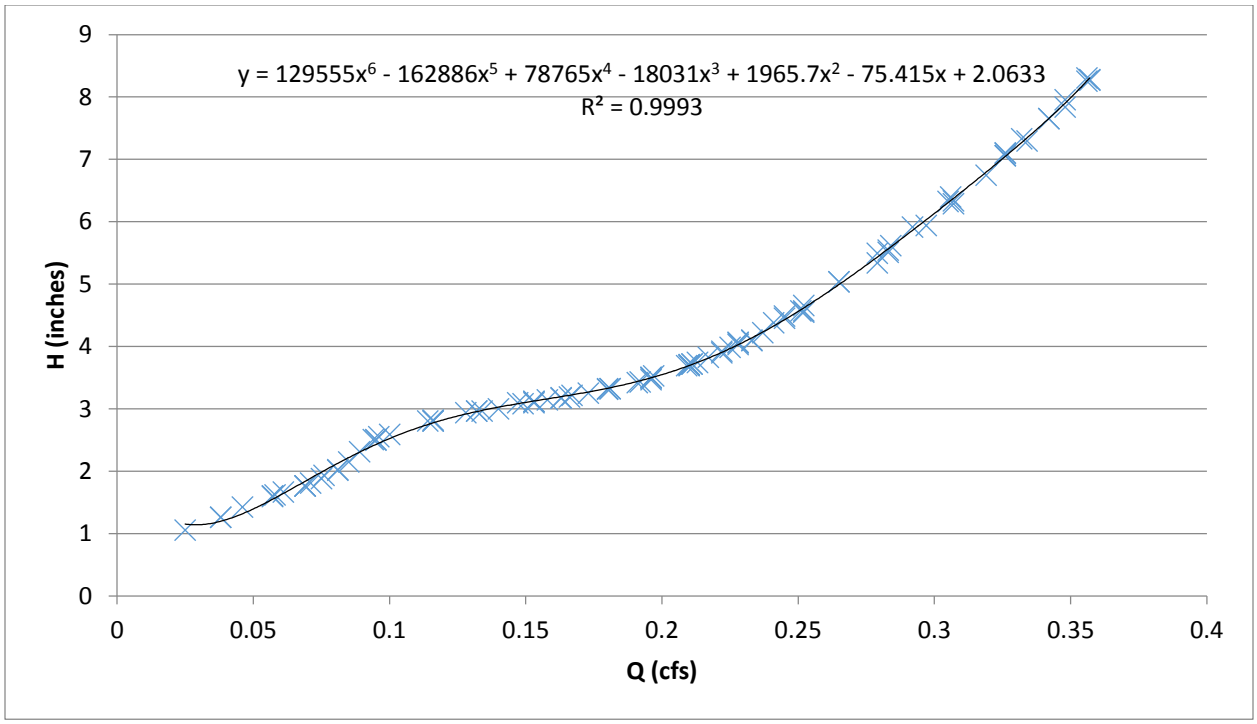

Figure 5.25 Prototype C Test 7: Rating curve for air vent tube modification.

One of the issues with the vent tube design is that vortexes formed sporadically. They predominantly formed in the second orifice pipe, however there were instances when vortexes formed in the third pipe even with the vent tube modification. Since they were extremely unpredictable, vent tubes would have to be placed in all three orifice pipes. The vent tube modification was a reluctant change because it would cause excessive intrusions into the design. The vent tubes could become clogged or shift which could potentially affect the rating curve. Further investigation examined Prototype C's design in order to determine why vortexes formed primarily in the second orifice pipe. The orifice pipes extended beneath the PVC cap's surface by varying lengths. It was discovered that the second orifice pipe had an excess of 3 in (7.6 cm) in length that protruded beneath the cap. The first and third orifice pipe extended less than two inches. The extra length of the second cylindrical pipe explains why vortexes predominantly formed there.

5.3.3 Prototype D – Organ Orifice 3.0

A new design was created with the orifice pipes flushed at the bottom of the PVC cap. The sizing and lengths of the orifice pipes remained the same as the previous design. A test was conducted to see if a rating curve could be developed with this design. Amazingly, a rating curve was developed and checked with several more tests (Figure 5.26). The results confirmed that the previous tests failed because of the excessive tube length. All three tests were executed by increasing and decreasing the flow rates incrementally.

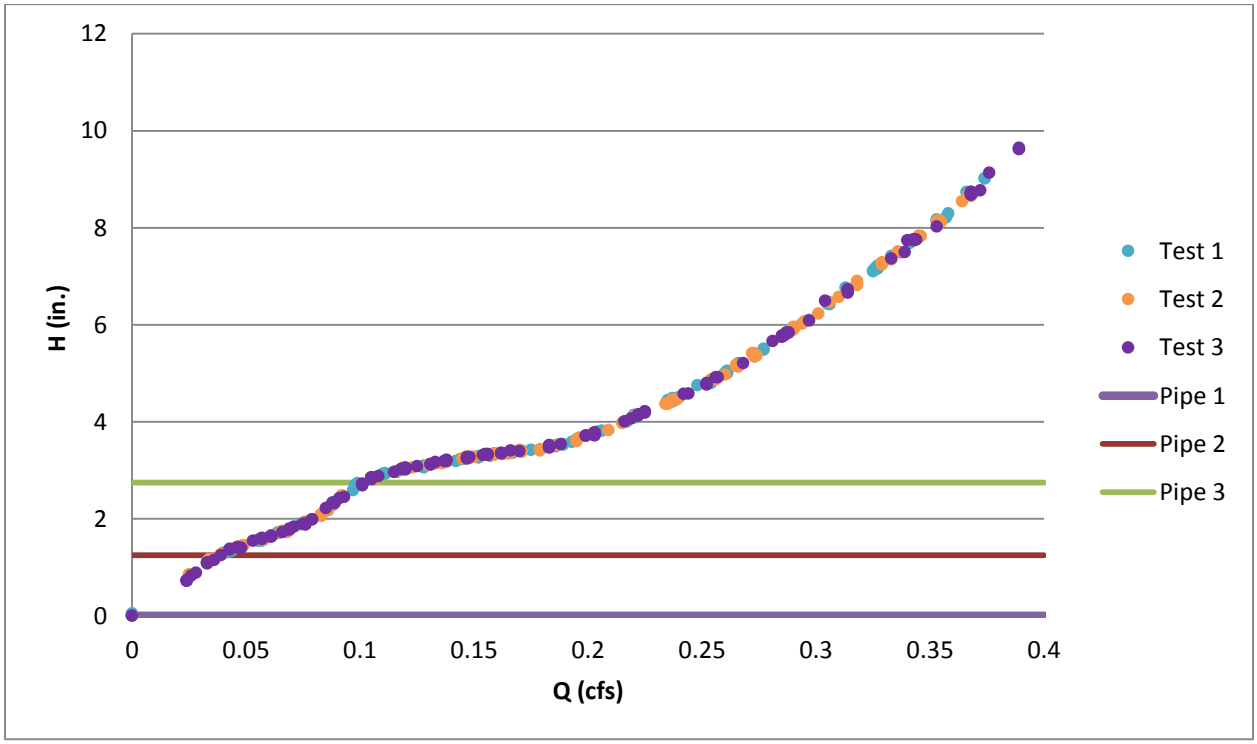

Figure 5.26 Prototype D testing of three tests with flush pipe design.

5.4. FINAL DESIGN – ORGAN ORIFICE

Prototype D was the inspiration for the final organ orifice design (see Appendix E, Figure E.4 for design drawings). The final design was manufactured by R.H. Benedix and constructed out of stainless steel. It is an 11.5 in (29.2 cm) plate with three pipes in the center that lay overtop the riser's 7.5 in (19.1 cm) opening (Figure 5.27). The orifice pipes' sizing and heights

remained the same as Prototype D. A 1 in (2.5 cm) tube with holes drilled into the side was also welded onto the plate as housing for the pressure transducer. Three tapped holes were also drilled into the design and a T-level was glued on the surface. This addition ensures the design is level for testing and installation. The organ orifice was temporary installed with a waterproof sealant as an adhesive.

Figure 5.27 Final Design of organ orifice manufactured by R.H. Benedix.

5.4.1 Laboratory Testing

Laboratory testing of the organ orifice involved five separate tests. The first three tests increased and decreased the flow incrementally from 0-0.4 cfs (0-0.011 m^3/s). The results were consistent for these tests. The last two tests varied the flow rates in order to create a more robust rating curve. The results were slightly scattered above and below the previous tests' results. The results were less consistent than the first three tests because the flow rates were independent of one another. Incrementally increasing and decreasing the flow rate does not randomize the flows. The first tests developed a rating curve with flow rates that were dependent upon the preceding data point. Therefore, variance is expected with fluctuating the flow rates. The combined results are displayed below in Figure 5.28. The varying test results slightly deviate from the first three tests. See Appendix E, Figures E.5-E.9 for all individual test results.

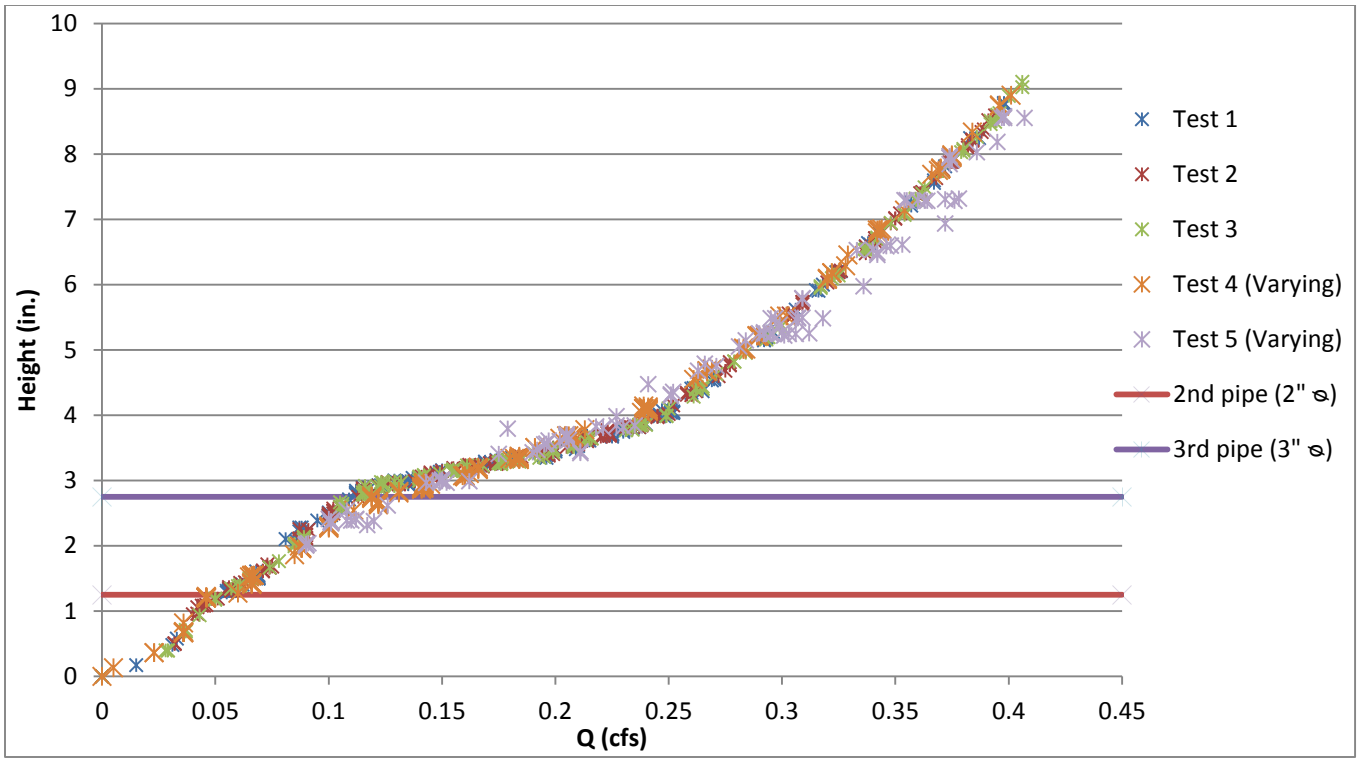

Figure 5.28 Combined Test Results of the Final Organ Device for rating curve.

5.4.2 Linear Regression Model

The organ orifice design has the label "orifice" in its name, but it actually operates as a weir and orifice. When water enters the first pipe it initially operates under weir flow until enough head increases and the opening becomes fully submerged. Once the pipe is fully submerged it operates as orifice flow. Orifice flow continues until water reaches the second pipe and it begins to operate as weir flow once again. Figure 5.29 displays the transition of orifice flow into weir flow in Prototype D's testing.

Figure 5.29 Transition of orifice flow into weir flow in organ orifice design

The weir and the orifice equations take on the same relationship of $Q = C_1 H^{C_2}$, where C_1 and C_2 are arbitrary constants unique to the discharge relationship. The weir and orifice pattern creates a unique rating curve in the combined tests plot above (Figure 5.28). The change in slopes is where the water transitions between weir and orifice flow. Since the weir and orifice equations have similar relationships, a linear regression model can be developed to create an equation for the device.

In order to create a linear regression model, the data was log transformed. The log transformation of Q and H created a plot that is linear to each slope. Minitab, a statistical software, was used to analyze the data. Before the data was inputted into Minitab, the data set of each test was investigated. During testing, flow rates were recorded on a one minute interval, but flow rates did not change every minute. Sometimes flow rates would remain constant for several minutes and repetitive data would be collected. Several data points clustered in the same region for the same flow rates and this would alter Minitab's linear regression model. Every data point has an equal weight in the model, therefore, repetitive data based on the same flow rates will inaccurately influence the model by creating a biased heavier weight to the model. As a

result, data clusters with similar flow rates and time intervals were averaged to a single data point. See Appendix E, Figure E.10 for the averaged test scores on a logarithmic scale.

The transition between weir and orifice flow was distinguished for the model. The weir flow's location started at the height of each pipe. The weir flow in the first, shortest pipe is minimal and shifts to orifice flow at 0.4 in (10.2 cm). Since there were only four data points within this region, one orifice equation was fitted to all of the first pipe's data. The weir flow began at 1.25 in (3.2 cm) for the second pipe and 2.75 in (7.0 cm) for the third pipe. The orifice flow's location was determined by the data's change in slope (Figure 5.30) and was confirmed by observations which adds confidence to the graph's accuracy. Full orifice flow occurs at 1.8 in (4.6 cm) for the second pipe and 4 in (10.2 cm) for the third pipe.

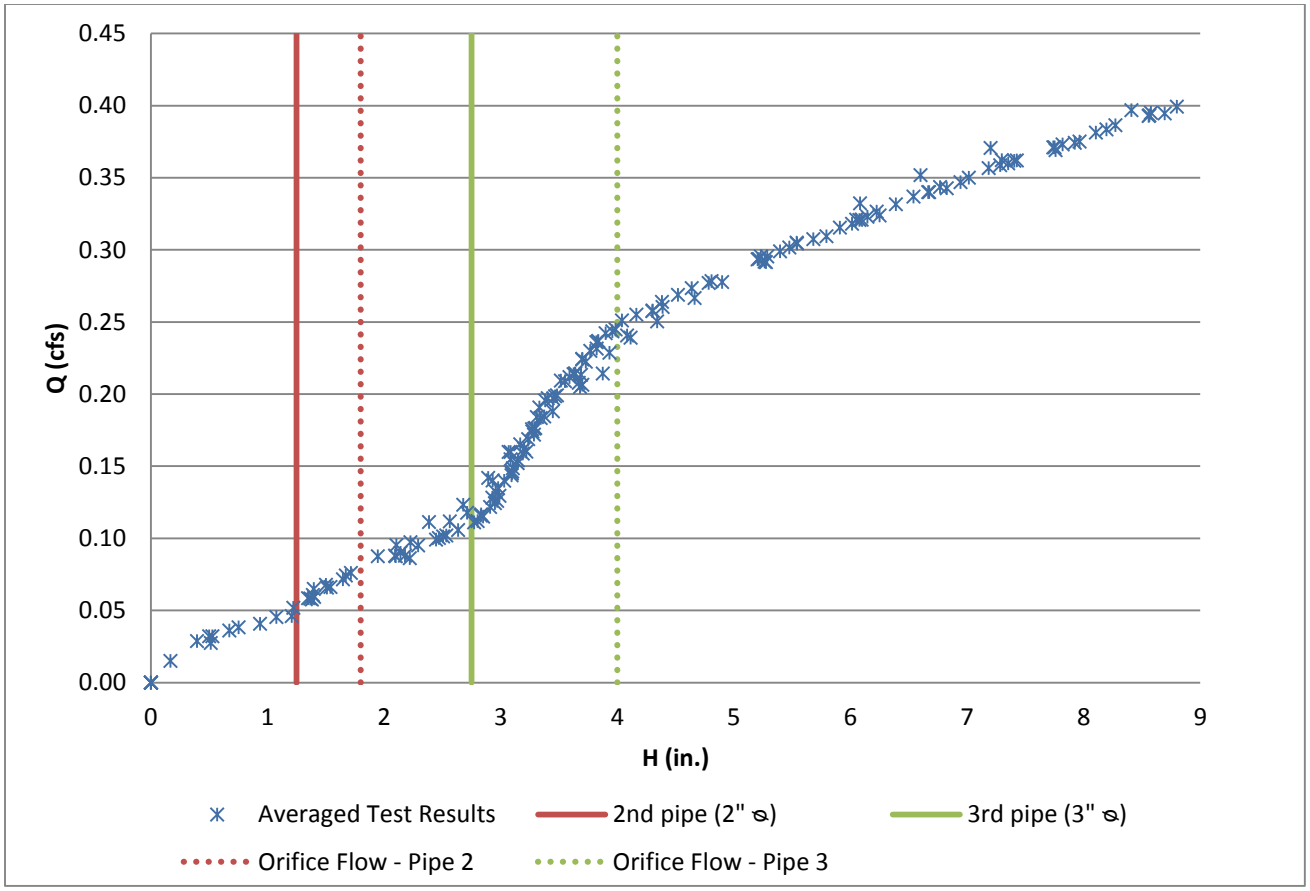

Figure 5.30 Average test data with weir and orifice flow locations.

The weir and orifice flow phases were entered into Minitab to create a linear regression that connects the graph's five flow phases. Minitab processed the data and yielded coefficients that relate to each corresponding weir or orifice flow. The output was back calculated to obtain the true flow rate equation on a non-logarithmic scale. The calculations create a five piece equation that relates to the locations of weir and orifice flow where,

$If\ H < 1.25\ inches,$

$$Q = 0.0455H^{0.602}$$

$If\ H < 1.8\ inches,$

$$Q = 0.0403H^{1.1481}$$

$If\ H < 2.75\ inches,$

$$Q = 0.0465H^{0.9031}$$

$If\ H < 4\ inches,$

$$Q = 0.0139H^{2.0944}$$

$If\ H \geq 4\ inches,$

$$Q = 0.1153H^{0.5704}$$

The data head measurements were graphed with the linear regression's five piece equation (Figure 5.31). According to the output (Appendix E, Figures E.11-E.12), the five-piece linear regression has an R^2 value of 99.56%, indicating that the linear regression is a good fit for the data. A confidence interval cannot be developed for the regression model because the test data points are not independent samples. Any copies of this design would have to be uniquely calibrated for its own linear regression model.

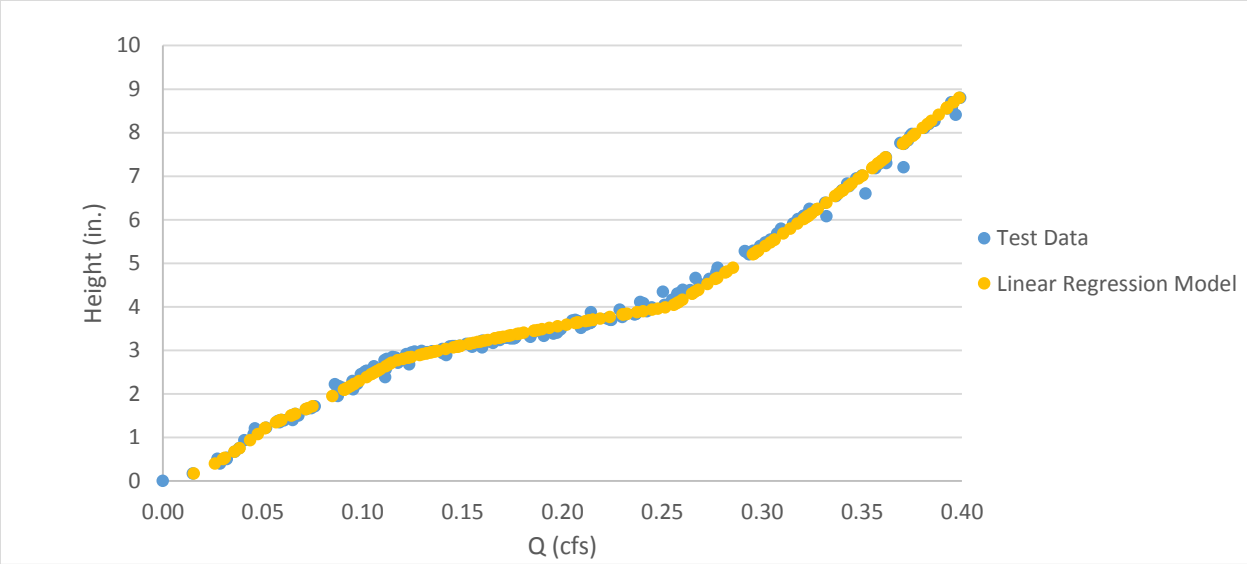

Figure 5.31 Linear Regression Model compared to Test Data

5.4.3 Analysis of Organ Orifice's Expected Performance

The linear regression model is a good fit for the organ orifice device, but is it the best technique to measure the overflow? Other hydraulic structures could also be used to measure the rain garden's outflow such as a Thelmar weir inside the 8 in (20.3 cm) pipe or a constructed weir box around the domed riser. At Villanova University, Dr. Ryan Lee created a processing tool called Green Infrastructure Flow Measurement Evaluation Tool (GIFMET) (Appendix E, Figure E.13) to evaluate the effectiveness of flow monitoring devices during large rain events (Dr. Ryan Lee, personal communication, October 2015). The system is based on rainfall data collected at Villanova University's bioinfiltration traffic island (BTI) between 2011 and 2015. The model considers rainfall events larger than 1.0 in (2.5 cm) and less than 3.2 in (8.1 cm) with a 6 hour drying time and excludes snowmelt.

Dr. Ryan Lee performed an investigation between the different flow measurement techniques comparing the organ orifice, Thelmar weir, and weir box overtop the domed riser. GIFMET's output analyzed how accurately the outflow device measures flows, how often the

site is expected to exceed capacity with the current configuration, and what is the overall volume capture percentage. Table 5.1 displays GIFMET's results for the orifice organ's performance regarding flow measurement at the Zoo rain garden site.

Table 5.1 Table of GIFMET's results comparing flow measurement devices and corresponding measurement error.

Flow measurement options	GIFMET flow measurement error based on 5 years of storm events
Option A: Thelmar weir inside 8 in (20.3 cm) pipe	31 %
Option B: Constructed weir box around domed riser	15%
Option C: Organ Orifice Flow-Meter	11%

The Thelmar weir inside the 8 in (20.3 cm) pipe outputted the largest flow measurement error at 31%, the constructed weir box around the domed riser resulted to a 15% measurement error, and the organ orifice had the lowest flow measurement error with only 11% error. The flow measurement error between the constructed weir box and the organ orifice is a marginal 4%, but the organ orifice still produces higher accuracy. Additionally, the organ orifice is aesthetically more appealing and as it fits inside the domed riser it is more protected from vandalism and trash. Therefore, it was concluded that the organ orifice is the best option to measure the system's overflow.

CHAPTER 6: FIELD TESTING – SIMULATED RUNOFF TEST (SRT)

Simulated Runoff Tests (SRTs) are part of PWD's Comprehensive Monitoring Plan in order to evaluate SCMs performance within Philadelphia. Portland, Oregon also utilizes SRTs as part of their monitoring program (§2.3.2). An SRT program at the Philadelphia Zoo rain garden is particularly useful since the site is heavily instrumented and therefore a full scale evaluation can be conducted on the site's functionality. Although SRTs are typically used for assessing a site's performance, they can also be used as a way to evaluate the adequacy of monitoring equipment, specifically with assessing inflow measurements. Since a known flow rate is entering the surface channel, it can be directly compared to the H-Flume's output. The focus of this SRT assessment is strictly on the inflow and outflow structures of the rain garden system. Existing soil moisture sensors and shallow wells aid in the understanding of the system's performance, but the focus of this report is on the inflow and outflow monitoring equipment.

6.1. SRT SITE CONFIGURATION

One necessary component of an SRT is having a nearby fire hydrant as the water source. A fire hose is connected between the fire hydrant and a downstream water meter. The fire hydrant has to be on the same street side as the rain garden to avoid running the fire hose across the street and interfering with traffic. West Girard Ave is heavily congested, therefore, traffic is an unavoidable issue (Figure 3.3, §3.3.1). An acceptable fire hydrant was discovered at the School of the Future approximately 300 ft (91.4 m) away from the site.

The flow rates entering the rain garden are controlled by a portable water meter, Sensus WL-1250 (Figure 6.1a). The portable water meter is connected to a diffuser to cause a more subtle discharge into the inlet channel (Figure 6.1b). Necessary equipment for the SRT includes

the water meter, fire hose, diffuser that is set upstream of the inlet and temporary pressure transducers (HOBO U20) that record water levels on a 1 minute interval throughout the rain garden at the same locations as the CS-451 pressure transducers (Figure 6.2).

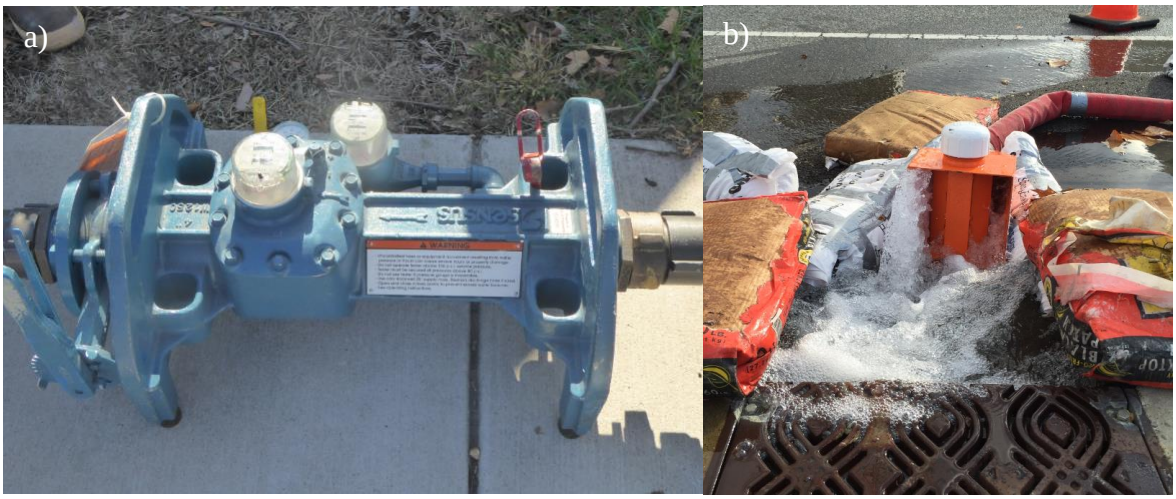

Figure 6.1 SRT equipment (a) Sensus WL-1250 portable water meter and (b) diffuser for the SRT.

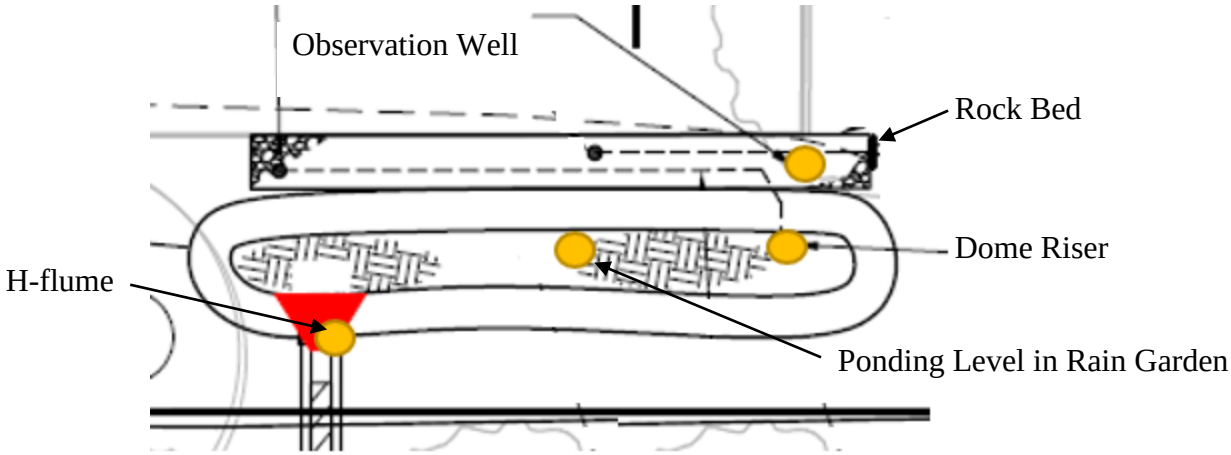

Figure 6.2 Location of pressure transducers in downstream rain garden indicated by yellow circles.

As the SRT is conducted, water levels are manually measured at all the pressure transducer locations. The manual measurements are taken on a ten minute interval and are used

to verify the readings of both sets of pressure transducers. Figure 6.3 shows the progression of an SRT where water enters the downstream rain garden via the H-flume, the rain garden begins to pond, and ultimately the entire system is full of water.

Figure 6.3 Progression of SRT (a-d) conducted on the downstream rain garden. (d) Yellow circle indicates submergence of H-flume

6.2. SRT TEST 1

The first SRT was conducted on December 3rd, 2015 with PWD's assistance. The upstream and downstream rain gardens were evaluated individually starting with the downstream rain garden. The focus of this research is on the downstream rain garden since it has a slightly larger drainage area and incorporates the H-flume and domed riser structure.

The CS-451 pressure transducers were logged on a five minute interval (which is the same time interval for continuous monitoring in the field.) The water meter flow rates were recorded and adjusted on a five minute interval. Flow is initialized at a low flow rate, steadily increased to an allowable peak rate, and then held constant. The fire hydrant's pressure determines the maximum allowable peak flow rates and the flow rates are held constant until the rain garden fills (depicted by the progression results in Figure 6.3).

The downstream rain garden was designed to manage a 1.42 in (3.6 cm) rain event and initially the rain garden was going to be evaluated only under this intended design. However, after the rain garden was subjected to the 1.42 in (3.6 cm) storm simulation, it was discovered that volume capacity was not reached and there was ample room for more water. Subsequently, more water was added into the system to evaluate its maximum potential resulting to the downstream rain garden effectively managing a volume equivalent of 2 in (5.1 cm). The flow was stopped prior to flooding the system. Flooding the system refers to the point where water overtops the rain garden and flows onto the adjacent parking lot and sidewalks. The SRT was conducted over an 88 minute duration and simulated an average intensity of 1.35 in/hr (3.42 cm/hr). The test ceased at approximately 2 in (5.1 cm) because the bowl of the rain garden was full of water and began approaching the sidewalk. The water meter recorded a total volume of 2086 CF (59.1 m^3) [which is ~2 in (5.1 cm) storm volume equivalent].

6.2.1. Test 1 Observations

During SRT 1, qualitative observations were made due to the discovery of a gap that caused a leak in the domed riser outflow structure. As ponding started in the rain garden, water levels began to rise contributing to the domed riser's submergence as water levels approached the domed riser's elevation (Figure 6.4).

Figure 6.4 An example of the ponding progression (a-d) contributing to the domed riser's submergence during an SRT.

As the domed riser's pipe submerged, the water level in the rock bed began to unexpectedly rise rapidly. There was a draining sound from the structure, but water was not exiting through the organ orifice device. Rock bed storage was surprising at this point because the water level was only half way up the domed riser's green pipe Figure (b-c) and never penetrated through the top iron domed casket. Side infiltration into the rock bed was anticipated, however, water was not expected to rise at a rapid rate from solely side infiltration. It was determined that there was a gap in the outflow structure between the domed riser's 7.5 in (19.1 cm) opening and the 8 in (20.3 cm) pipe that allowed water into the pipe below the iron domed casket, which discharged directly into the rock bed. It is indicated in Figure 6.5 where the water

began rising in the rock bed (20 min) prior to water being measured in the outflow device (55 min).

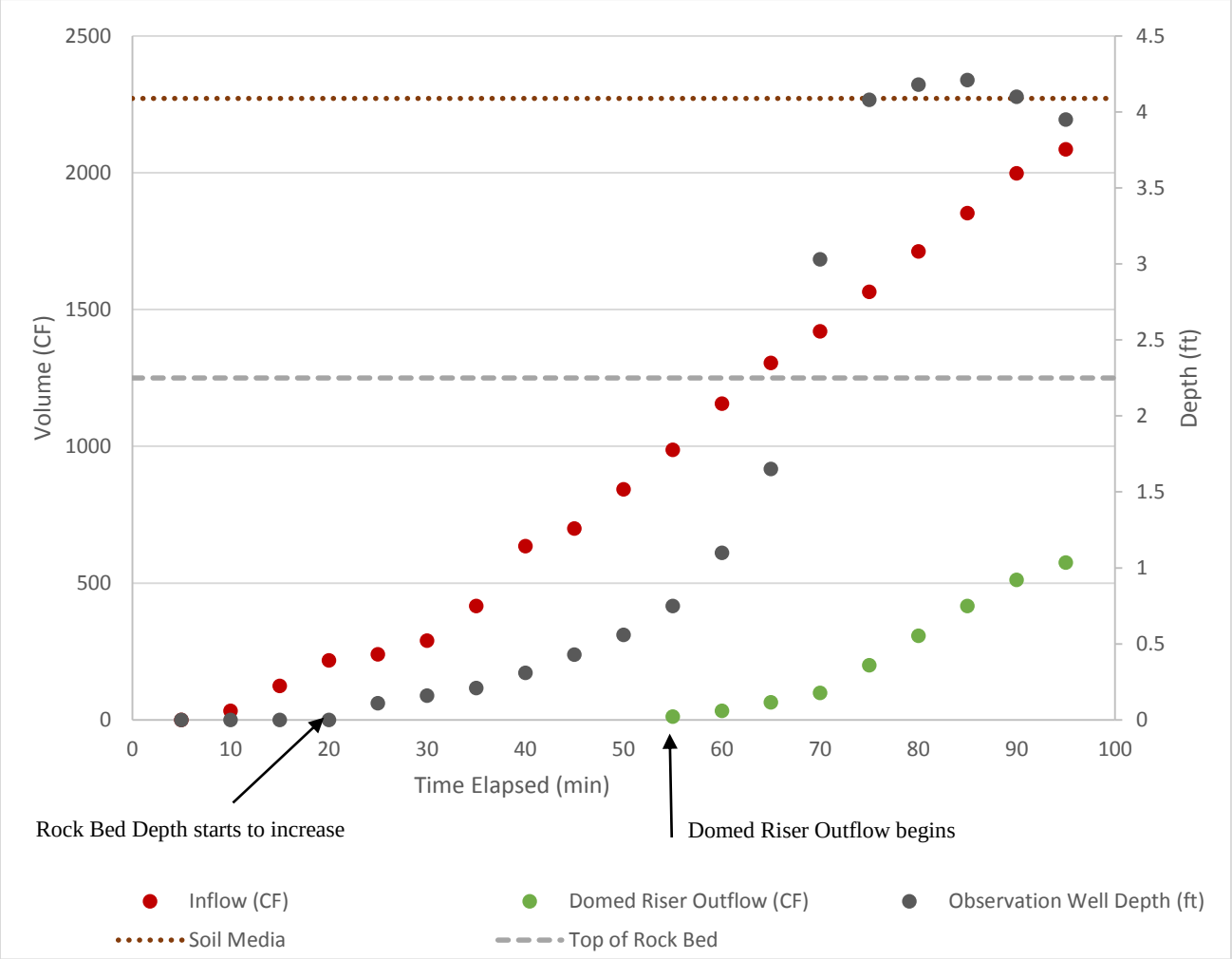

Figure 6.5 SRT results of rock bed depth (ft) increasing prior to outflow measurements through the organ orifice device (CF) due to gap in outflow structure.

6.2.2. SRT 1 Results & Analysis

Simulated Runoff Test 1 illustrated a discrepancy between design and construction. The outflow structure is only supposed to be utilized in the case of an overflow event. Water has been exiting the rain garden system prior to the ponding at the iron domed casket, consequently

escaping prior to an overflow event. An analysis could not be conducted on the organ orifice device due to the gap in the outflow structure.

Inflow measurements of the H-flume were compared to the WL-1250's readings. The WL-1250 water meter recorded a total volume of 2086 CF (59.1 m^3), and the H-flume recorded a total volume of 2214 CF (62.7 m^3). There is a 6% difference between the two measurements. Figure 6.6 shows the 5 minute interval flow rate measurements and exhibits that overall the H-flume records higher flow rates than the Sensus WL-1250. Note, Figure 6.6 displays at 15 minutes the WL-1250 measures zero flow rate. The flow rate was stopped for 3 minutes during testing (from 15-18 minutes) due to checking the fire hydrant's maximum allowable water pressure. The goal for this SRT was to have the highest allowable constant flow rate and as precaution the pressure was double checked mid-test, prior to increasing the flow. The slightly higher measurement error could be attributed to either the H-flume and pressure transducer's measurements, the water meter's measurements, or both. The WL-1250 specifications declare there is an error range between 1-2% of the flow depending on application and flow rates. However, the device is a meter tester and designed to verify the accuracy of meters in a distribution system and is being used as part of monitoring programs in an unconventional application, which signifies that measurement error potentially exists on the water meter's end. The H-flume was tested in a laboratory setting (§4.1), but the WL-1250 has not been tested in a laboratory environment for this specific application. Objectively comparing the results, the error between both instruments is reasonable and further verification of the water meter's accuracy can be evaluated via future laboratory experiments.

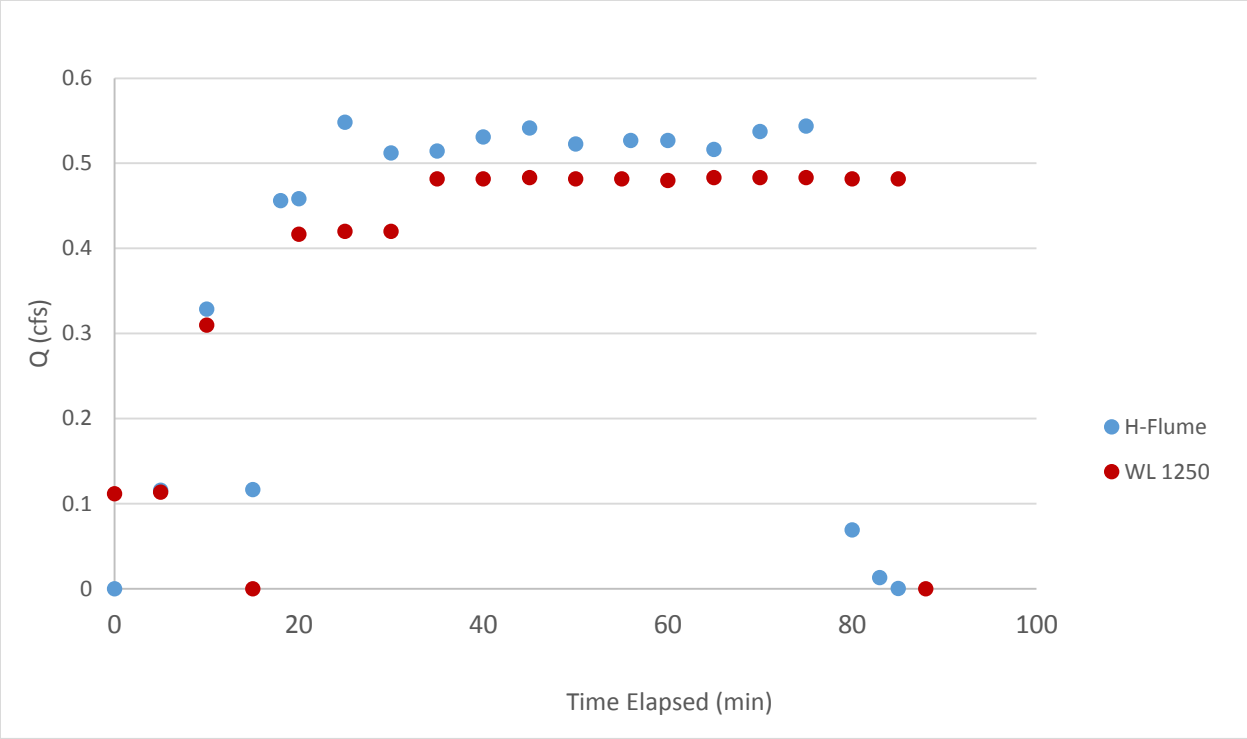

Figure 6.6 SRT (downstream rain garden) flow rate results comparing H-flume and WL-1250 water meter.

Overall, SRT 1 provided valuable information about the site's performance and instrumentation. The downstream rain garden can adequately manage a 2 in (5.1 cm) rain storm event, exceeding its design. Also, discoveries were made about the outflow structure's functionality and utilization prior to an overflow event. The domed riser's gap was addressed by PWD and sealed so that water now enters through the top dome. The SRT provided further confidence in the H-flume's performance for accurately quantifying inflow measurements.

6.3. SRT TEST 2

6.3.1. Test 2 Differences

A second SRT was conducted on March 18th, 2016 for further analysis on the H-flume's performance and the fixed outflow structure. The SRT configuration altered from the previous test, where instead of evaluating the upstream and downstream rain garden individually, a splitter

was installed on the water meter (Figure 6.7) so that both rain gardens could be tested simultaneously. The splitter allows a simulation similar to a real storm event, where water enters both upstream and downstream rain gardens concurrently. This assessment's primary focus still remains on the downstream rain garden with some additional considerations.

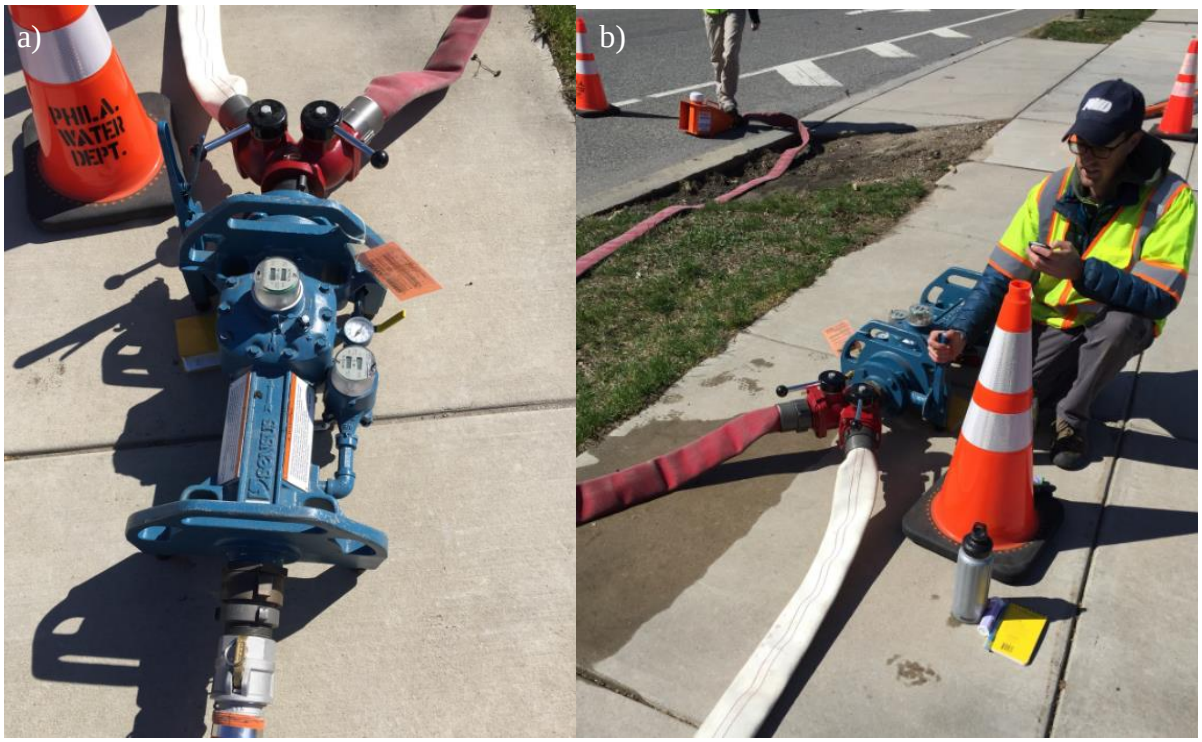

Figure 6.7 (a) Sensux WL-1250 water meter with splitter attachment and (b) fire hoses connected to the water meter and discharging to upstream and downstream rain gardens.

The downstream rain garden is separated from the upstream rain garden by a vegetated swale (Figure 3.3; §3.3.1). When the upstream rain garden overflows, water enters the vegetated swale and ultimately travels into the downstream rain garden. There is a 30 degree V-notch weir directly upstream of the downstream rain garden to measure the additional overflow entering the system (Figure 6.8). The V-notch weir's additional inflow only affects the organ orifice analysis and does not contribute the H-flume's evaluation.

Figure 6.8 Thirty degree V-notch weir and check dam directly upstream the downstream rain garden.

An additional consideration is that the splitter diverts the water meter's recorded flow. It is assumed that the flow is split in half with minimal losses and therefore the total inflow entering each H-flume is one-half the water meter's output. The total output of the WL-1250 water meter was 4683 CF (132.6 m^3) and thus is was assumed that approximately 2341.5 CF (66.3 m^3) entered the upstream and downstream rain garden simultaneously. The simulated storm event represented a 2.3 in (5.8 cm) storm event over a 178 minute duration, which represents a duration 0.8 in/hr (2.0 cm/hr) storm.

Another discrepancy is the amount of water added to the downstream rain garden. Flow was stopped during the first SRT prior to flooding the system. Test 2 determined the rain garden's 'point of failure' – the location where the system overtops the rain garden's bowl and

overflows onto the adjacent parking lot or sidewalk. Water input ceased once the system failed, which was at the total volume of 4683 CF (132.6 m^3) entering both rain gardens. Figure 6.9a shows the ponded rain garden prior to it overflowing onto the sidewalk. The point of failure location was directly downstream the downstream rain garden's outflow structure near the sidewalk pavement (Figure 6.9b). The total volume in the downstream rain garden was approximately 2356.5 CF (66.7 m^3) (including the additional 15 CF (0.42 m^3) inflow from the V-notch weir).

Figure 6.9 Overflow of zoo rain garden onto adjacent sidewalk; (a) ponded rain garden prior to it overflowing onto the side walk, (b) failure point of the Philadelphia Zoo rain garden system, located directly downstream of the domed riser near the sidewalk pavement

The CS-451 pressure transducers were logged on a one minute interval, which differs from test 1 and the continuous field monitoring (5 minute interval). The 1 minute interval allows for a more robust analysis on interpreting what is happening within the rain garden. The duration of testing was also longer since the flow was being split to the upstream and downstream rain garden. The water meter flow rates were still recorded and adjusted on a five

minute interval following the pattern of increasing the flow rate and maintaining a constant flow. The flow rate was increased and held constant three times.

6.3.2. SRT 2 Results and Analysis

An analysis was conducted on the instrumentation's performance in the rain garden system. The inflow of the H-flume was analyzed with similar circumstances as SRT 1, by a direct comparison of the measurement recordings. The sealed gap in the outlet structure permitted an analysis on the organ orifice device. It is difficult to verify the organ orifice's performance since there is no distinct comparison available (such as a flowmeter installed in the outlet structure, etc.) Therefore, a definitive comparison of measurements is impossible, however there are ways to analyze the device's performance with estimations, which is further discussed in the outflow evaluation (§6.3.2.3)

Prior to assessing each individual monitoring device, the initial data analysis involved objectively examining the flow rates of the inflow and outflow structure compared to the water meter's inflow measurements in order to determine if the data is consistent (Figure 6.10).

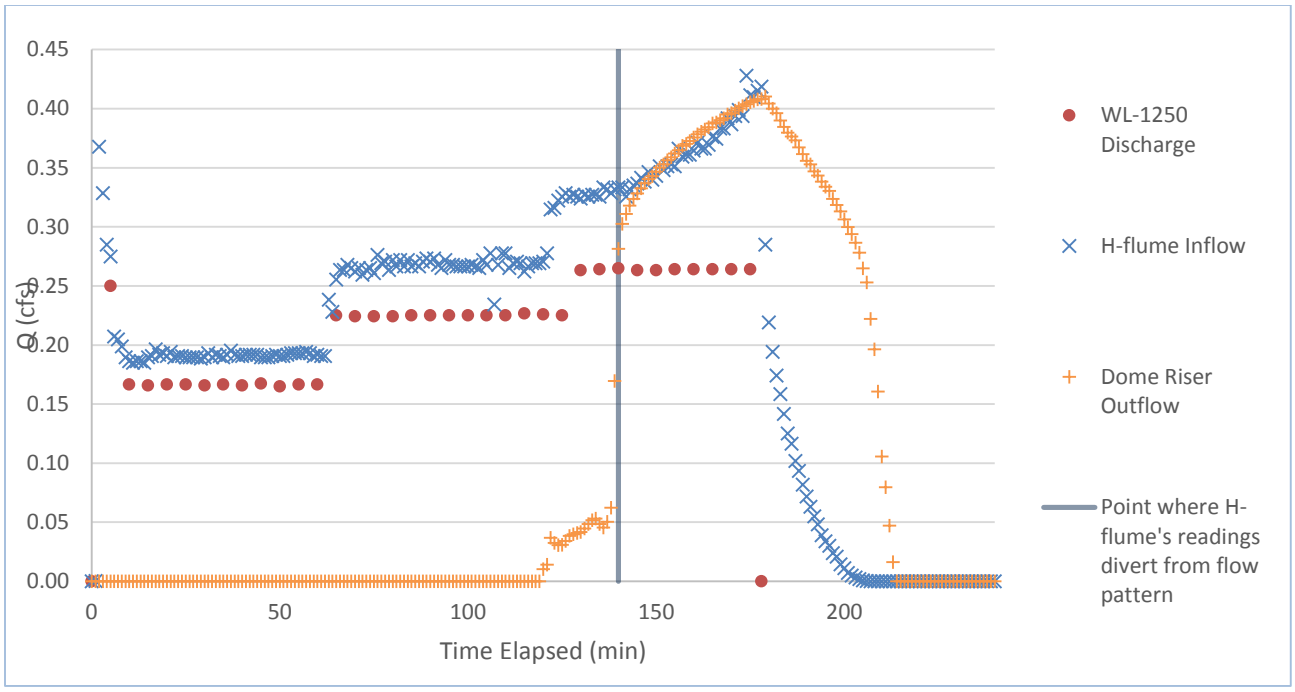

Figure 6.10 Flow rate results of WL-1250 Discharge, H-flume inflow, and domed riser outflow from SRT Test 2.

Strictly examining the first 100 minutes (approximately 50% of the storm event), the performance of the inflow seems reasonable. Similar to SRT 1, the H-flume measured a slightly higher flow rate than the WL-1250 water meter. Initially, the flow rates are very high because the WL-1250 discharged 0.25 cfs (0.007 m^3/s) for the first ten minutes. However, the high flow rate is not the sole contribution to the H-flume's initial large measurements and could be a result of sedimentation and trash flowing through the system. Prior to SRT 1, sedimentation and trash was cleaned out of the H-flume and corresponding inflow channel. Test 2 tried to simulate a real storm event as close as possible, therefore the inflow channel was not cleaned out prior to the test. Figure 6.11a displays a thick layer of sedimentation that was gathered in the H-flume's channel and ultimately swept through the H-flume's outfall. During the first few minutes of the test, leaves and sticks also got trapped in the H-flume's outfall (Figure 6.11b). The trash could have potentially altered the water levels of the system for the initial readings. The initial peak

data point [at 2 min, Q=0.37 cfs (0.010 m^3/s] was presumptively a result of the first wave of trash passing through the H-flume, but the succeeding high flow rates may be exclusively recording the water meter's discharge and is not affected by the minimal remaining sedimentation. Within five minutes, all the sedimentation and trash was washed through the H-flume allowing it to operate under its intended design.

Figure 6.11 Trash and sedimentation in H-flume during SRT 2; (a) sedimentation swept through the H-flume's channel during the initial minutes of Test 2. (b) leaves and sticks being trapped by the H-flume's outfall.

Under initial observation, Figure 6.10 displays inconsistent data towards the end of the SRT from 140 to 178 minutes for the H-flume. The data is concerning because H-flume's flow rate is increasing significantly while the water meter is remaining constant. Typically, the H-flume measures a higher flow rate than the water meter, but it generally follows the same flow pattern (demonstrated in Test 1 and early minutes of Test 2). During 140 to 178 minutes the flow rates divert from the meter's constant flow rate pattern and begins to increase significantly. Since the increasing measurements occur later in the test, the preliminary assumption is that the

rain garden ponding levels were submerging the H-flume (Figure 6.12) as observed during the test. Clearly the measurements during this time interval are not reasonable and requires further investigation as part of the H-flume's analysis and comprehending the instrument's limitations.

Figure 6.12 Submergence of H-flume during SRT Test 2.

As for the domed riser, there are no initial red flags depicted in Figure 7 that indicate a failure in its measurements. Later investigation determined that the organ orifice's operations were sufficient, but not applicable under specific site conditions. Further analysis required evaluating the domed riser with respect to the entire system.

6.3.2.1. Inflow Analysis

Figure 6.10 indicates that there is a discrepancy with the inflow rates specifically towards the end of Test 2. Figure 6.13 illustrates the rain garden's ponding depth increasing as inflow enters the system. The depth measurements are with respect to the lowest point in the rain

garden and depicts the point when ponding reaches the H-flume and increases passed the H-flume's 30% submergence level. As the depth increases pass the 30% submergence line, the inflows begin to increase which elucidates the error between the H-flume and water meter. The H-flume's literature explains that flow rates can accurately be measured up to 30% of its 9 in (22.9 cm) depth, which is 2.7 in (6.9 cm). Figure 6.13 demonstrates that the H-flume can accurately measure flow rates passed the 30% depth during SRT 2. At approximately 140 minutes, the H-flume's depth is 4 in (10.2 cm) [1.4 ft (0.4 m) with respect to the rain garden's ponding depth] and the H-flume's inflow measurements remained constant. Passed this depth, the H-flume's inflow rate begins to increase. Figure 6.13 suggests that during SRT 2, the H-flume can potentially measure inflow up to 4 in (10.2 cm), which is approximately 44% submergence.

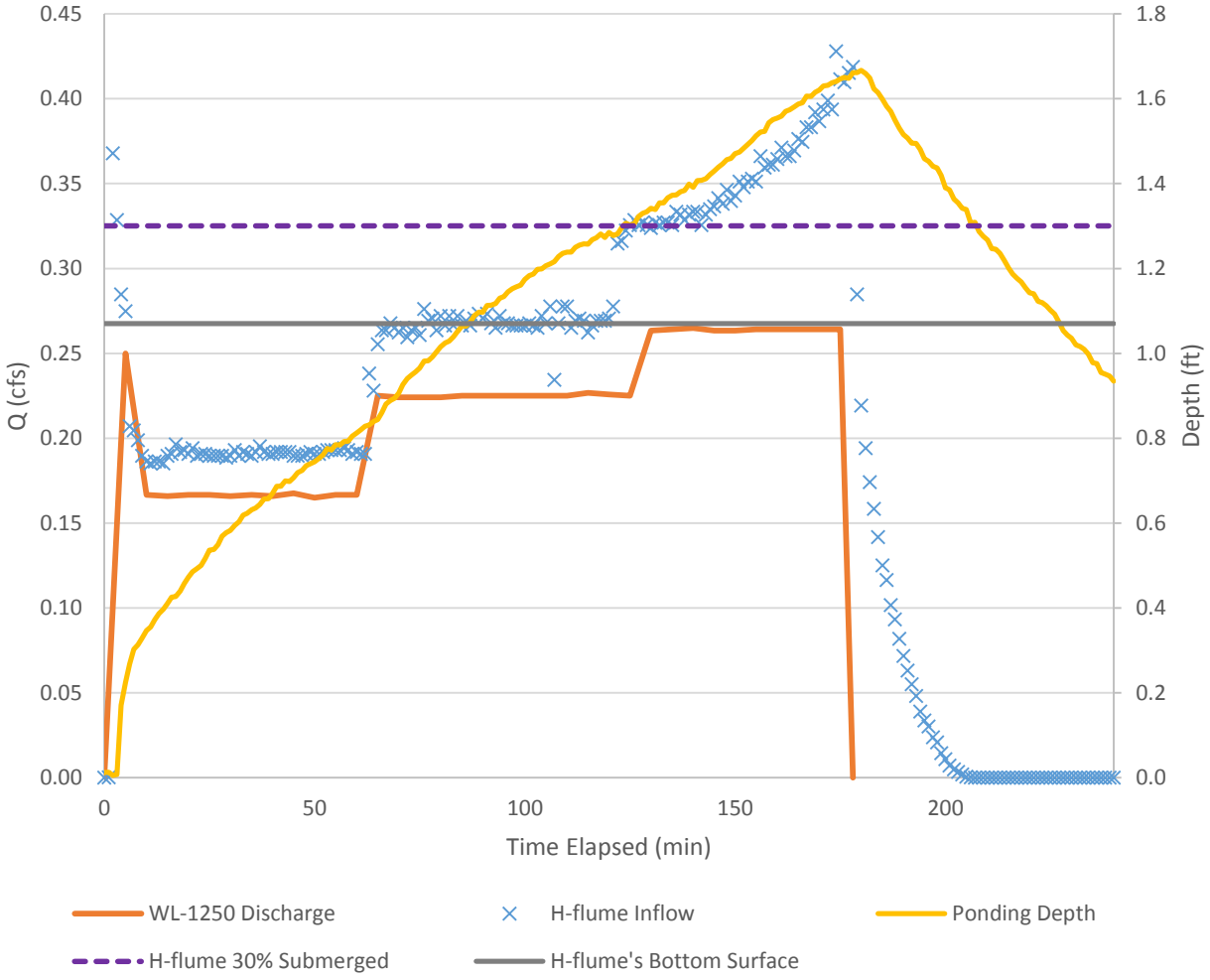

Figure 6.13 Results comparing the H-flume's inflow and rain garden ponding depth with respect to the H-flume's bottom surface and 30% submergence level.

Evidently there is going to be a higher percent difference on the total inflow due to the H-flume's submergence. Table 6.1 depicts the results comparing the total volume measured over 30 minute intervals. After the first 30 minutes there is a 12% difference and the error steadily increases over time. There is a jump in percent difference explicitly after 150 minutes, which is expected due to the H-flume increasing measurements as depicted in Figure 6.10 and Figure 6.13. Table 6.1 displays percent difference above 140 minutes (44% submergence) where there is evidently a larger discrepancy between the H-flume and WL-1250. This difference is only

displayed to indicate the significant difference outside the H-flume's usability and applicable range. The total percent difference between the H-flume and the WL-1250 is 29%, with the water meter outputting a total volume of 2343 CF (66.3 m^3) and the H-flume measuring a total volume of 3011 CF (85.3 m^3) at the conclusion of 210 minutes.

Table 6.1 Elapsed time comparison of total volume (CF) entering the inflow channel measured by the WL 1250 water meter and H-flume. ** indicates recordings outside H-flume's applicable range and measurements recorded against manufacturer's specifications (i.e. pass 30% submergence)

Time Elapsed (min)	WL 1250 Total Vol/2 (CF) (m^3)	H-flume$_{down}$ Total Vol (CF) (m^3)	% Difference
0	0	0	-
30	323 (9.1)	362 (10.3)	12%
60	622 (17.6)	707 (20.0)	14%
90	1017 (28.8)	1174 (33.2)	16%
120	1421 (40.2)	1657 (46.9)	17%
**150	1894 (53.6)	2247 (63.6)	19%
**180	2342 (66.3)	2914 (82.5)	24%

Figure 6.13 clarifies why there was an increase in volume measurements after the inflow ceased. The ponding depth peaks at the same moment the inflow stops. At this moment, the H-flume's measurements are actually recording the rain garden's ponding depth and not the H-flume's inflow depth. Depth measurements are continuously recorded as water infiltrates into the soils, which accumulates volume recordings explaining why the total percent difference is 29% at 210 minutes when inflow concluded at 180 minutes where percent difference was only 24%. From SRT 1 (§6.2.2), Figure 6.6 demonstrates how the H-flume ceases inflow

measurements and how measurements drop to zero. Figure 6.13 depicts an inflow curve that is based off the infiltration depths of the system and does not portray inflow. As a result, the submergence phenomenon affects how to determine the best method of evaluating the system.

The H-flume's purpose is to contribute to the rain garden's whole assessment. The big picture requires determining the best method for analyzing the total inflow volume in regards to a submergence event. Indicated by the percent differences in Table 6.1, including all inflow data leads to insufficient results that are significantly larger than the storm event. Therefore, several approaches can be taken regarding which portion of data should be accounted for in the estimation. Figure 6.14 displays the marked values when the H-flume is passed 44% submergence (during 140-180 minutes).

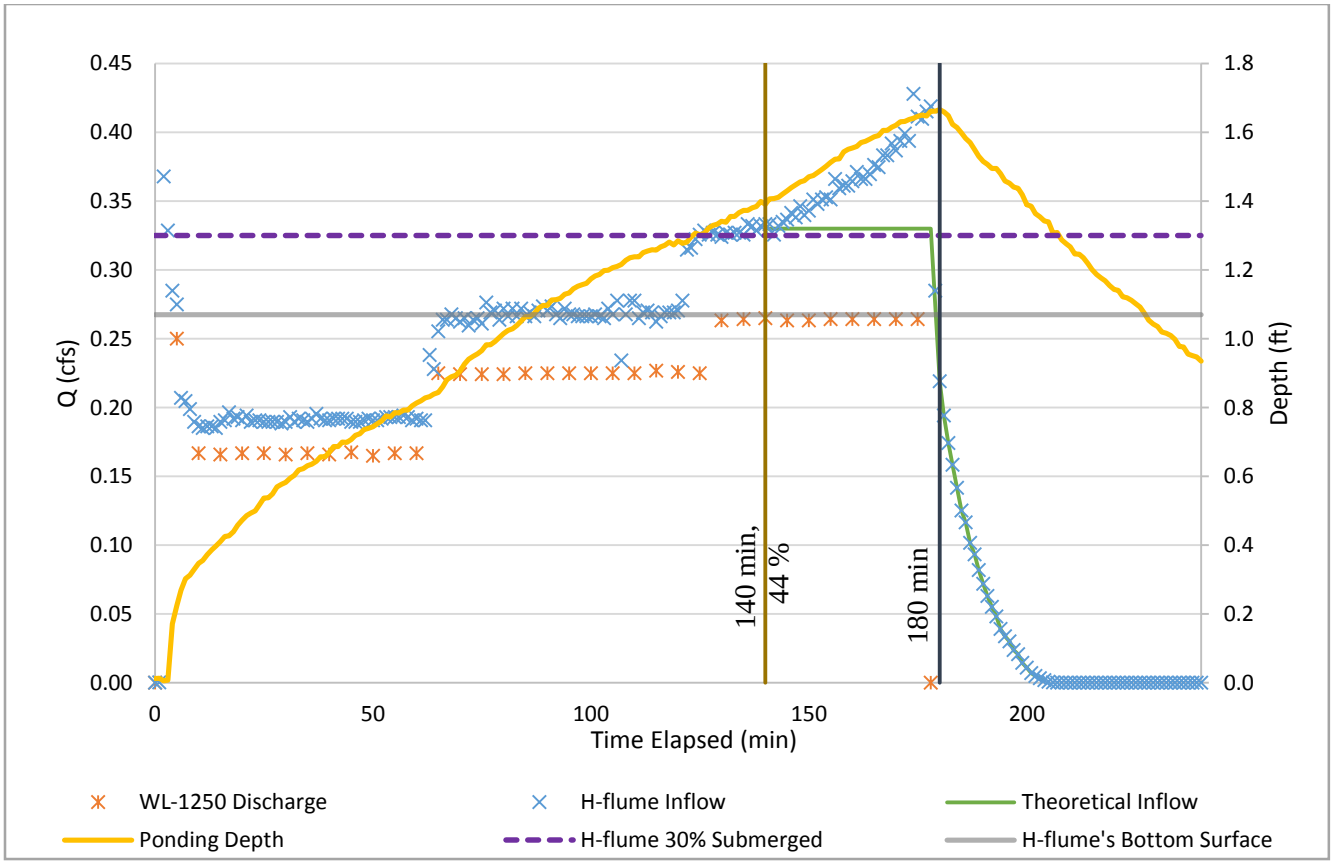

Figure 6.14 H-flume and WL-1250 inflow specifying the time interval greater than 44% submergence (140 – 180 min).

The first approach is to analyze the data from the time interval, 0-140 min, and disregard the succeeding values. This approach assumes that once submergence occurs, data is insufficient for the remainder of the event. The second approach is to include all the recorded values up to the highest peak (where it is presumptively assumed that flow has ceased) at 180 minutes and neglect the falling limb data. This approach assumes that once inflow stops, the falling limb is strictly the rain garden's ponding depth infiltrating and does not contribute any additional inflow volume. The third approach is identified as a 'theoretical inflow' depicted in Figure 6.14. The theoretical inflow replaces all inflow greater than the 44% submergence with the constant flow rate at the time submergence occurred. Once the submergence subsides beneath 44% submergence, then the inflow is equal to the recorded measurements. The final approach is to neglect all data greater than 44% submergence (140 to 180 min) and compute inflow with all recordings (on the rising and falling limbs) beneath the submergence. All results were compared to the WL-1250 water meter's final volume of 2341.5 CF (66.3 m^3). Table 6.2 displays each method's computed volume and associated percent error. Each method makes different assumptions regarding what is considered adequate data. The table indicates that the best method for estimating volume is the last method, to include all data below the 44% submergence and neglect any measurements above 44% submergence.

Table 6.2 Methods and results for estimating inflow volume during the H-flume submergence event.

Method	WL-1250 (CF) (m^3)	H-flume (CF) (m^3)	% Difference
0 to 140 min (disregard all data pass 44% submergence)	2341.5 (66.3)	2045 (57.9)	12.7%
0 to 180 min (include all submergence data up to peak, disregard falling limb)	2341.5 (66.3)	2913 (82.5)	24.4%
Theoretical Line	2341.5 (66.3)	2893 (81.9)	23.6%
All Data below 44% submergence	2341.5 (66.3)	2143 (60.7)	8.5%

Simulated Runoff Test 2 was only 178 minutes and the inflow into the channel concluded at approximately 180 minutes. One flaw with this analysis is that since the WL-1250 was never tested within a laboratory setting and as a result, the water meter's error is unknown. Prior to submergence, it is assumed that difference between the H-flume and water meter would be minimal, but at 140 minutes the water meter measured 1736 CF (49.2 m^3) and the H-flume measure 2045 CF (57.9 m^3), which estimated a 17.8% difference. The error is significantly higher than expected especially considering that SRT 1 produced overall a 6% difference. Table 6.1 indicates that the larger discrepancy was present from the beginning of the test and steadily increased throughout. The significant increase could be attributed to the techniques of using splitter attachment in congruence with the water meter. The attachment was intended to divert the flow in half so that the upstream and downstream rain garden captured inflow simultaneously. The WL-1250 specifications state not to bend the fire hose connected downstream of the water meter because it could result to back pressure propagating difficulties with the water meter's functionality (SENSUS 2016). Figure 6.7b (§6.3.1) indicates that the fire hose connection is bent from the water meter to the upstream rain garden in two locations. The

bent fire hose could have implications and potentially caused backflow into the water meter resulting to either incorrect measurements or causing more water to divert downstream. The disproportionate flow could result in the H-flume being more accurate than the water meter. Further investigation on the upstream rain garden could address the large discrepancy.

The results determined that the H-flume inflow measurements for SRT 2 should only be considered up to 44% submergence and recordings pass this depth should be disregarded. Disregarded inflow data passed 44% submergence levels will rarely occur because Philadelphia typically experiences lower volume storms. The simulated storm event represented a 2.3 inch (5.8 cm) storm event over a 178 minute duration, which represents a long duration 0.8 in/hr (2.0 cm/hr) storm, an intense event. It is recommended a storm event that replicates SRT 2 where the H-flume is submerged for a 0.8 in/hr (2.0 cm/hr) storm event, readings are considered reasonable up to 44% [4 inch (10.2 cm)] submergence.

6.3.2.2. Depth Analysis

A depth analysis was also investigated at all pressure transducer locations (Figure 6.2, §6.1). Figure 6.15 displays depth recordings at the rock bed, domed riser, rain garden, and H-flume. Everything is graphed with respect to the surveying data and the datum is set to the bottom of the observation well in the rock bed. According to the site's drawings (Appendix B, Figure B.5) the rock bed is 45 ft (13.7 m) long by 4 ft (1.2 m) wide and has a 2.25 ft (0.7 m) depth. The increase in height passed 2.25 ft (0.7 m), depicted in Figure 6.15, is the measurement of water increasing in the observation well within the rock bed.

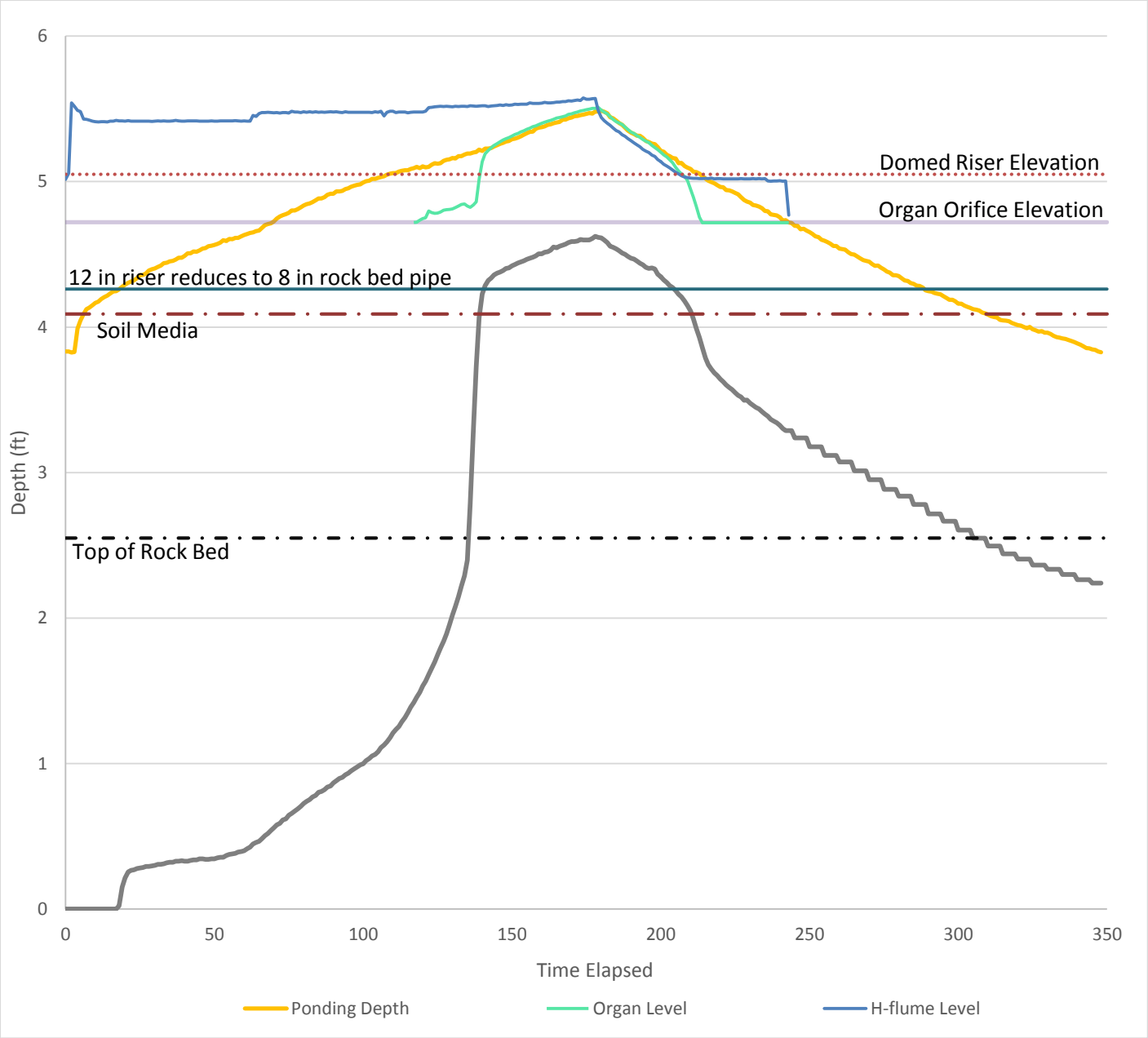

Figure 6.15 SRT Test 2 depth measurement results throughout the system with the bottom of the observation well as the datum.

Figure 6.15 demonstrates that the peak of all depth levels occur at the same time, approximately at 180 minutes (when the inflow, represented by the H-flume level, subsided). The ponded depth of the rain garden at 180 minutes is 1.67 ft (0.5 m) which is the point where the system began to flood over the edge of the rain garden onto the sidewalk. It is interesting to

note that immediately after the system's peak, all four locations have a similar descending slope. At this point, the recorded change in ponded and rock bed depth is based on the rain garden's infiltration as recorded by the pressure transducers at the shallow well, H-flume, and organ orifice device. For a short period of time even the rock bed, which is situated on a 6 in (15.2 cm) layer of sand, has the same slope as the pressure transducers installed in the rain garden which is peculiar since the rock bed has different soil characteristics than the rain garden. The rock bed depth and domed riser depth have a sharp rise at approximately 135 minutes, then both steadily increase with a similar slope to the rain garden's ponding depth.

Once the rock bed is completely full, the outlet pipe from the domed riser begins to fill with water. The organ orifice is acting similar to the H-flume where its outflow is being restricted and thus is incapable of recording accurately to the calibrated rating curve. As a result, an analysis on the organ orifice's performance is intricate.

6.3.2.3. Outflow Analysis

The initial approach is to determine if the data is sensible. It is difficult to conclude if it is accurate data since there is no direct comparison, but an indicator of unreasonable data would be if the device recorded a total volume larger than total inflow. The total recorded volume for the outflow was 1538 CF (43.6 m^3), which is less than the water meter and weir's inflow of 2357 CF (66.7 m^3).

The next approach is to the compare outflow volume to the rock bed storage. As discussed in §6.3.2.2, the depth analysis concludes that the organ orifice's outflow is potentially being restricted and cannot adequately measure depth for the associated rating curve. Therefore, the organ orifice can only be evaluated where the device is operating properly under its intended

design. Figure 6.16 displays the organ orifice's water level without the restricting rock bed assumption from 115 to 140 minutes.

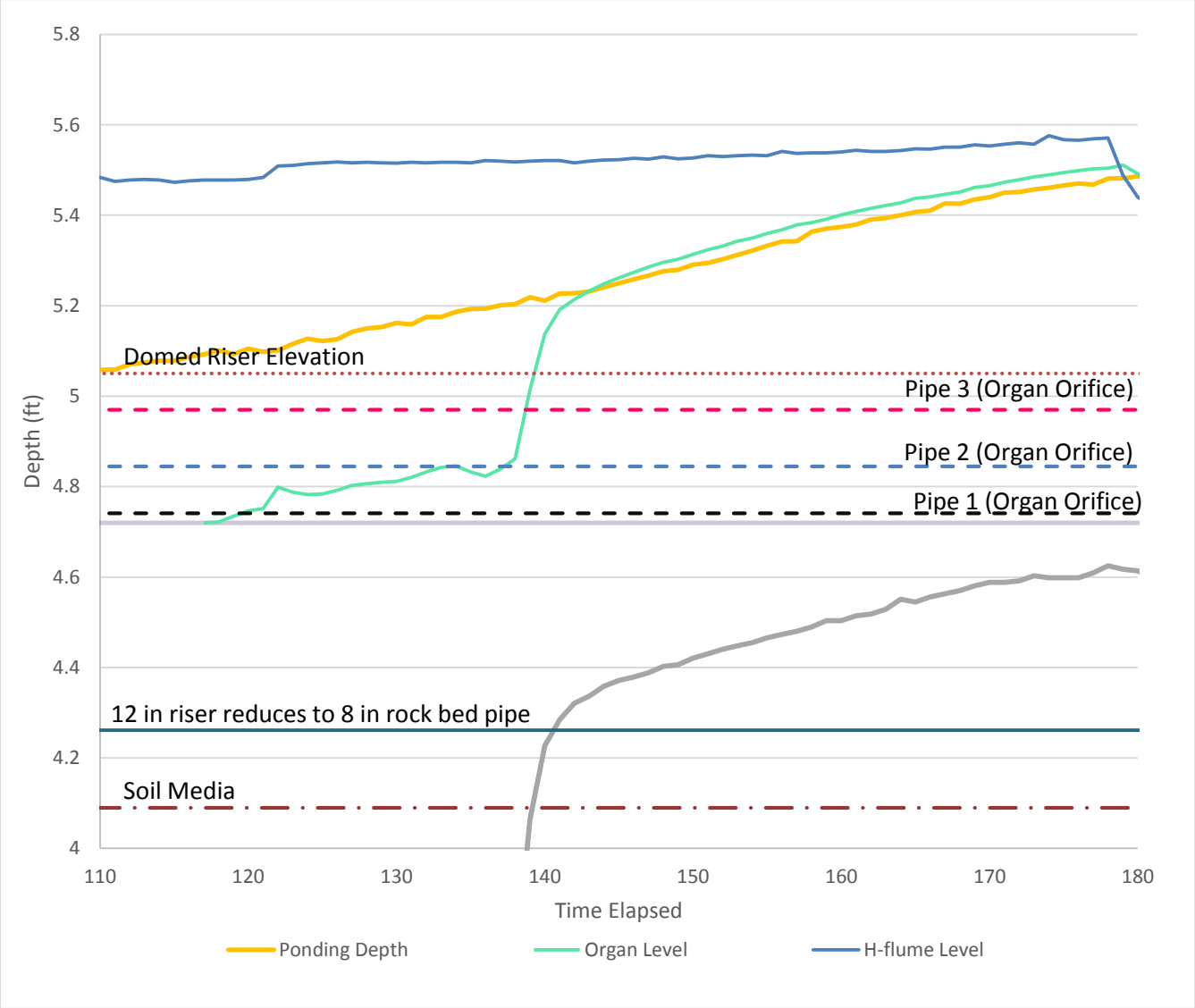

Figure 6.16 Organ orifice and rock bed depth from 115 to 140 minutes.

During this time interval, the level of the observation well increases from 1.49 ft (0.45 m) to 4.22 ft (1.29 m). There are several impediments with using the difference of 4.22 ft (1.29 m) and 1.49 ft (0.45 m) as depth for estimating the rock bed storage. The rock bed has already risen to a depth of 1.49 ft (0.45 m) prior to any outflow the domed riser, which insinuates that there is

side infiltration and possibly still a small leak existing in the domed riser that is attributing to the rock bed storage. Another factor is that the rock bed only has a maximum depth of 2.25 ft (0.69 m) (according to drawings) and the remaining depth is the water increasing solely in the observation well. At 133 min, the level in the observation well is 2.21 ft (0.67 m) (which is within the rock bed storage) therefore the rock bed storage was estimated between 119 and 133 min. The depth at 133 min (2.21 ft) was subtracted by the pre-existing 1.49 ft (0.45 m) depth, computing a final depth of 0.72 ft (0.22 m). The final rock bed volume calculation values had depth equaled to 0.72 ft (0.22 m), length as 45 ft (13.72 m), and width as 4 ft (1.22 m) with assuming porosity of 0.38. The rock bed storage estimated 49.3 CF (1.39 m^3) and at 133 minutes the organ estimates an outflow volume of 32.9 CF (0.93 m^3) which is a 39.8% difference. A 39.8% difference is expected with the previous storage estimation because side infiltration (or any potential pipe leaks) was not accounted for in the calculation. The estimated depth should deduct the excessive contributing flow. Prior to the domed riser outflow, the depth increases from 1.22 (0.37 m) to 1.48 ft (0.45 m) the preceding 14 minutes (104 to 118 min). The difference in height is 0.26 ft (0.08 m) over a 14 min interval (same time interval for the estimation of the rock bed storage). The depth was adjusted from 0.72 ft (0.22 m) to 0.46 ft (0.14 m) and thus the computed rock bed volume was 31.5 CF (0.89 m^3) which is a 4.3% difference from the organ orifice's output 32.9 CF (0.93 m^3).

Although the comparison between the rock bed storage and organ orifice outflow is within 1.4 CF (0.04 m^3), many assumptions were made for the estimation. The comparison was only made over a 14 minute period with fairly low flow rates. Also, the exact rock bed's dimensions and porosity size are unknown. The results appear to be accurate, however, there is no certainty of the reliability and exact accuracy of the system. The SRTs demonstrated the

difficult process of accurately capturing flow and establish that even with extensive testing, there is never 100% certainty with monitoring. Nevertheless, the advantage of SRTs is to look at the functionality of the system components and instrumentation's measurement ability.

6.4 SRT Inflow Test Comparison

Further evaluation was conducted on the differences between the two SRTs. Both SRTs experienced large volume storm events, but the durations and intensities differ greatly. SRT 1 was directed for an 88 minute duration and simulated an average intensity of 1.35 in/hr (3.42 cm/hr), which computes to a total volume of 2086 CF (59.1 m^3). SRT 2 was conducted for 178 minutes at an average simulated intensity of 0.8 in/hr (2.0 cm/hr), creating a total volume of 2356.5 CF (66.7 m^3). Unfortunately, due to the construction error, a comparison could not be determined for the outflow structure and only the H-flume was examined.

The H-flume captured inflow more effectively for SRT 1 than SRT 2, which could be attributed to a number of variables (as discussed per §6.3.3.1). H-flumes are typically applied only where there is free-spilling discharge because submergence can result to higher flow rates than those actually experienced. The large volumes from both simulated storms caused significant ponding within the system and observationally it appeared that both H-flumes experienced substantial submergence. Therefore, it was questionable why the H-flume did not experience similar increased flow rates during SRT 1 as it did during SRT 2. The TRACOM H-flume allows for 30% submergence, but Figure 6.17 clearly dictates two situations where the H-flume's performance is adequate surpassed 30% submergence.

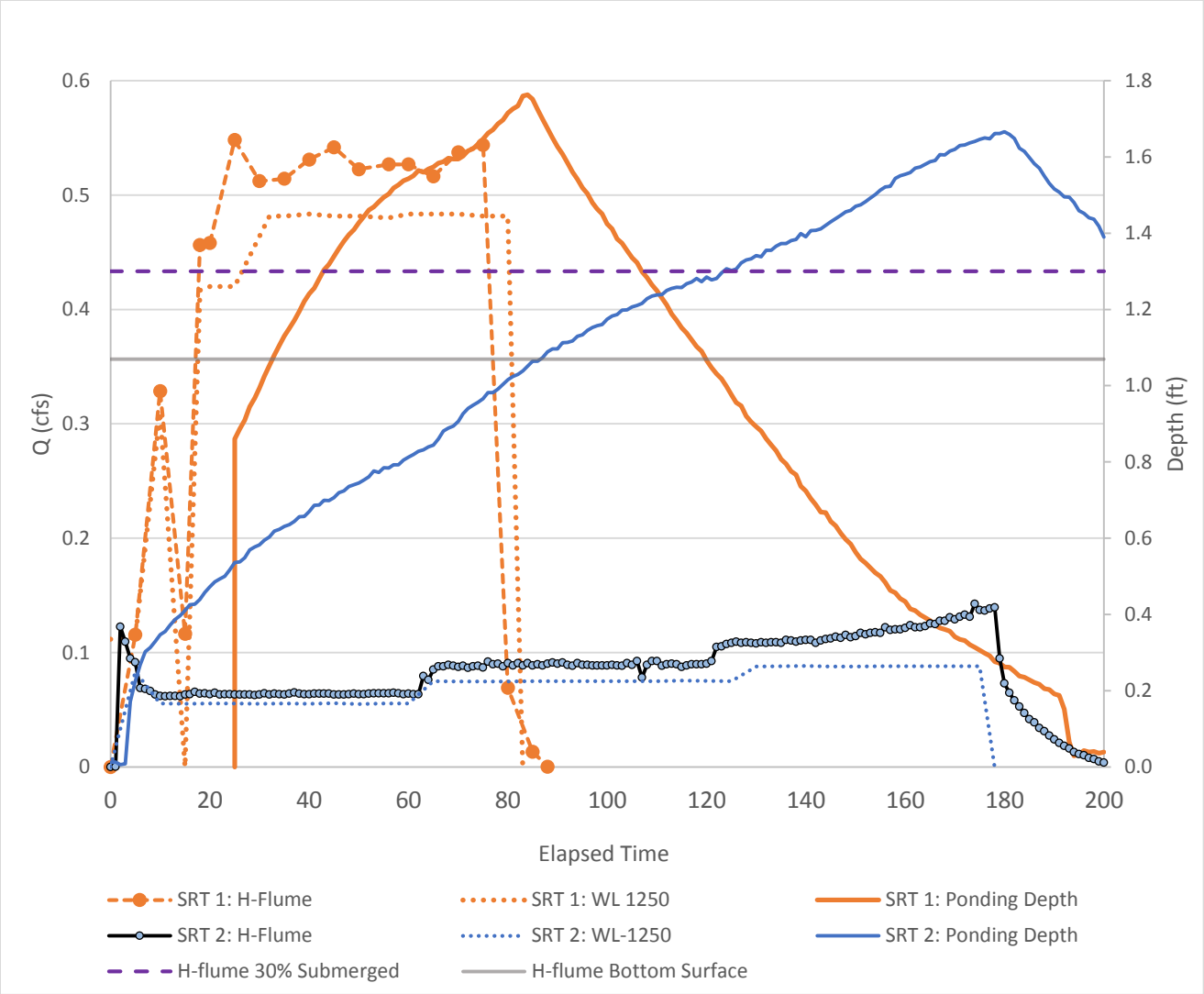

Figure 6.17 H-flume performance comparison between SRT 1 and SRT 2

Figure 6.17 displays an inflow comparison between the two SRTs, particularly examining the inflow and ponding depth in the rain garden. The ponding depth between both SRTs is within 1 in (2.5 cm). Both ponding depths significantly surpassed the H-flume's allowable 30% submergence and in SRT 2 the H-flume was only capable of measuring flow rates up to 44% submergence. However, SRT 1 was able to capture flow rates significantly pass this point, which suggests that the H-flume's submergence capabilities is dependent on the flow rate entering the H-flume. The H-flume makes measurements based on critical depth, thus for a

different flow rate there will be a different critical depths. As a result, changing the critical depth would consequently alter the allowable critical submergence. This assumption calls for further research testing varying critical depths compared to different submergence levels. Parshall flumes also experience a similar relationship with submergence, where the tailwater causes discontinuity for incoming headwater and there are different correction factors and plots dependent on the upstream head and percent submergence (USBR 1988). Further research needs to be conducted to verify if this is phenomenon is occurring within the Zoo rain garden's H-flume.

6.5 SRT Summary

Both SRTs discovered components of the rain garden's performance specifically under large storm events. The simulated storms' intensity and long duration truly push the monitoring equipment's limitations with subjecting the devices to significant ponding. Considering the variables in field monitoring, the monitoring equipment proved to be sufficient with capturing the storm events. A model built to correspond with the field data could further evaluate the rain garden's performance. The collected data from the SRT contributes to comprehending measurements for real storm events, specifically with the inflow and outflow monitoring equipment, to determine if the system is functioning under its intended inflow and outflow design or under submergence. The SRTs provided a further understanding about how the rain garden functions and the collected data can enhance a model for the system.

CHAPTER 7: SUMMARY

Instrumentation governs the quality of recorded data that significantly affects meaningful results from any research project. The selection and verification of monitoring equipment can be a tedious process, but is essential to understanding a sensor's specific function in desired research applications. For example, in urban stormwater monitoring, there is no go-to monitoring system that can be bought off the shelf; each monitoring goal requires a custom sensor-equipment configuration. It is imperative to test instrumentation in laboratory environments and also in field settings in order to determine if sensors are operating under their intended design. Three monitoring devices were evaluated for inflow and outflow structures in urban SCMs. An H-flume was selected as an inflow measuring device for a rain garden's surface inlet channel from street flow, an ADV sensor was selected as an inflow measuring device for a tree trench's 8 in (20.3 cm) subsurface pipe, and a custom unique designed orifice meter was developed for a rain garden's domed riser outlet structure. The objective of this research was to verify each instrument's reliability for capturing flow rates, determine its functionality under each specific site's conditions, and understand the sensor's overall operation in congruence with the site's performance. Laboratory experiments were conducted on each device to verify its accuracy, along with field analysis. If laboratory experiments were successful, then Simulated Runoff Tests were used to investigate each sensor's capabilities in the field under simulated storm conditions.

7.1 CONCLUSION

A 0.75 ft (0.23 m) (22.86 cm) TRACOM H-flume was selected for the Philadelphia Zoo rain garden's surface inlet channel primarily because it could accurately record a wide range of flow rates [0-0.957 cfs (0-0.0271 m^3/s)]. Laboratory testing was conducted in order to verify

factory calibration. Eight laboratory tests encompassed incrementally increasing/decreasing flow rates and varying flow rates in which all tests confirmed factory calibration a with a 3% root mean square error (§4.1.1.5). Two SRTs were conducted at the Philadelphia Zoo's downstream rain garden to assess the field installed H-flume. Each test directly compared inflow from the WL-1250 water meter to the H-flume's measurements. Test 1 evaluated a volume of 2086 CF (59.1 m^3) entering the rain garden and the H-flume recorded a total volume of 2214 CF (62.69 m^3) which resulted to a 6% difference. In SRT 2, the downstream rain garden was subjected to an approximate volume of 2356 CF (66.71 m^3) as measured by the WL-1250 water meter. This is a tremendous amount of water [2.3 in (5.8 cm) storm event], and ponding depths caused the flume to be submerged. The H-flume specifications indicate that the H-flume can adequately measure flow rates while under 30% submergence. Test 2 demonstrated that the H-flume was sustaining flow measurements under 44% submergence [an inflow up to 4 in (10.2 cm) depth], however, passed this point the recorded data was insufficient for an analysis. Prior to submergence, the H-flume recorded 2045 CF (2045 m^3) and the water meter recorded 1736 CF (49.2 m^3) which resulted to a 17.8% difference. It is inconclusive whether the difference in measured inflow volume originated from an error with the H-flume or WL-1250 water meter. Considering the H-flume's accuracy in laboratory investigations, it is presumptively assumed that error may be associated with the unconventional techniques of using the splitter attachment and water meter. Future laboratory exploration can address the error between the two systems.

The FloWav-PSA ADV sensor was selected for the Morris Leeds tree trench's subsurface pipe because of the sensor's low intrusiveness, versatility, and ease of installation. In order to expedite research, two sensors were immediately installed in the field and one was used for laboratory investigation. A custom Arduino datalogging system was used in conjunction with

the sensor in the lab that resulted inaccurate measurements. Laboratory experiments attempted to account for inaccuracies by troubleshooting errors with the ADV sensor's pressure transducer and Doppler velocity sensor. All laboratory tests were insufficient and as a result, the sensors were removed from the field. Additional research and consultations with the manufacturer provided information about the ADV sensor's learning software. This information was not known prior to laboratory testing and could have altered testing procedures and outcomes. The field data provided information about sedimentation in field conditions and maintenance requirements.

The research conducted on the ADV sensor taught valuable lessons for future sensor selection and testing procedures. It is necessary to fully understand sensor properties as it relates to hydraulics of the field research conditions, specifically with new technologies that may be deployed in research applications that were not intended for the sensor's design. Also, testing multiple technologies simultaneously conflicts with addressing sensor accuracy and identifying error sources. This difficulty was encountered with testing the ADV sensor in congruence with the Arduino datalogging system, without knowledge of the internal data processing attributes. There was not enough background knowledge on how both sensors would operate together, and therefore, the Arduino datalogging system should have been separated from the ADV sensor. The field maintenance enlightened the potential future problems with sedimentation and it is necessary to understand the nature of the sediment effects on the system. Also, the Morris Leeds site encounters low intensity storm events with flow effects less than the deadbands. Overall further examination is required to understand the statistical conditioning methods within the sensor and associated datalogger's settings, specifically within its application at the Morris Leeds site.

The unique design of the Philadelphia Zoo rain garden's outflow structure, the domed riser, required a custom in-house design in order to record a range of flow rates. The objective was to create a device with a reliable head-discharge relationship that would not conflict with the site's performance. Several prototypes were created that influenced the development of the final organ orifice design comprising of a 11.5 in (29.21 cm) plate with three pipes in the center increasing in size and elevation: 2 in (5.1 cm) pipe at a 0.25 in (0.635 cm) above the plate, 2 in (5.1 cm) pipe at 1.5 in (3.81 cm), and 3 in (7.62 cm) pipe at 3 in (7.62 cm). A five piece linear regression model was developed for the device that mimicked a similar relationship as the weir and orifice equations, $Q = C_1 H^{C_2}$ where C_1 and C_2 were arbitrary constants unique to the device's discharge relationship. The five sections of the regression model dictate the location of water measurements in each pipe with respect to weir or orifice flow. SRT 1 determined that the domed riser was bypassed and thus was not able to evaluate its results because of a construction error and consequently no conclusion was made on the organ orifice's performance. The construction error discovery stresses the importance for field testing. An estimation of the rock bed storage was used for comparing the organ orifice's device for SRT 2. The analysis evaluated the organ orifice's performance from 115 to 134 minutes when it was functioning according to its intended design of free outflow. The device measured 32.9 CF (0.93 m^3) and the rock bed storage estimated 34.1 CF (0.97 m^3), a difference of 1.2 CF (0.03 m^3). A full time interval analysis could not be conducted on the organ orifice because it was restricted in its measurements by the rock bed filling up with water and constricting further inflow.

Successful laboratory experiments provided confidence in each sensor's measurements, but it was necessary to examine their functionality within the urban environment. Field conditions greatly differ from laboratory settings, especially in urban environments which

encounter sedimentation, trash, vandalism, etc. The SRT is a method that can simulate storm events to evaluate each monitoring device's measurements and also understand the site's performance. Simulated runoff tests demonstrate how an SCM operates and reveals any faults with the SCM and the monitoring design. During large rain storm events at an intensity 0.8 in/hr (2.0 cm/hr), it was discovered that the H-flume's submergence is effective in monitoring inflow up to 4 in (10.16 cm) depth, which is higher the expected 2.7 in (6.86 cm). During SRT 1, submergence did not affect the H-flume's performance due to a discharge from a higher intensity at 1.35 in/hr (3.4 cm/hr). Further exploration is required in order to determine the relationship and capabilities of measuring flow rates under submerged conditions. Additional comprehension of the system's hydraulics were discovered, specifically regarding the domed riser and how the rock bed can constrict the flow from the overflow device. Regulated field tests, where possible, are encouraged to gain confidence in the monitoring equipment and subsequent collected data.

The ADV sensor's complications is one example why it is imperative to test monitoring equipment under its desired research application. Care must be taken when applying manufacturer's accuracy specifications since each sensor is installed in a unique environment that typically differs from the manufacturer's laboratory settings. An example would be that the majority of storm events would be not able to be recorded due to low depths and velocities. Laboratory experiments should replicate field conditions and investigate all projected situations that is substantial for research. The laboratory tests in this research provided further knowledge about each device's capabilities as well as further understanding on its measurement reliabilities.

7.2 FUTURE WORK

The instrumentation is installed as part of a research grant to evaluate the current generation of green infrastructure SCMs in order to develop, design, and validate next generation

SCMs in coordination with Philadelphia's Green City, Clean Waters Initiative. Further testing will be conducted on the sites to evaluate each SCM's performance and the testing will correspond with further research on this project. With proper maintenance, monitoring equipment's accuracy can be maintained over time and reassessments should be conducted periodically.

7.2.1. Additional SRT Investigations

Further testing should be conducted on every instrument to thoroughly understand the performance of each device under different circumstances. Although this research is focused on the operation of monitoring equipment, the previous SRTs proved that the site's performance affects a device's measurements. So far the only simulated storms for SRTs have been a constant duration of a high steady flow rate, but this systematic simulation is not the case for every storm event. Storm events can vary intensities and also stop for periods of times and then continue. All SRTs were conducted without any storm events in the preceding days. Simulated runoff tests could be conducted while the soil is saturated, over numerous flow rates, and also over various seasons to see if the site's performance and instrumentation's measurements alters. Numerous SRTs can provide additional confirmation on monitoring equipment's accuracy, which brings further confidence in the collected data for each site's continuous monitoring program.

The WL-1250 water meter should be tested in a laboratory setting to verify its accuracy. Laboratory testing needs to replicate the water meter's operation in field studies since it is being utilized in an unconventional assessment for SCMs.

7.2.2 H-flume

The urban environment subjects the H-flume to perpetual trash and sedimentation (Figure 7.1a) altering the water levels in the H-flume's stilling basin. Future SRTs conducted should specifically consider the inflow of trash to determine if there is a prominent impact on flow rate measurements. Test 2 evaluated a small sample of sediment and trash passing through the H-flume. However, different trash (i.e. plastic bags, bottles, empty chip bags, etc.) could vary the H-flume's performance for some unknown amount of time and one future experiment could evaluate the system with different debris scenarios. Seasonal variability is also another future test consideration as the H-flume is exposed to leaves in the fall (Figure 7.1b)

Figure 7.1 Urban effects on H-flume (a) Natural, urban sedimentation, trash, and debris that the H-flume encounters. (b) Seasonal debris the H-flume is subjected to during fall.

7.2.3 ADV Sensor

Tests are currently being conducted on the FloWav sensor with its corresponding datalogger (FW-33 DCL). Laboratory experiments are investigating the FloWav's accuracy and learning software under the manufacturer's intended design. If conclusions declare the ADV

sensor sufficient then the sensor may be redeployed at the Morris Leeds tree trench site. Simulated runoff tests will also be conducted if and when the ADV sensor is installed in the field. Since the FloWav has a learning software, then special considerations should be made for the SRTs. Only expected storm events should be simulated because the in-field testing could alter the sensor's future measurements.

7.2.3 Orifice Organ

There has been no storm event thus far that resulted to an overflow event. Therefore, the domed riser has only been evaluated under SRT simulations. The previous inactivity of the organ orifice could be a result of there being gap in the riser (§5.2.1), which was corrected in March 2016. It would be interesting to evaluate the organ orifice device in congruence with a real storm event to see if it functions similarly to the SRT (i.e. the rock bed constricting inflow into the domed riser), or see its performance under a high intensity storm event that is faster than the rain garden's infiltration rate. Once a comparison is made between the SRT and a real storm event, then it could determine how to perform the future SRTs. An SRT should be conducted to represent a similar storm event that the domed riser experiences. Understanding the rain garden's performance in congruence with the organ orifice will further help in modeling the site.

7.3 CLOSING THOUGHTS

Acquiring reliable instrumentation for a specific research application is a tedious process that involves preliminary research, laboratory experimentation, and field testing. The preliminary research includes comprehending the manufacturer's specifications in addition to investigating background information for the site's design. Understanding the manufacturer's specifications in correspondence with the research site is essential, but also limiting with interpreting collected data. Therefore, further investigation is required through laboratory and

field exploration. Laboratory exploration can verify the sensor's accuracies and additionally, reveal exactly how the sensor operates under ideal laboratory conditions. Laboratory testing may justify a sensor's reliability, but the ultimate comprehension of the sensor's data for a specific research application is through field testing. Field testing not only confirms the sensor's operation, but also reveals any discrepancies encountered in the sensor's measurements consequently of the site's design. It is particularly beneficial to perform laboratory and field experiments to correctly address any uncertainties in field data. Comparing laboratory results and the tested field results specifies if an uncertainty is attributed to the sensor, site's performance, or combination of both. The thorough instrumentation process, from preliminary investigation to laboratory and field testing, is the best method for correctly comprehending the relationship between the monitoring site and its associated equipment as well as the optimal technique for accurately interpreting collected data in applied research.

Regarding instrumentation, the procedural methods discovered many entities of the H-flume, ADV sensor, and unique organ orifice design. The laboratory tests were significant on understanding the manufacturer's intended design for the device and helped determine if it was applicable in the field. For example, the laboratory testing determined the inefficiency for the ADV sensor in the specific Morris Leeds site application. The laboratory investigations additionally supplied confidence in the H-flume's performance when comparing it to the water meter discharge. The laboratory results validated the manufacturer's calibration, therefore, inflow discrepancies could confidently be attributed elsewhere. Even though the laboratory results provided prominent background about a sensor's capabilities, the ultimate test is investigating the device's performance in the field. The SRTs are the most beneficial tests for truly comprehending the functionality of sensors in their applied settings. Sensors can be

endlessly tested under ideal laboratory conditions, but the best understanding of sensors' limitations is through analyzing instrumentation's measurements through simulated storms in the field. This process has given a thorough understanding and confidence in the monitoring equipment's capabilities installed at specific urban SCMs part of PWD's Green City, Clean Waters.

REFERENCES

Andoh, R., Faram, M., and Osei, K. "Vortex flow controls in integrated stormwater management for urban environments." *Proc., 6th International Water Sensitive Urban Design Conference and Hydropolis*.

ASTM D5389 – 93 (2013). Standard Test Method for Open-Channel Flow Measurement by Acoustic Velocity Meter Systems

ASTM D5640 – 95 (2014). Standard Guide for Selection of Weirs and Flumes for Open-Channel Flow Measurement of Water

Aguilar, M. F., McDonald, W. M., and Dymond, R. L. (2015). "Laboratory evaluation of flow sensor technology for use in storm sewer measurements." *Proc., World Environmental and Water Resources Congress 2015: Floods, Droughts, and Ecosystems, May 17, 2015 - May 21, 2015*, American Society of Civil Engineers (ASCE), 2579-2589.

Bonakdari, H., and Zinatizadeh, A. A. (2011). "Influence of position and type of Doppler flow meters on flow-rate measurement in sewers using computational fluid dynamic." *Flow Measurement and Instrumentation*, 22(3), 225-234.

Boornazian, L., and Pollins, M. (2007). "Use of Green Infrastructure in NPDES Permits and Enforcement." *Memorandum from Water Permit and Enforcement Divisions Directors to the EPA regions and enforcement coordinators, and state NPDES directors*.

Booth, D. B., and Jackson, C. R. (1997). "Urbanization of aquatic systems: Degradation thresholds, stormwater detection, and the limits of mitigation." *Journal of the American Water Resources Association*, 33(5), 1077-1090.

Delleur, J. W. (2003). "The evolution of urban hydrology: past, present, and future." *Journal of hydraulic engineering*, 129(8), 563-573.

Dotto, C. B. S., Kleidorfer, M., Deletic, A., Rauch, W., and McCarthy, D. T. (2014). "Impacts of measured data uncertainty on urban stormwater models." *Journal of Hydrology*, 508, 28-42.

Environmental Protection Agency (EPA) (1999). "Combined Sewer Overflows Guidance for Monitoring and Modeling." Office of Wastewater Management, *Policy*, 1, 6.

Federal Interagency Stream Restoration Working Group (FISRWG) (1998). “Stream Corridor Restoration: Principles, Processes, and Practices.” *National Engineering Handbook*, USDA-Natural Resources Conservation Service.

FloWav (2016). "FW-33 DCL Logger (Direct Connect Logger).”

Gulliver, J. S., Asleson, B. C., Nestingen, R. S., Nieber, J. L., and Hozalski, R. M. (2009). "Four levels of assessment for LID practices." *Proc., 2008 International Low Impact Development Conference, November 16, 2008 - November 19, 2008*, American Society of Civil Engineers (ASCE), Council of the Environmental and Water; Low Impact Development Technical Committee; of the Urban Water Resources Research; Resources Institute (EWRI) of ASCE.

Harmel, R. D., Smith, D. R., King, K. W., and Slade, R. M. (2009). "Estimating storm discharge and water quality data uncertainty: A software tool for monitoring and modeling applications." *Environmental Modelling and Software*, 24(7), 832-842.

Herschy, R. W. (1995). *Streamflow measurement*, CRC Press.

Kazimer, M. (2014). "HS/H/HL - Type Flume Specification and Installation." TRACOM.

Lee, H., Swamikannu, X., Radulescu, D., Kim, S.-j., and Stenstrom, M. K. (2007). "Design of stormwater monitoring programs." *Water Research*, 41(18), 4186-4196.

Lee, R. (2015). “Green Infrastructure Flow Measurement Evaluation Tool (GIFMET). Villanova, Pennsylvania.

Leopold, L. B. (1968). *Hydrology for urban land planning: A guidebook on the hydrologic effects of urban land use*, US Government Printing Office Washington, DC, USA.

Locke, D. B. (2012). "Measurement of Stream Discharge Using Weirs and Flumes." *Measurement of Stream Discharge*, Maine.

Maheepala, U. K., Takyi, A. K., and Perera, B. J. C. (2001). "Hydrological data monitoring for urban stormwater drainage systems." *Journal of Hydrology*, 245(1-4), 32-47.

McIntyre, N., and Marshall, M. (2008). "Field verification of bed-mounted ADV meters." *Proceedings of the ICE-Water Management*, 161(4), 199-206.

McMillan, H., Krueger, T., and Freer, J. (2012). "Benchmarking observational uncertainties for hydrology: rainfall, river discharge and water quality." *Hydrological Processes*, 26(26), 4078-4111.

O'Bannon, D. a. N., J. (2012). "Detailed Rain Garden Flow Monitoring." *World Environmental and Water Resources Congress 2012*, 3565-3572.

Philadlephia Water Department (PWD) (2009). "Precipitation Analysis." *Philadelphia Combined Sewer Overflow Long Term Control Plan Update*.

Phialdelphia Water Department (PWD) (2011). "Green City Clean Waters." *The City of Philadelphia's Program for Combined Sewer Overflow Control*

Philadelphia Water Department (PWD) (2012). "Green City, Clean Waters, Comprehensive Monitoring Plan."

Portland (2010). "2010 Stormwater Management Facility Monitoring Report." *Bureau of Environmental Services*, Bureau of Environmental Services, Portland, Oregon.

Quigley, M. M., Strecker, E. W., and Urbonas, B. (2002). "Overview of the Urban Stormwater BMP Performance Monitoring: A Guidance Manual for Meeting the National Stormwater BMP Database Requirements." *Global Solutions for Urban Drainage*, 1-14.

Rantz, S. (1982). "Measurement and computation of stream flow. Volume 2: Computation of discharge." *US Geological Survey water-supply paper*, 2175, 631.

Sauer, V. B., and Meyer, R. (1992). *Determination of error in individual discharge measurements*, US Department of the Interior, US Geological Survey.

Schenk, J. E., Smith, K., and Stinson, M. K. (2001). "Verification Testing of Wet-Weather Flow Technologies." *Bridging the Gap*, 1-10.

Silberstein, R. (2006). "Hydrological models are so good, do we still need data?" *Environmental Modelling & Software*, 21(9), 1340-1352.

Struck, S. D., Hufnagel, C. L., and Field, R. (2012). "Prioritization of green infrastructure for CSO communities - Identifying effective implementation opportunities." *Proc., World Environmental and Water Resources Congress 2012: Crossing Boundaries, May 20, 2012 - May 24, 2012*, American Society of Civil Engineers (ASCE), 478-494.

Sturm, T. W. (2010). *Open channel hydraulics*, McGraw-Hill Higher Education.

Tackett, T. (2009). "Seattle's policy and pilots to support green stormwater infrastructure." *Proc., 2008 International Low Impact Development Conference, November 16, 2008 - November 19, 2008*, American Society of Civil Engineers (ASCE), Council of the Environmental and Water; Low Impact Development Technical Committee; of the Urban Water Resources Research; Resources Institute (EWRI) of ASCE.

TUVNEL (2010). "An introduction to non-invasive ultrasonic flow metering." National Measurement System.

United Nations (UN) (2014). "World Urbanization Prospects: The 2014 Revision, Highlights." P. D. Department of Economic and Social Affairs, ed.

United States Bureau of Reclamation (USBR) (2001). “Water Measurement Manual: A guide to effective water measurement practices for better water management.” U.S. Department of the Interior Bureau of Reclamation, ed., Government Printing Office.

Voyde, E., Fassman, E., and Simcock, R. (2010). "Hydrology of an extensive living roof under sub-tropical climate conditions in Auckland, New Zealand." *Journal of Hydrology*, 394(3–4), 384-395.

Yu, S. L., Kuo, J.-T., Fassman, E. A., and Pan, H. (2001). "Field test of grassed-swale performance in removing runoff pollution." *Journal of Water Resources Planning and Management*, 127(3), 168-171.

Zahmatkesh, Z., Burian, S. J., Karamouz, M., Tavakol-Davani, H., and Goharian, E. (2015). "Low-impact development practices to mitigate climate change effects on urban stormwater runoff: Case study of New York City." *Journal of Irrigation and Drainage Engineering*, 141(1).

APPENDIX

Appendix A: Philadelphia Climate Study

Table A.1 Annual and Seasonal Average Temperature and Total Precipitation from 1961 to 2000 from climate data processing tool 'CMIP' (Miller et al. 2014)

	Annual	Winter (DJF)	Spring (MAM)	Summer (JJA)	Fall (SON)
Temperature (°F)	54.4	41.9	NA*	84.5	NA*
Precipitation (inches)	44.0	9.9	11.4	12.2	10.5

**The CMIP climate data processing tool does not provide average spring or fall temperatures.*

Appendix B: Philadelphia Zoo Rain Garden Preliminary Research

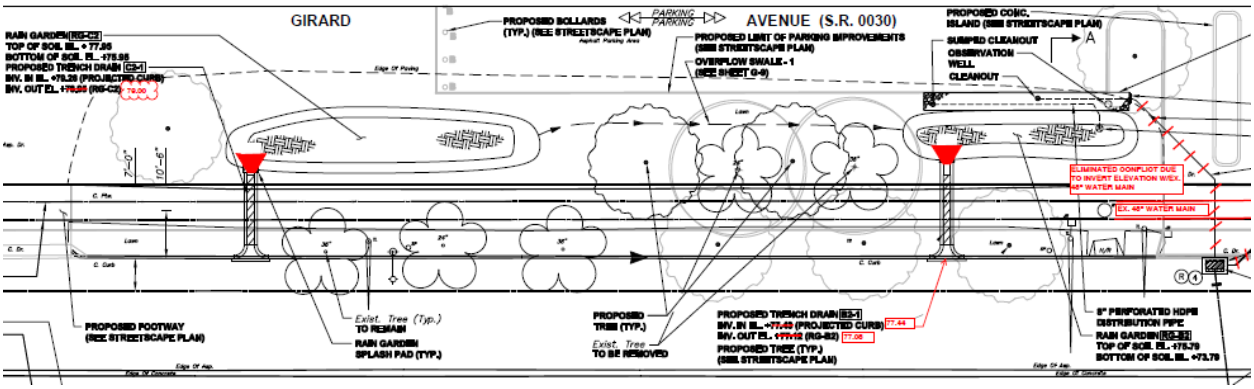

Figure B.1 Philadelphia Zoo Rain Garden As-Builts

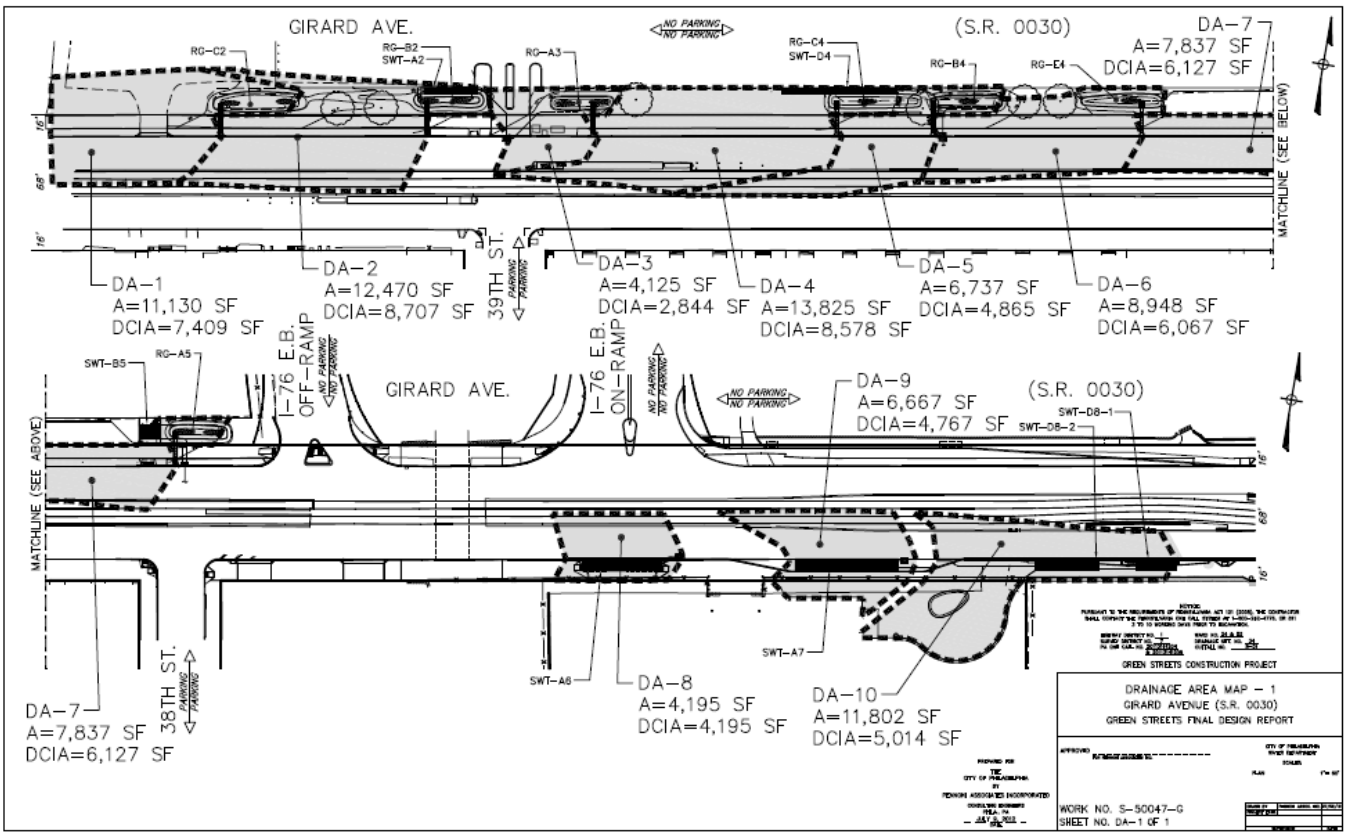

Figure B.2 Philadelphia Zoo Rain Garden's drainage area maps provided by PWD.

Table B.1 Predicted Peak Discharge for Philadelphia Zoo Inlet Upstream Rain Garden using the Equation 2

Peak Flow Rates			**5 minute duration**		**15 minute duration**	
Storm Event	0.5 in (1.3 cm)	1 in (2.5 cm)	2 Year	10 Year	2 Year	10 Year
Q (cfs) **(m^3/s)**	0.07 (0.002)	0.15 (0.004)	0.74 (0.021)	0.96 (0.027)	0.50 (0.014)	0.65 (0.018)

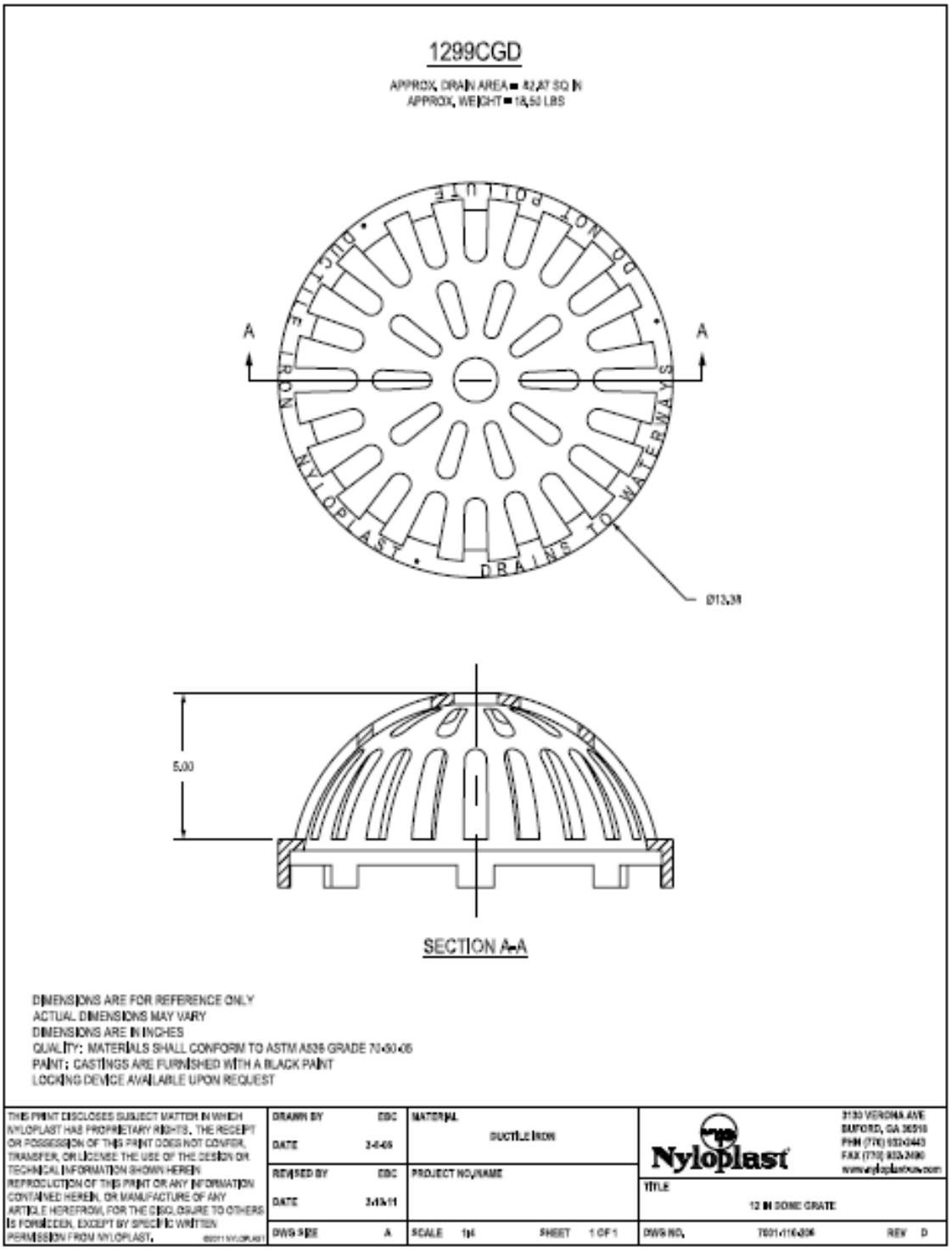

Figure B.3 Domed riser specs for 12 inch (30.5 cm) iron domed.

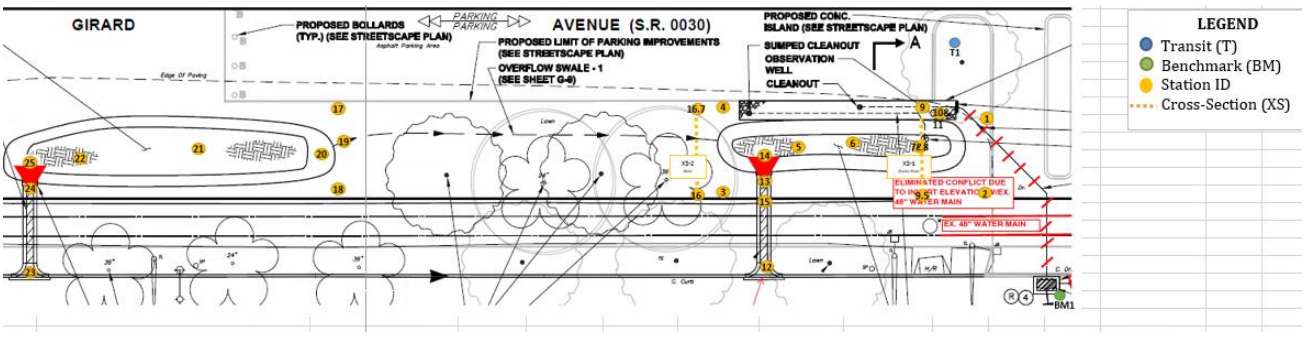

Location	Notes	ID	Middle Reading (ft)	Top Reading (ft)	Bottom Reading (ft)	Known Elevation (ft)	Height of Instrument (ft)	Elevation (ft)	Horizontal Distance (ft)
-	Storm Drain	BM1	5.68	5.96	5.41	76.59	82.27	-	55
RG-B2	Corner RG-B2	1	3.71	3.79	3.62	-	-	78.57	17
	Corner RG-B2	2	5.06	5.22	4.90	-	-	77.21	32.5
	Corner RG-B2	3	3.95	4.28	3.63	-	-	78.32	65
	Corner RG-B2	4	3.93	4.22	3.63	-	-	78.35	59
	Low Depth 1 - Close to swale	5	6.31	6.58	6.05	-	-	75.96	52.5
	Low Depth 2 - Closer to transit	6	6.43	6.61	6.25	-	-	75.84	36
	Dome Riser - Ground Elevation	7	5.82	5.93	5.70	-	-	76.46	23
	Dome Riser - Top Dome	8	5.21	5.32	5.09	-	-	77.07	23
	Cross Section 1 - Dome Riser (close to transit)	9	4.17	4.25	4.09	-	-	78.10	16
	Cross Section 1 - Dome Riser	9.1	5.02	5.11	4.93	-	-	77.25	18
	Cross Section 1 - Dome Riser	9.2	5.73	5.84	5.63	-	-	76.54	20.5
	Cross Section 1 - Dome Riser	9.3	6.24	6.36	6.11	-	-	76.04	25
	Cross Section 1 - Dome Riser	9.4	5.93	6.07	5.78	-	-	76.34	29
	Cross Section 1 - Dome Riser (close to street)	9.5	4.59	4.76	4.42	-	-	77.69	34
	Observation Well - Ground Elevation	10	4.33	4.42	4.25	-	-	77.94	17
	Observation Well - Depth	11	10.25	10.34	10.17	-	-	72.02	17.5
	Surface Inflow - Street Side	12	4.83	5.14	4.52	-	-	77.44	62
	Surface Inflow - End Sidewalk	13	5.14	5.40	4.88	-	-	77.13	52
	Surface Inflow - Bottom of riprap	14	6.37	6.61	6.13	-	-	75.90	48
	Sidewalk	15	4.09	4.35	3.83	-	-	78.18	51.5
Swale	Cross Section 2 - Weir (close to street)	16	3.85	4.19	3.51	-	-	78.42	68
	Cross Section 2 - Weir	16.1	4.23	4.56	3.90	-	-	78.04	66
	Cross Section 2 - Weir	16.2	4.87	5.20	4.55	-	-	77.40	65.5
	Cross Section 2 - Weir	16.3	5.35	5.65	5.03	-	-	76.93	62.5
	Cross Section 2 - Weir (low point)	16.4	5.59	5.90	5.28	-	-	76.68	62
	Cross Section 2 - Weir	16.5	5.36	5.67	5.05	-	-	76.91	62
	Cross Section 2 - Weir	16.6	4.38	4.69	4.07	-	-	77.89	62
	Cross Section 2 - Weir (close to transit)	16.7	3.74	4.04	3.44	-	-	78.53	60
	Corner Swale (parking lot side)	17	2.83	3.44	2.22	-	-	79.44	122
	Corner Swale (parking lot side)	18	3.08	3.71	2.45	-	-	79.19	126
	Spillway Entrance - Swale low side	19	3.78	4.39	3.27	-	-	78.49	112
RG-C2	Spillway Exit from RG-C2	20	3.54	4.17	3.92	-	-	78.73	24.5
	Low Depth 1 - Close to swale	21	3.92	4.64	3.19	-	-	78.35	145
	Low Depth 2 - Closer to Surface Inflow	22	4.12	5.08	3.17	-	-	78.15	191
	Surface Inflow - Street Side	23	2.92	3.93	1.92	-	-	79.35	201
	Surface Inflow - End Sidewalk	24	3.12	4.12	2.12	-	-	79.15	200
	Surface Inflow - Bottom of riprap	25	4.00	4.99	3.00	-	-	78.27	199
		26				-	-	82.27	0

Figure B.4 Surveying analysis of Philadelphia Zoo Rain Garden

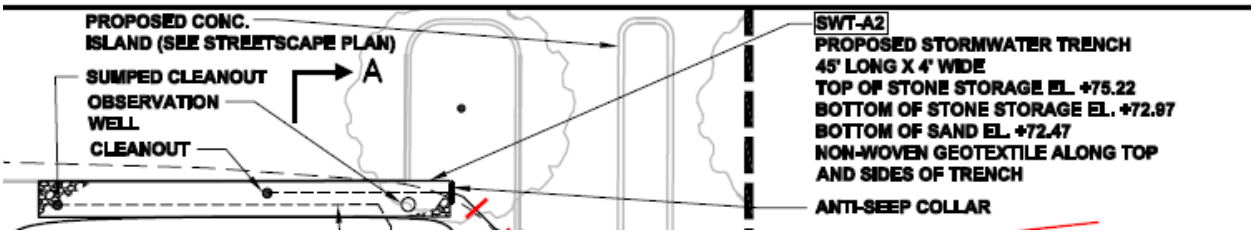

Figure B.5 Rock Bed Dimensions from PWD Drawings

Appendix C: Morris Leeds Tree Trench Preliminary Research

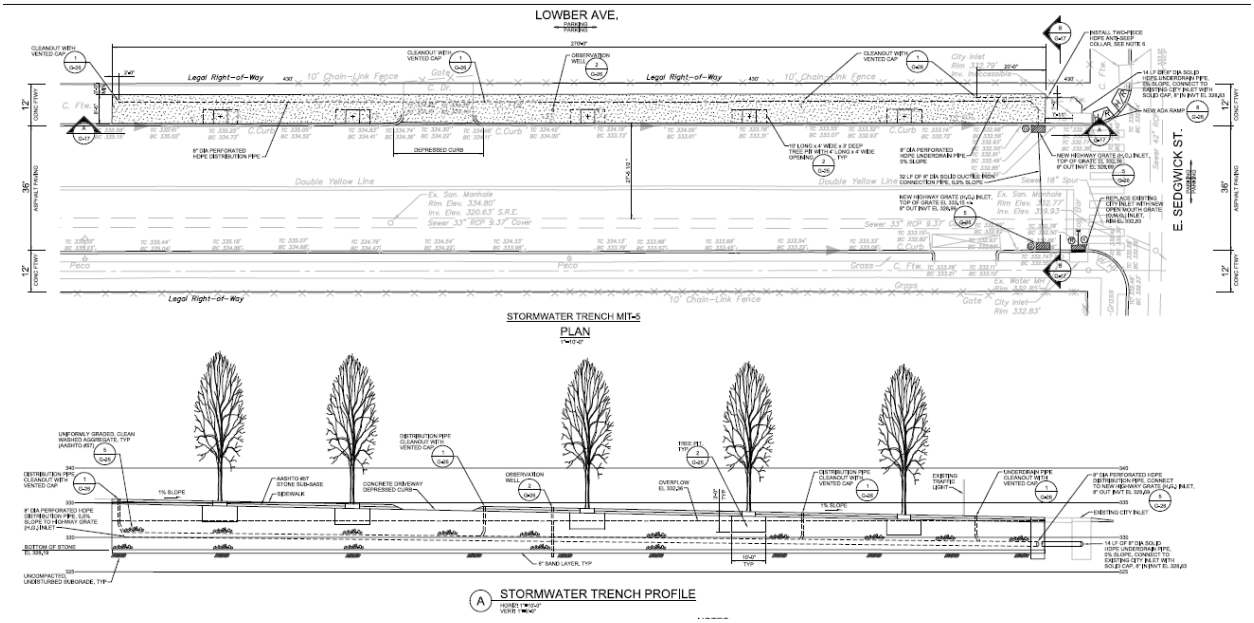

Figure C.1 PWD drawings of subsurface pipe and tree pits at Morris Leeds Tree Trench site.

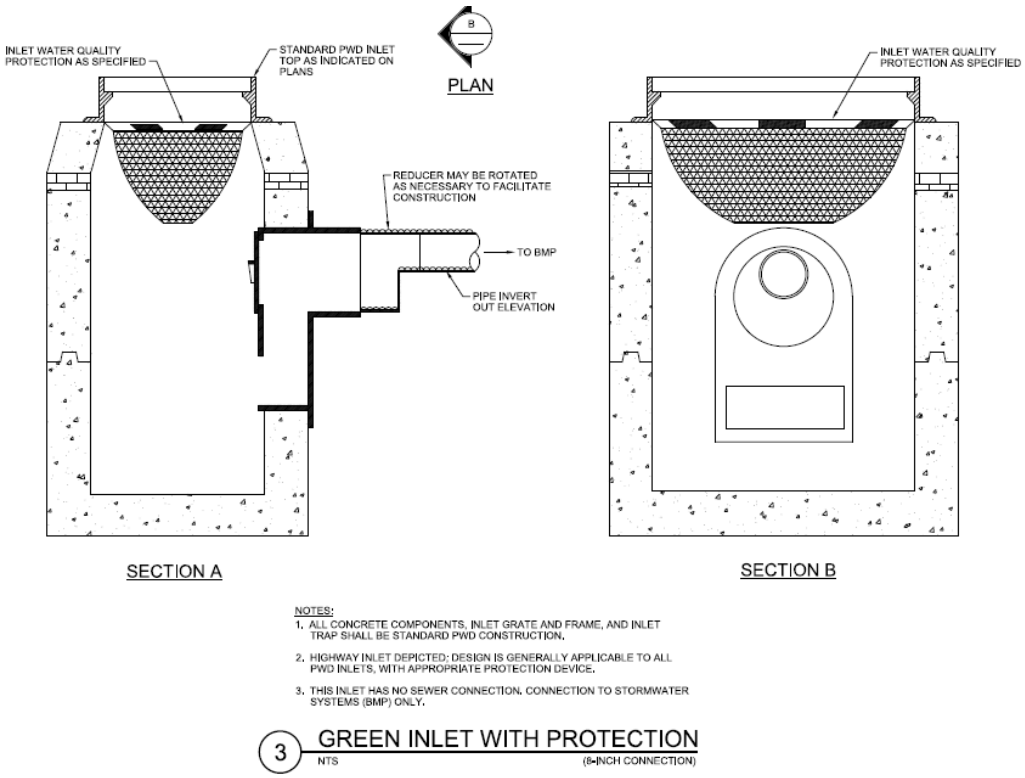

Figure C.2 Typical cross section of green inlet with trap door component.

Appendix D: H-Flume Laboratory Tests

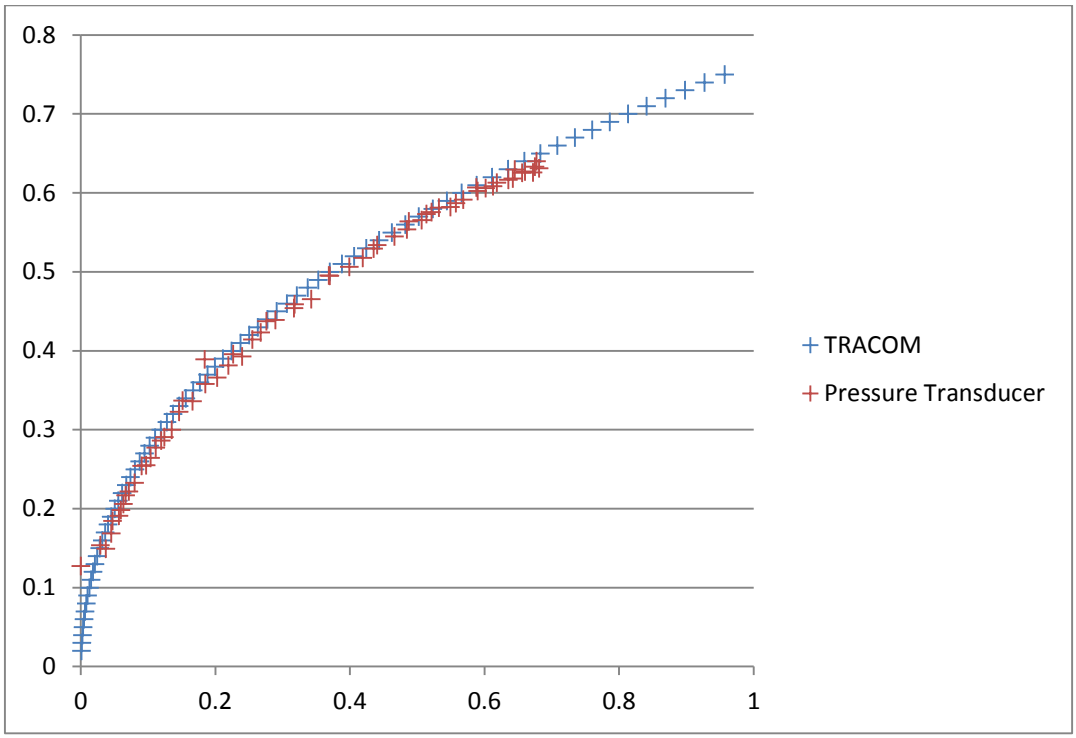

Figure D.1 H-Flume laboratory test 1 results

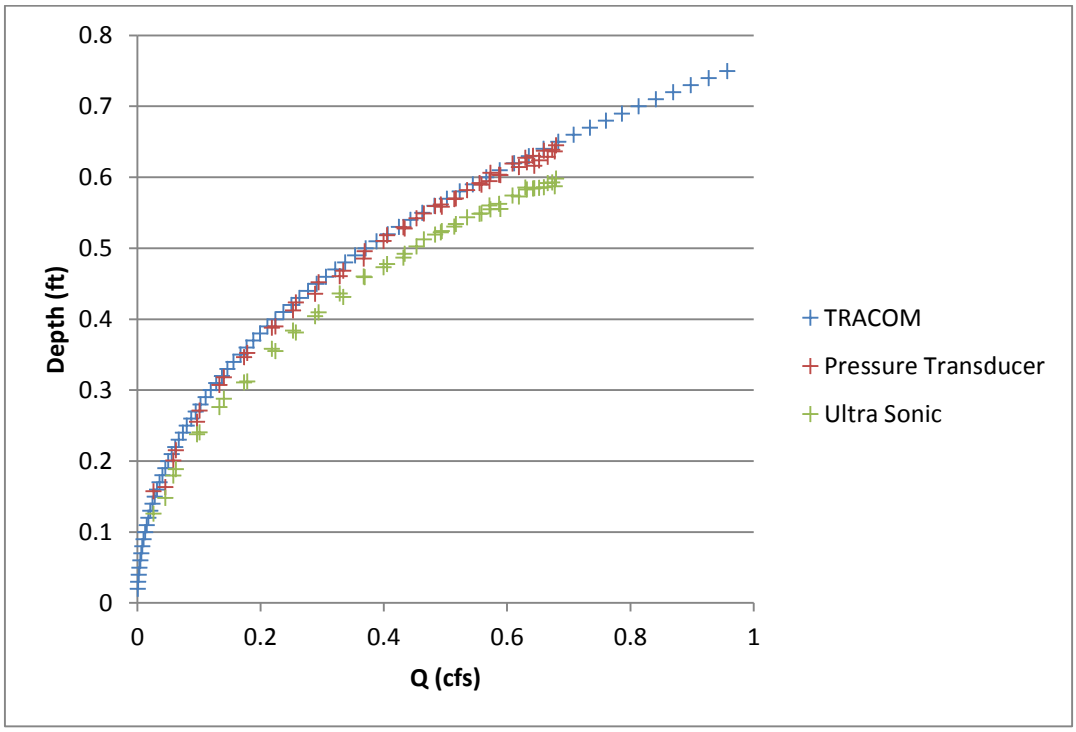

Figure D.2 H-Flume laboratory test 2 results

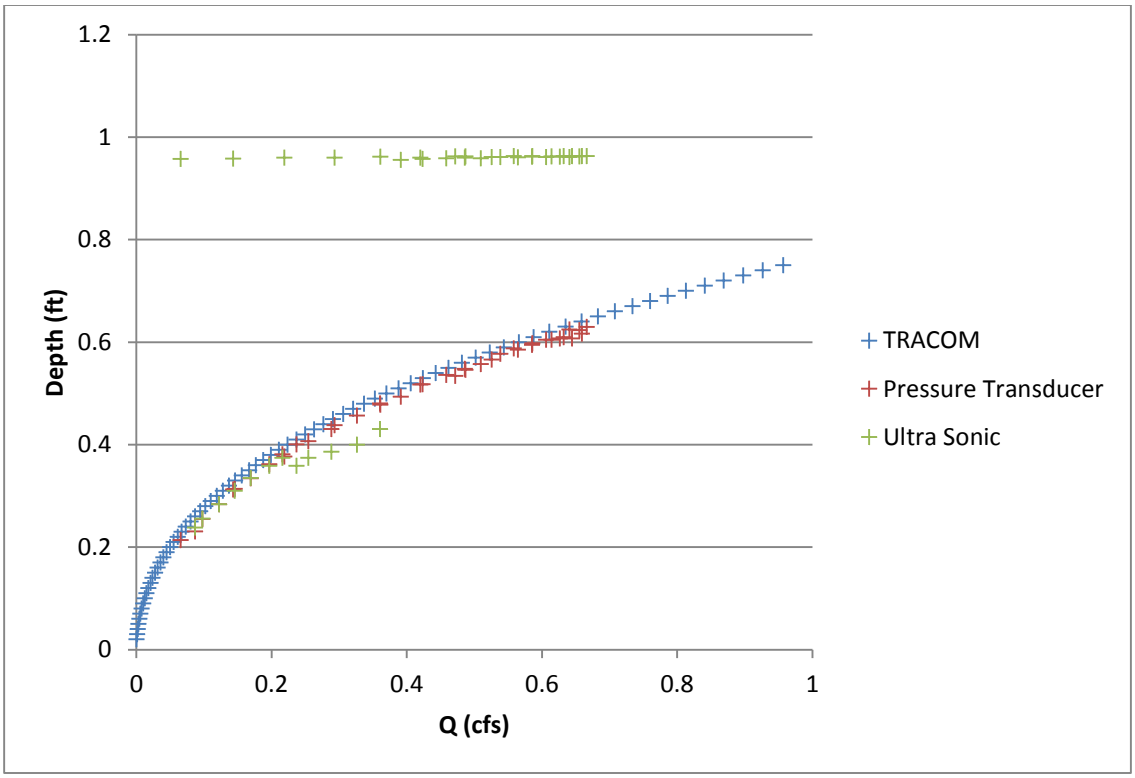

Figure D.3 H-Flume laboratory test 3 results

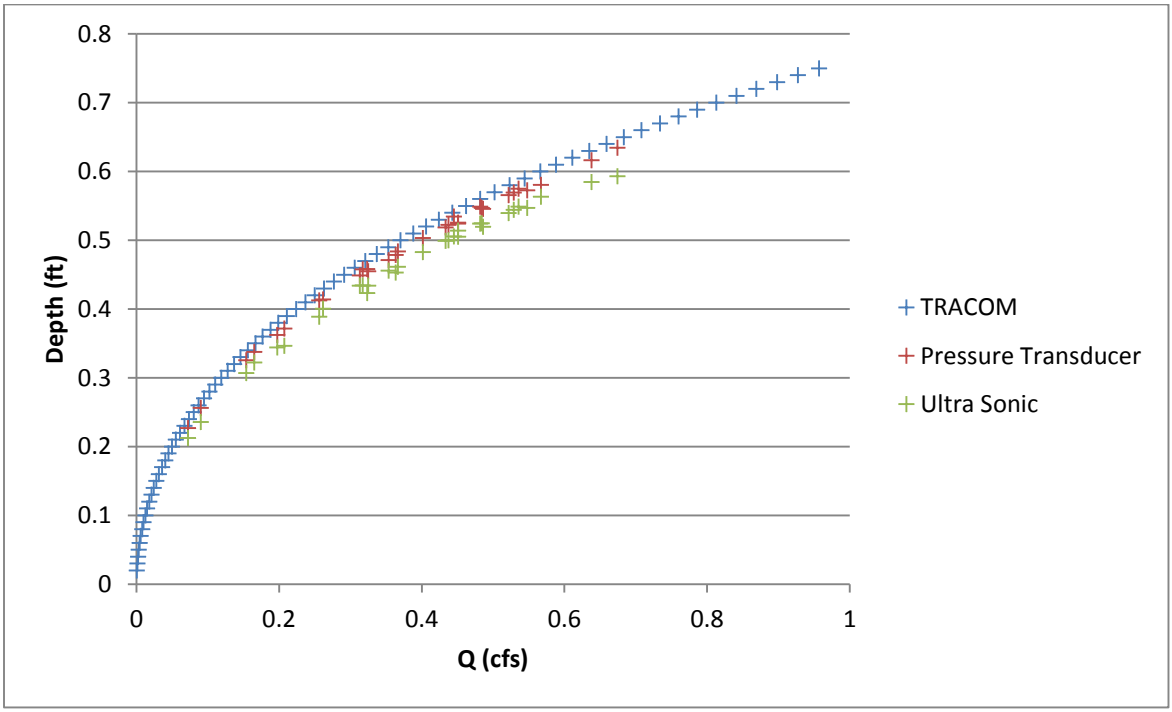

Figure D.4 H-Flume laboratory test 4 results

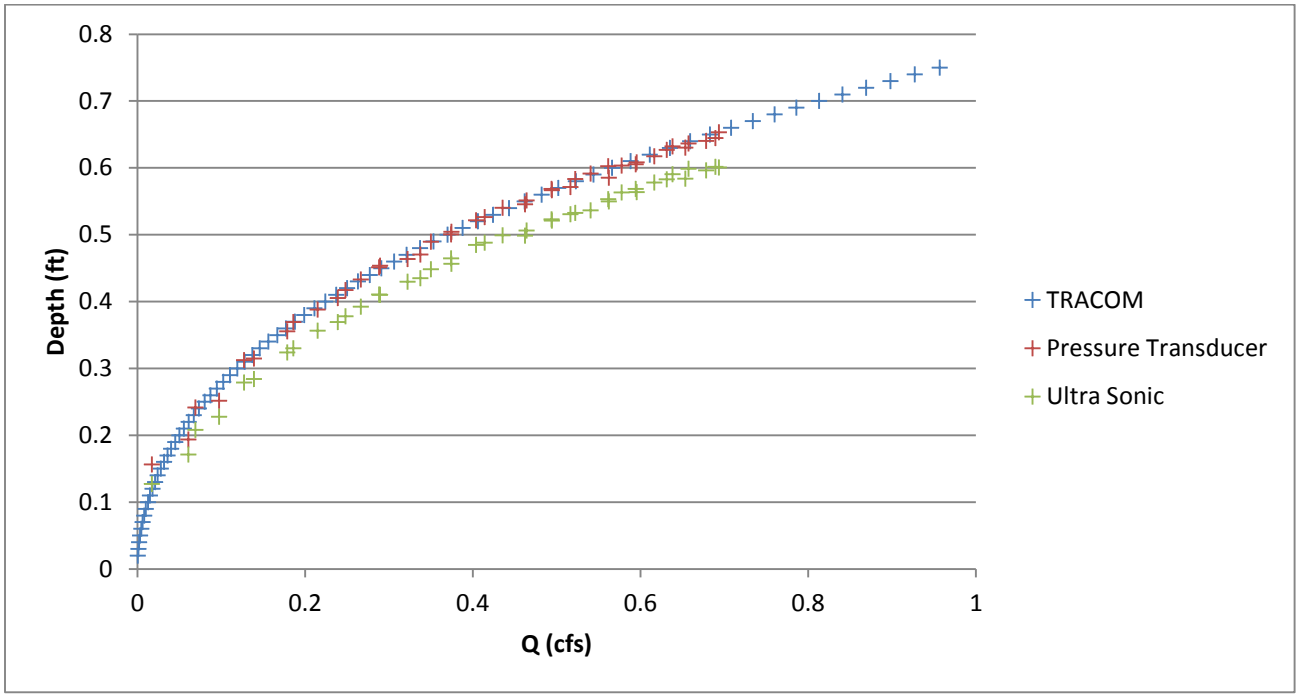

Figure D.5 H-Flume laboratory test 5 results

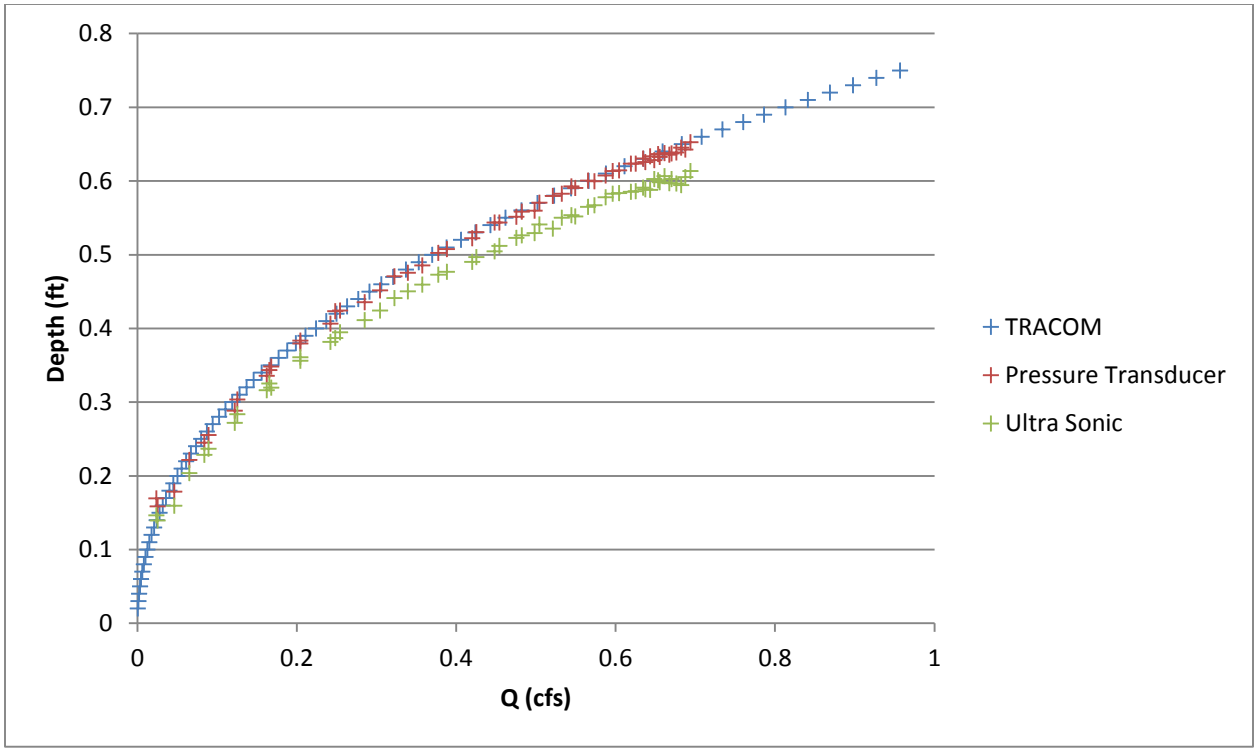

Figure D.6 H-Flume laboratory test 6 results

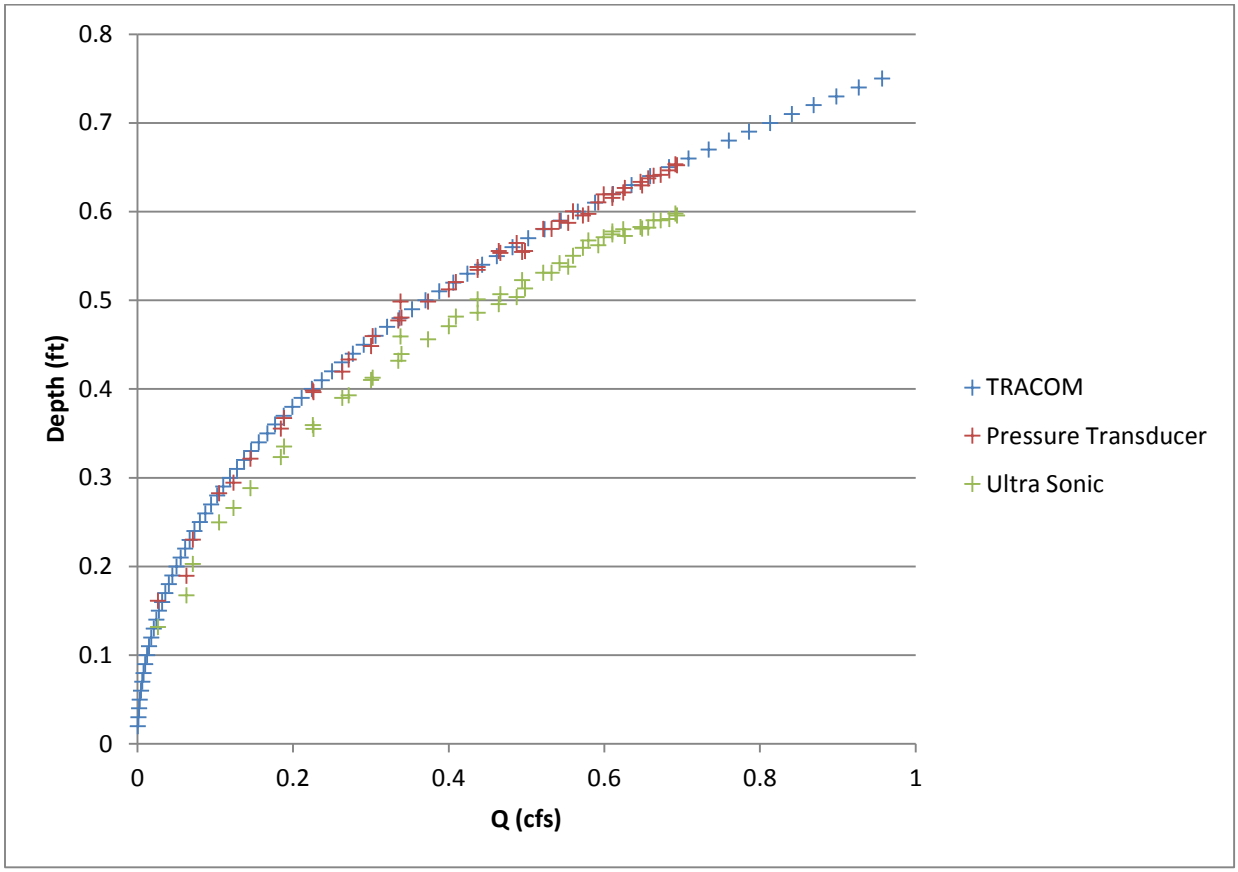

Figure D.7 H-Flume laboratory test 7 results

TRACOM

770.664.6513 (V) 770.664.6565 (F)

Discharge Table
For
0.75' H Flume

Document: H75-D-T Rev.: 0 Date: 4-6-00 By: Jon Wachter

LEVEL		FLOW		
FEET	INCHES	CFS	GPM	MGD
0.01	0.12			
0.02	0.24	0.0006	0.2693	0.0004
0.03	0.36	0.0013	0.5834	0.0008
0.04	0.48	0.0022	0.9874	0.0014
0.05	0.60	0.0032	1.436	0.0021
0.06	0.72	0.0046	2.064	0.0030
0.07	0.84	0.0061	2.738	0.0039
0.08	0.96	0.0080	3.590	0.0052
0.09	1.08	0.0101	4.533	0.0065
0.10	1.20	0.0126	5.655	0.0081
0.11	1.32	0.0151	6.777	0.0098
0.12	1.44	0.0179	8.034	0.0116
0.13	1.56	0.0210	9.425	0.0136
0.14	1.68	0.0242	10.86	0.0156
0.15	1.80	0.0278	12.48	0.0180
0.16	1.92	0.0317	14.23	0.0205
0.17	2.04	0.0358	16.07	0.0231
0.18	2.16	0.0403	18.09	0.0260
0.19	2.28	0.0451	20.24	0.0291
0.20	2.40	0.0501	22.48	0.0324
0.21	2.52	0.0555	24.91	0.0359
0.22	2.64	0.0612	27.47	0.0396
0.23	2.76	0.0672	30.16	0.0434
0.24	2.88	0.0735	32.99	0.0475
0.25	3.00	0.0802	35.99	0.0518
0.26	3.12	0.0872	39.14	0.0564
0.27	3.24	0.0946	42.46	0.0611
0.28	3.36	0.1023	45.91	0.0661
0.29	3.48	0.1104	49.55	0.0714
0.30	3.60	0.1190	53.41	0.0769
0.31	3.72	0.1280	57.45	0.0827
0.32	3.84	0.1370	61.49	0.0885
0.33	3.96	0.1460	65.52	0.0944
0.34	4.08	0.1560	70.01	0.1008
0.35	4.20	0.1670	74.95	0.1079
0.36	4.32	0.1770	79.44	0.1144
0.37	4.44	0.1880	84.37	0.1215
0.38	4.56	0.1990	89.31	0.1286
0.39	4.68	0.2110	94.70	0.1364
0.40	4.80	0.2240	100.5	0.1448
0.41	4.92	0.2370	106.4	0.1532
0.42	5.04	0.2500	112.2	0.1616
0.43	5.16	0.2630	118.0	0.1700
0.44	5.28	0.2770	124.3	0.1790
0.45	5.40	0.2910	130.6	0.1881
0.46	5.52	0.3060	137.3	0.1978
0.47	5.64	0.3210	144.1	0.2075
0.48	5.76	0.3370	151.2	0.2178
0.49	5.88	0.3530	158.4	0.2281
0.50	6.00	0.3700	166.1	0.2391
0.51	6.12	0.3880	174.1	0.2508
0.52	6.24	0.4060	182.2	0.2624
0.53	6.36	0.4240	190.3	0.2740
0.54	6.48	0.4430	198.8	0.2863
0.55	6.60	0.4620	207.3	0.2986
0.56	6.72	0.4820	216.3	0.3115
0.57	6.84	0.5020	225.3	0.3244
0.58	6.96	0.5230	234.7	0.3380
0.59	7.08	0.5440	244.1	0.3516
0.60	7.20	0.5660	254.0	0.3658
0.61	7.32	0.5880	263.9	0.3800
0.62	7.44	0.6110	274.2	0.3949
0.63	7.56	0.6350	285.0	0.4104
0.64	7.68	0.6590	295.8	0.4259
0.65	7.80	0.6830	306.5	0.4414
0.66	7.92	0.7080	317.8	0.4576
0.67	8.04	0.7340	329.4	0.4744
0.68	8.16	0.7600	341.1	0.4912
0.69	8.28	0.7860	352.8	0.5080
0.70	8.40	0.8130	364.9	0.5254
0.71	8.52	0.8410	377.4	0.5435
0.72	8.64	0.8690	390.0	0.5616
0.73	8.76	0.8980	403.0	0.5804
0.74	8.88	0.9270	416.0	0.5991
0.75	9.00	0.9570	429.5	0.6185

Figure D.8 TRACOM Discharge Table (Factory's calibration)

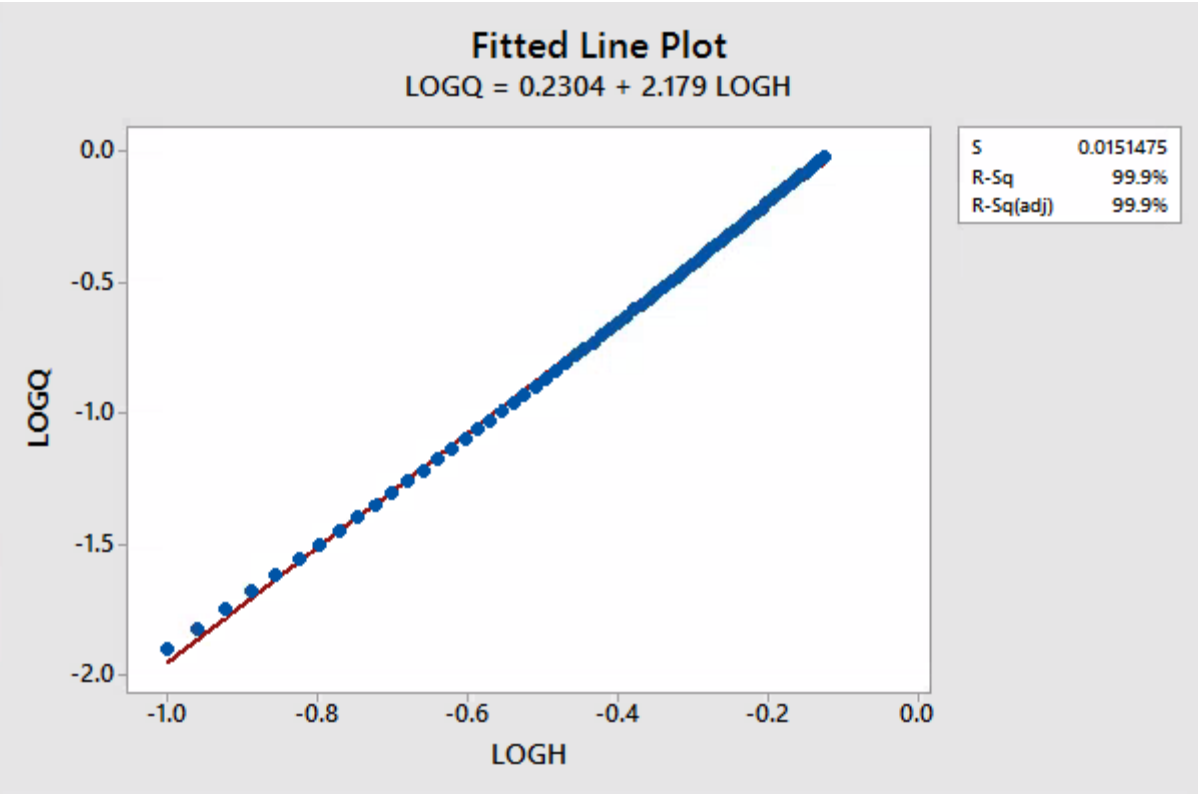

Figure D.9 Linear regression of H-flume's calibrated curve for corresponding discharge table

Appendix E: Development of Organ Orifice Meter

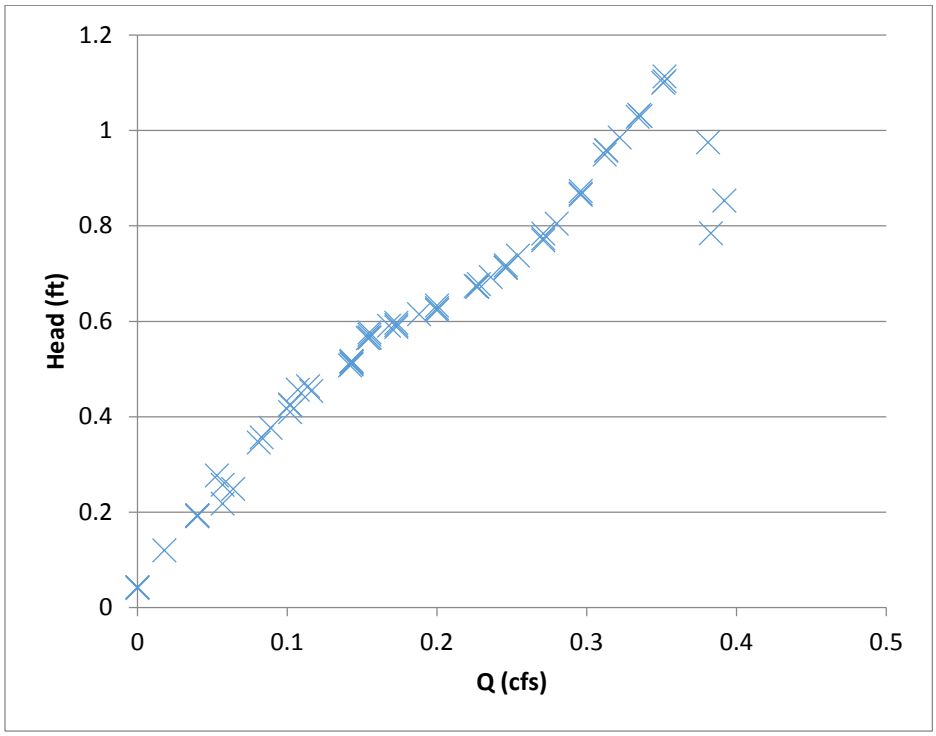

Figure E.1 Prototype B test 2 results for increasing flow rates

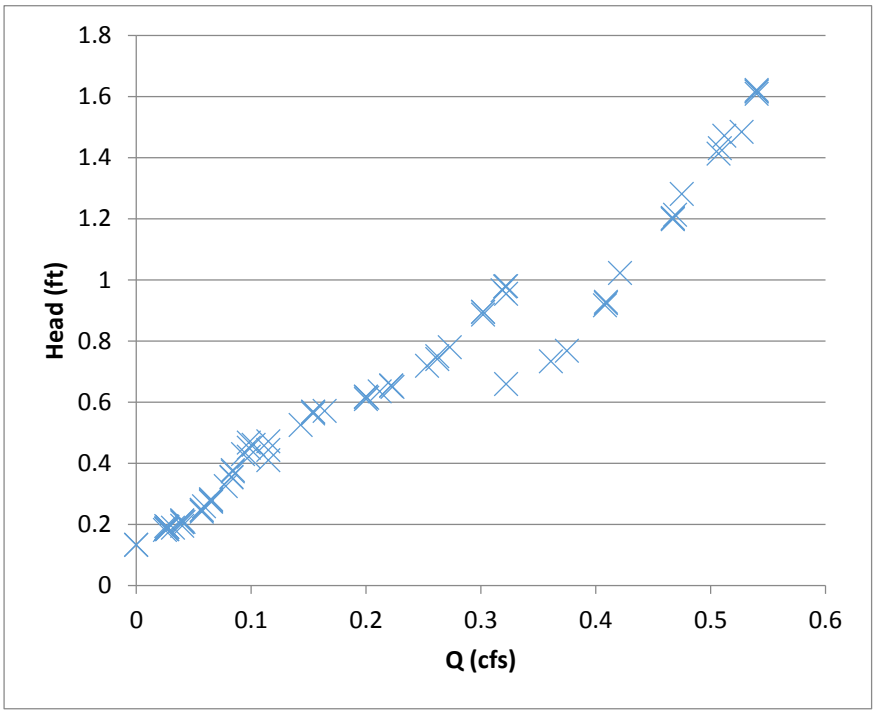

Figure E.2 Prototype B test 2 results for decreasing flow rates

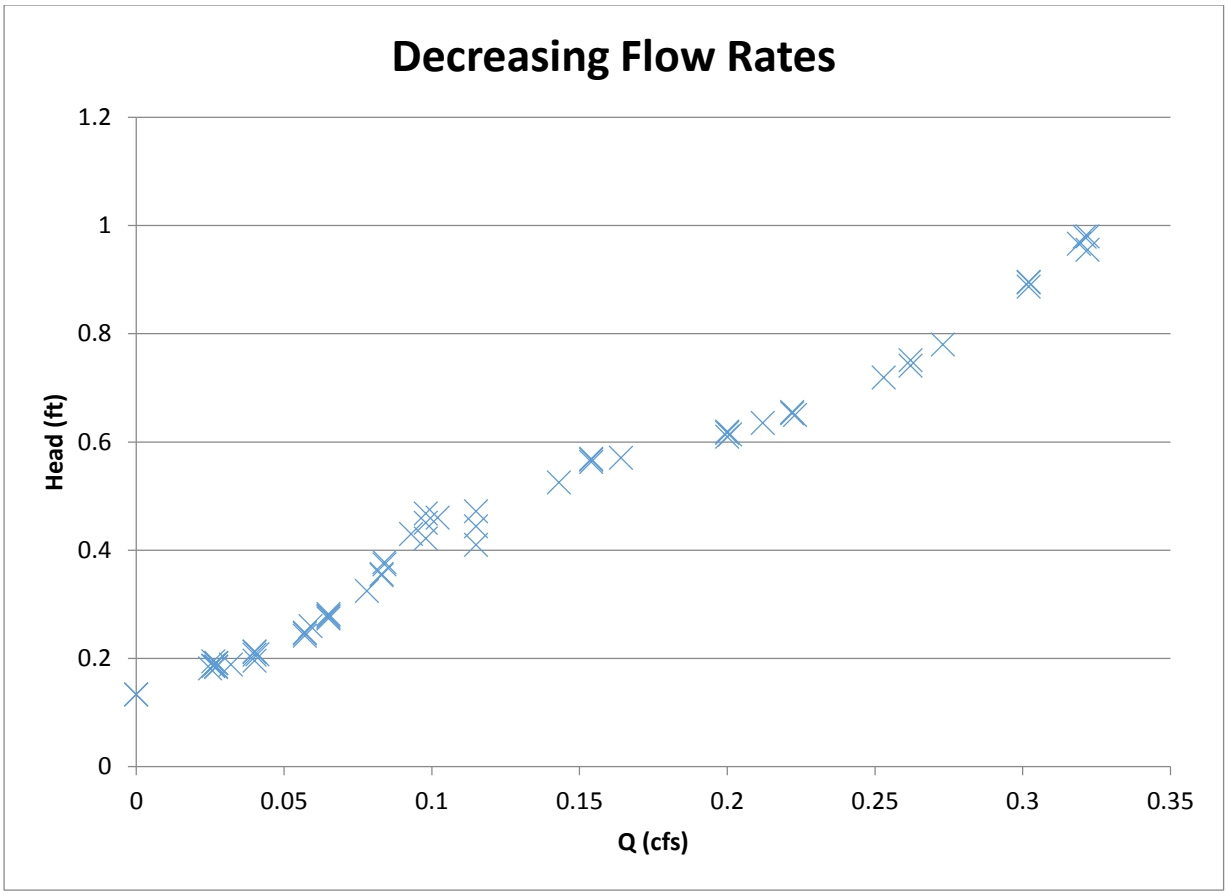

Figure E.3 Prototype B test 3 results for decreasing flow rates

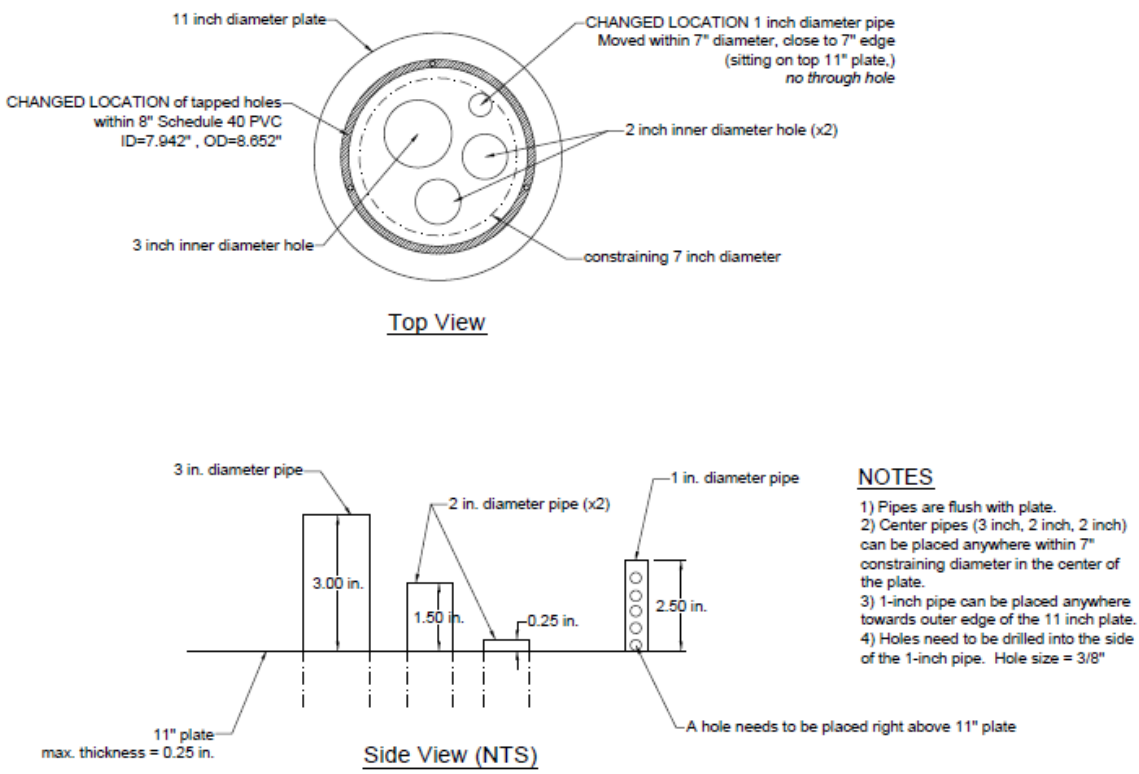

Figure E.4 Drawings and specs of final organ orifice design

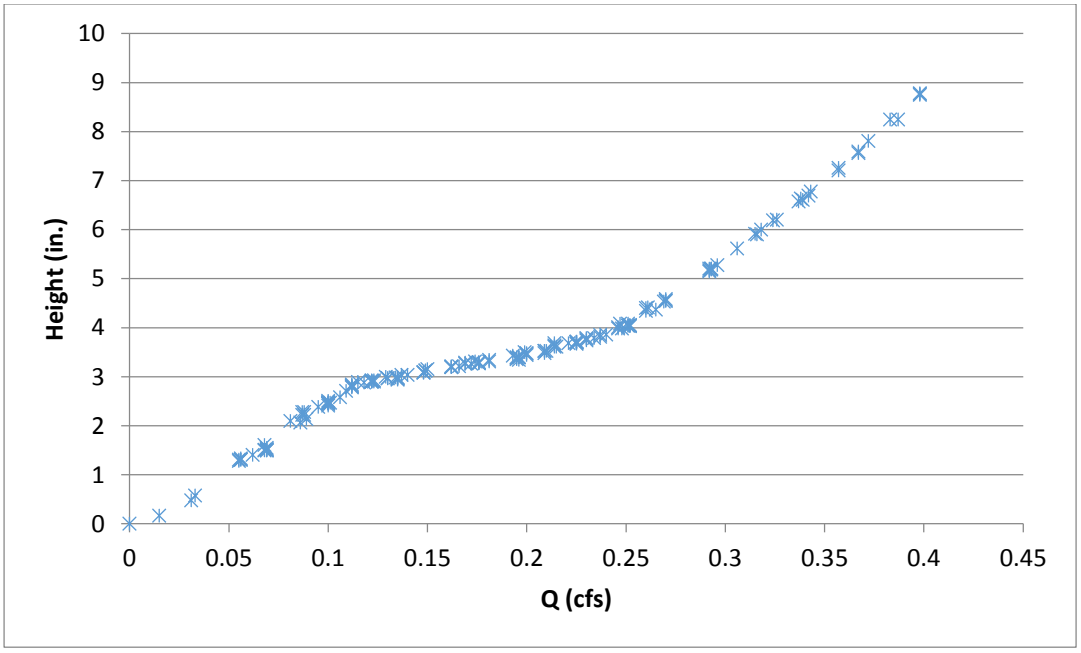

Figure E.5 Test 1 of final organ orifice design manufactured by Benedix.

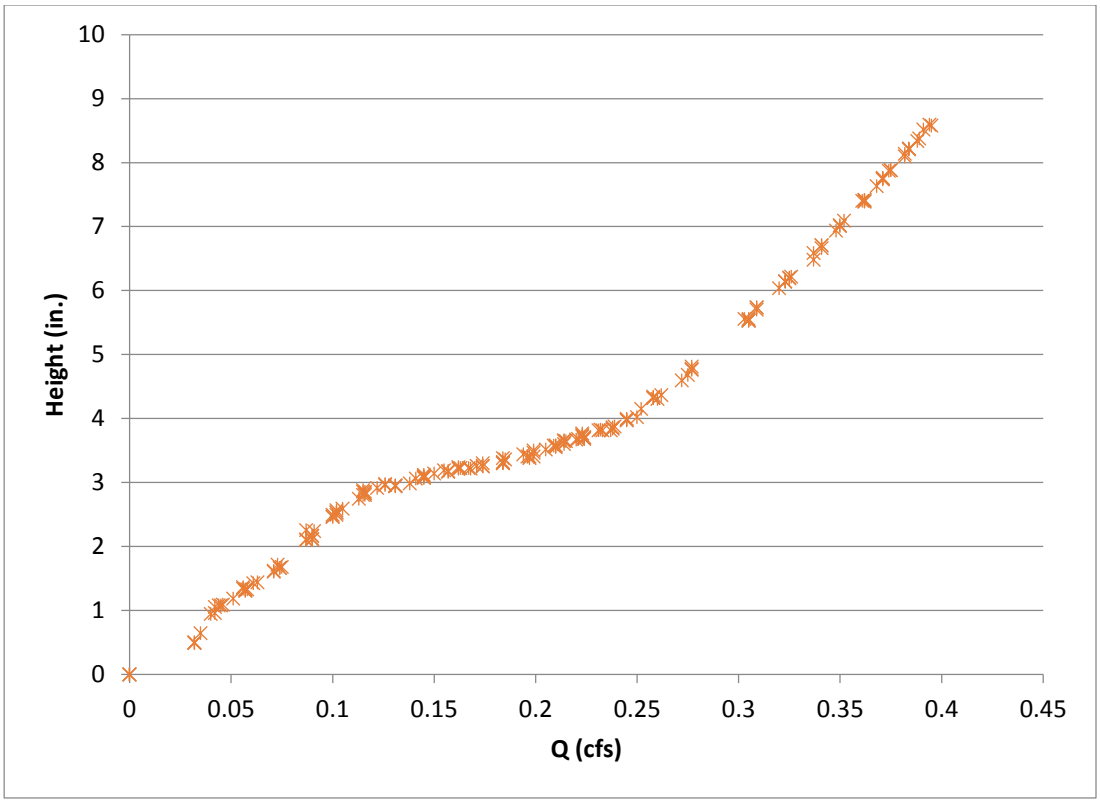

Figure E.6 Test 2 of final organ orifice design manufactured by Benedix

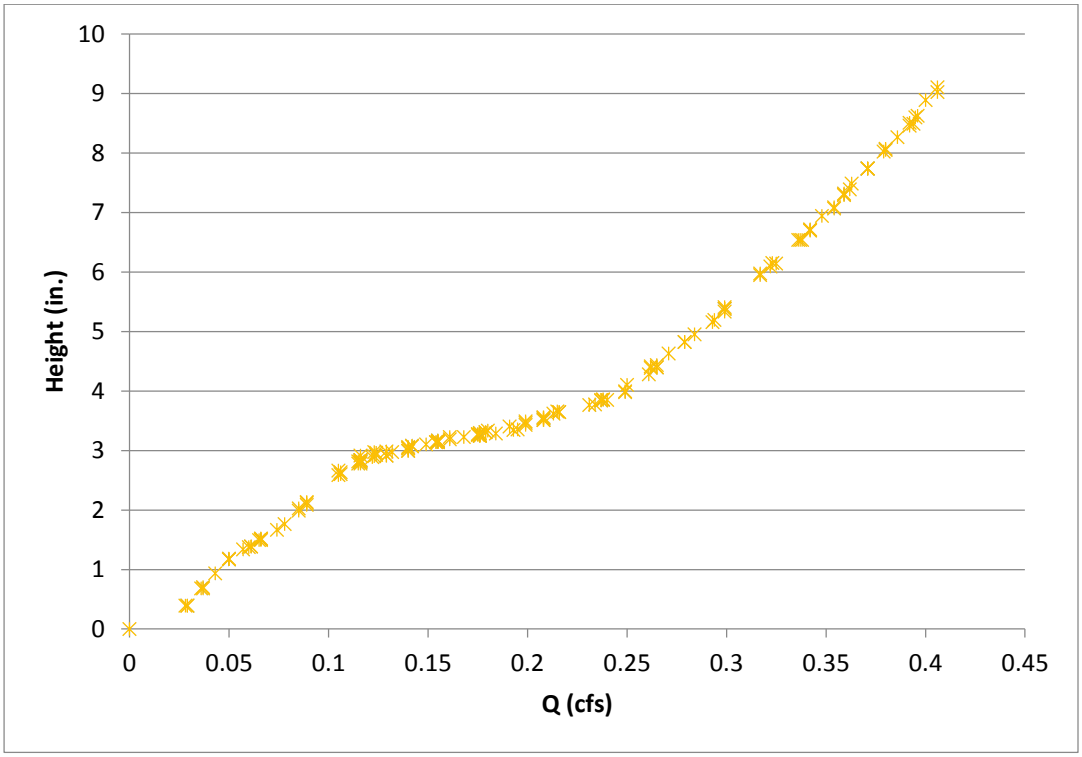

Figure E.7 Test 3 of final organ orifice design manufactured by Benedix

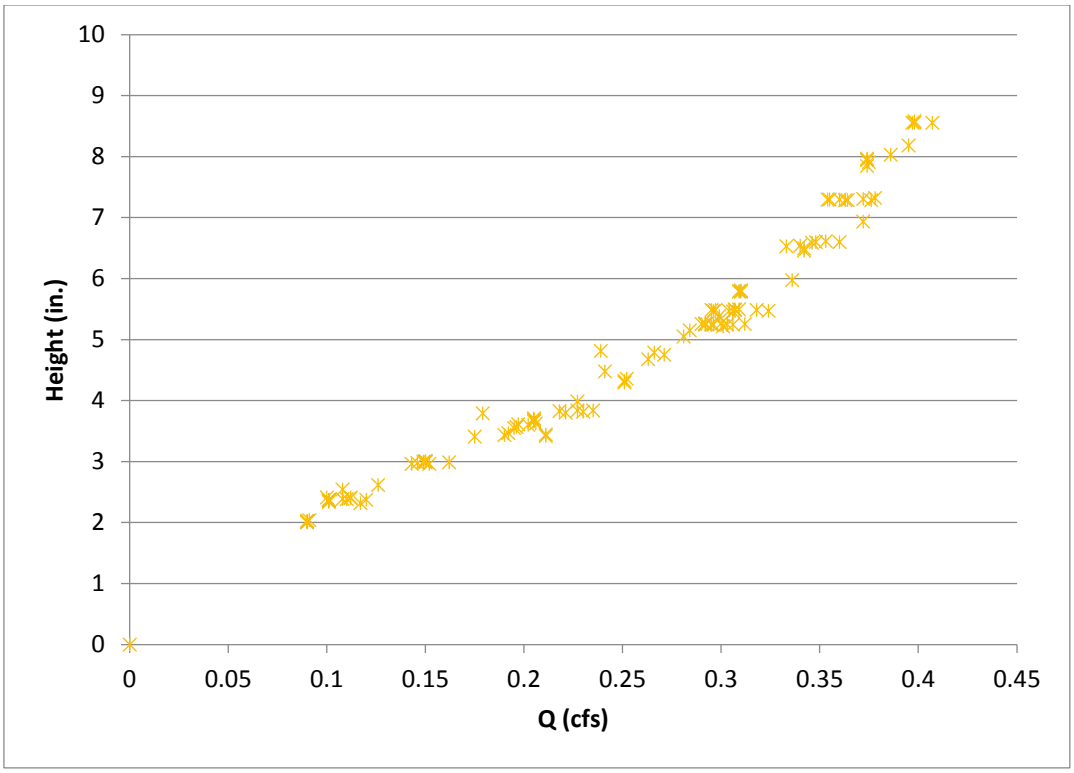

Figure E.8 Test 4 of final organ orifice design manufactured by Benedix

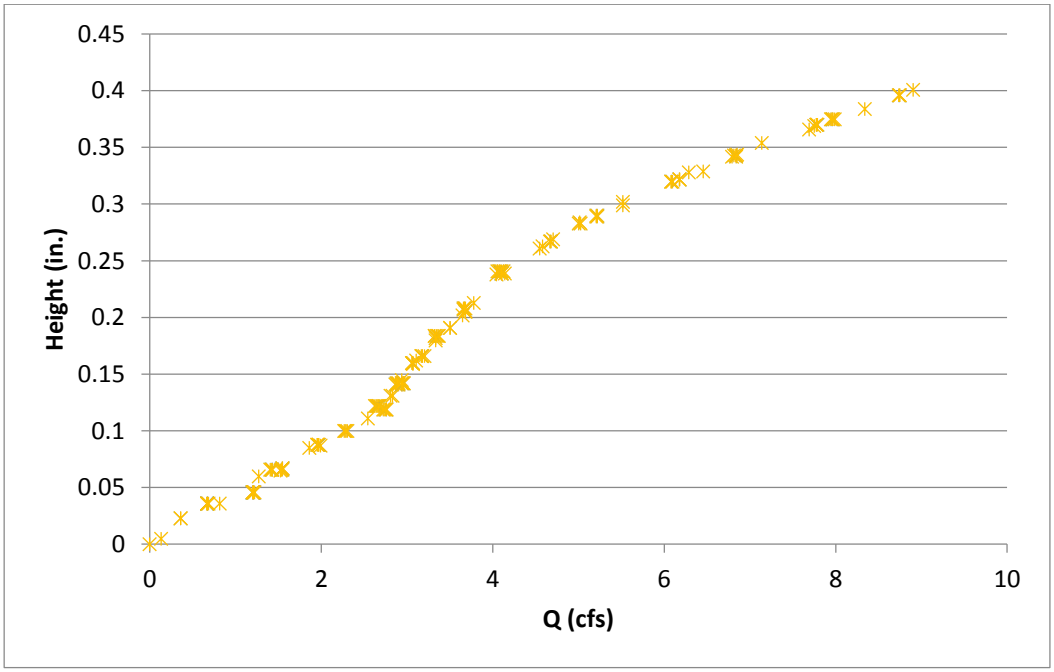

Figure E.9 Test 5 of final organ orifice design manufactured by Benedix

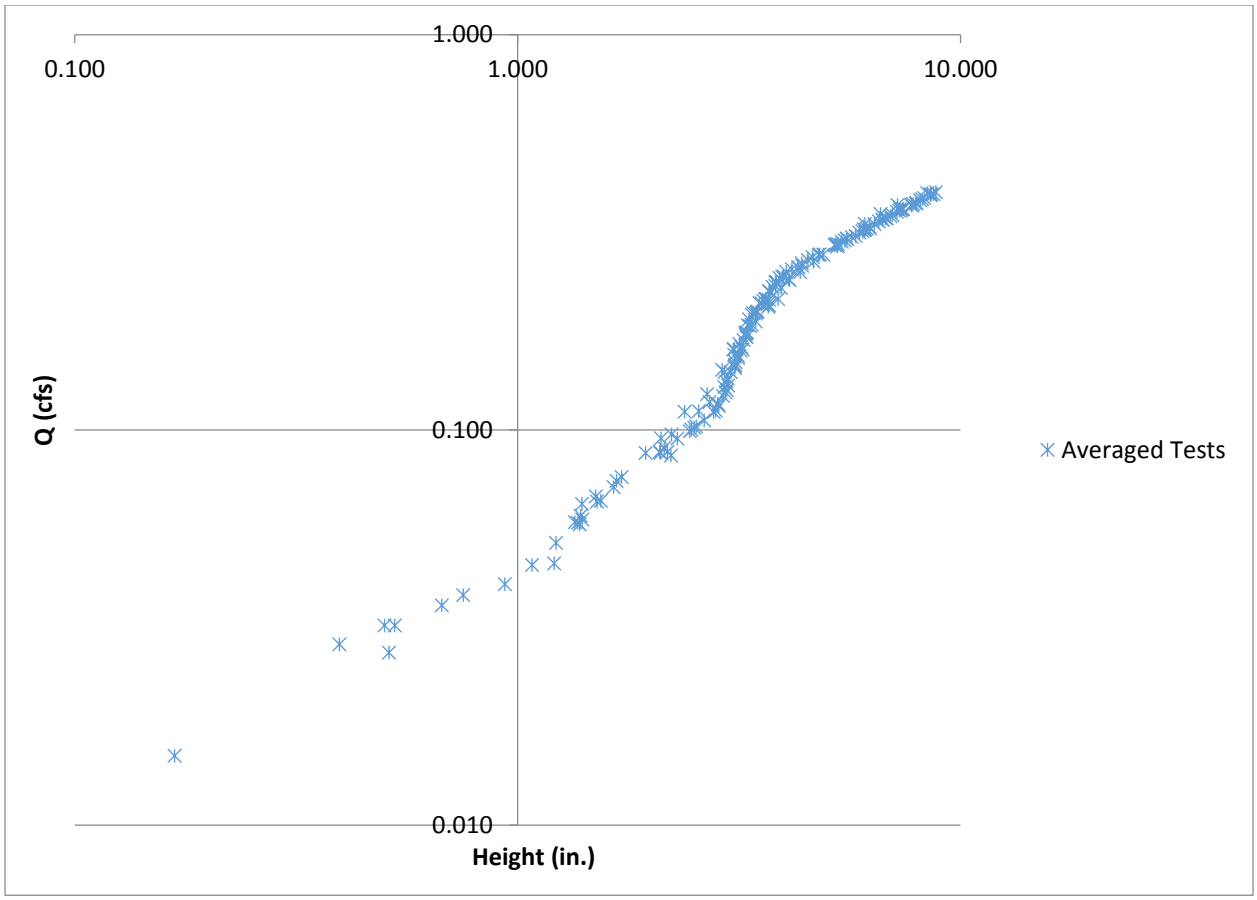

Figure E.10 Log transformation of organ orifice test data.

Results for: LR IV.MTW

Regression Analysis: LOG Q versus LOG H1, LOG H2, LOG H2b, LOG H3, LOG H3b

Analysis of Variance

Source	DF	Adj SS	Adj MS	F-Value	P-Value
Regression	5	14.7079	2.94157	8487.62	0.000
LOG H1	1	0.3106	0.31063	896.30	0.000
LOG H2	1	0.0136	0.01359	39.21	0.000
LOG H2b	1	0.0015	0.00146	4.20	0.042
LOG H3	1	0.0814	0.08139	234.85	0.000
LOG H3b	1	0.3296	0.32963	951.12	0.000
Error	169	0.0586	0.00035		
Lack-of-Fit	165	0.0576	0.00035	1.44	0.404
Pure Error	4	0.0010	0.00024		
Total	174	14.7664			

Model Summary

S	R-sq	R-sq(adj)	R-sq(pred)
0.0186164	99.60%	99.59%	99.56%

Coefficients

Term	Coef	SE Coef	T-Value	P-Value	VIF
Constant	-1.34200	0.00563	-238.56	0.000	
LOG H1	0.6020	0.0201	29.94	0.000	16.01
LOG H2	0.5461	0.0872	6.26	0.000	202.21
LOG H2b	-0.245	0.120	-2.05	0.042	294.69
LOG H3	1.1913	0.0777	15.32	0.000	80.03
LOG H3b	-1.5240	0.0494	-30.84	0.000	14.57

Figure E.11 Minitab output 1 for linear regression model of organ orifice design

Regression Equation

LOG Q = -1.34200 + 0.6020 LOG H1 + 0.5461 LOG H2 - 0.245 LOG H2b + 1.1913 LOG H3
- 1.5240 LOG H3b

Fits and Diagnostics for Unusual Observations

Obs	LOG Q	Fit	Resid	Std Resid		
1	-1.82400	-1.80851	-0.01549	-1.24		X
2	-1.56300	-1.51717	-0.04583	-2.60	R	
3	-1.54300	-1.58398	0.04098	2.40	R	X
5	-1.49500	-1.52319	0.02819	1.60		X
10	-1.33700	-1.29264	-0.04436	-2.55	R	X
11	-1.28600	-1.28963	0.00363	0.21		X
17	-1.18700	-1.22850	0.04150	2.30	R	
23	-1.11900	-1.12517	0.00617	0.35		X
24	-1.06400	-1.02007	-0.04393	-2.41	R	
25	-1.05800	-1.07152	0.01352	0.77		X
39	-0.95400	-0.99154	0.03754	2.05	R	
47	-0.90900	-0.94580	0.03680	2.01	R	
56	-0.84800	-0.88950	0.04150	2.26	R	
65	-0.79600	-0.83655	0.04055	2.20	R	
80	-0.72000	-0.76116	0.04116	2.22	R	
81	-0.70900	-0.74765	0.03865	2.09	R	
83	-0.70500	-0.74232	0.03732	2.02	R	
94	-0.66900	-0.62411	-0.04489	-2.44	R	

R Large residual
X Unusual X

Figure E.12 Minitab output 2 for linear regression model of organ orifice design

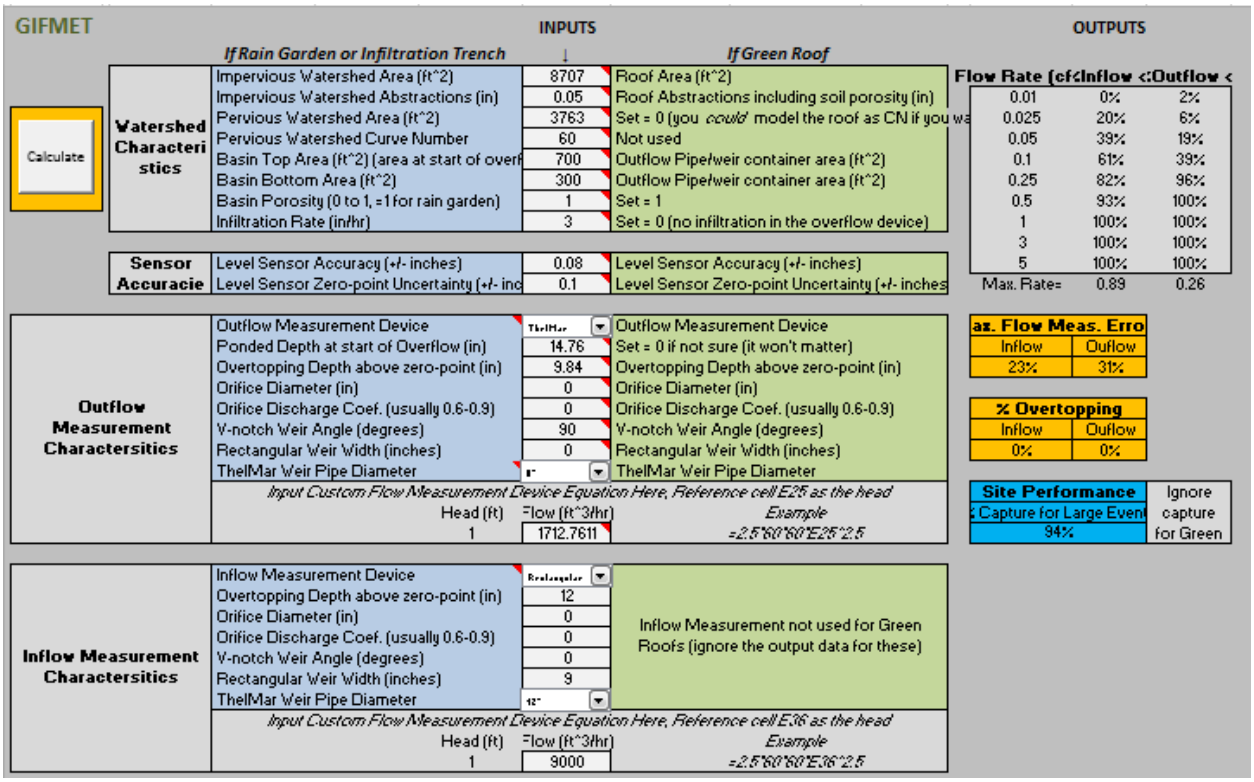

GIFMET

INPUTS

OUTPUTS

Calculate

	If Rain Garden or Infiltration Trench	↓	If Green Roof
Watershed Characteristics	Impervious Watershed Area (ft^2)	8707	Roof Area (ft^2)
	Impervious Watershed Abstractions (in)	0.05	Roof Abstractions including soil porosity (in)
	Pervious Watershed Area (ft^2)	3763	Set = 0 (you *could* model the roof as CN if you wa
	Pervious Watershed Curve Number	60	Not used
	Basin Top Area (ft^2) (area at start of overf	700	Outflow Pipe/weir container area (ft^2)
	Basin Bottom Area (ft^2)	300	Outflow Pipe/weir container area (ft^2)
	Basin Porosity (0 to 1, =1 for rain garden)	1	Set = 1
	Infiltration Rate (in/hr)	3	Set = 0 (no infiltration in the overflow device)
Sensor Accuracie	Level Sensor Accuracy (+/- inches)	0.08	Level Sensor Accuracy (+/- inches)
	Level Sensor Zero-point Uncertainty (+/- inc	0.1	Level Sensor Zero-point Uncertainty (+/- inches
Outflow Measurement Charactersitics	Outflow Measurement Device	ThelMar	Outflow Measurement Device
	Ponded Depth at start of Overflow (in)	14.76	Set = 0 if not sure (it won't matter)
	Overtopping Depth above zero-point (in)	9.84	Overtopping Depth above zero-point (in)
	Orifice Diameter (in)	0	Orifice Diameter (in)
	Orifice Discharge Coef. (usually 0.6-0.9)	0	Orifice Discharge Coef. (usually 0.6-0.9)
	V-notch Weir Angle (degrees)	90	V-notch Weir Angle (degrees)
	Rectangular Weir Width (inches)	0	Rectangular Weir Width (inches)
	ThelMar Weir Pipe Diameter	8"	ThelMar Weir Pipe Diameter
	Input Custom Flow Measurement Device Equation Here, Reference cell E25 as the head		
	Head (ft)	Flow (ft^3/hr)	*Example*
	1	1712.7611	*=2.5*60*60*E25^2.5*
Inflow Measurement Charactersitics	Inflow Measurement Device	Rectangular	Inflow Measurement not used for Green Roofs (ignore the output data for these)
	Overtopping Depth above zero-point (in)	12	
	Orifice Diameter (in)	0	
	Orifice Discharge Coef. (usually 0.6-0.9)	0	
	V-notch Weir Angle (degrees)	0	
	Rectangular Weir Width (inches)	9	
	ThelMar Weir Pipe Diameter	12"	
	Input Custom Flow Measurement Device Equation Here, Reference cell E36 as the head		
	Head (ft)	Flow (ft^3/hr)	*Example*
	1	9000	*=2.5*60*60*E36^2.5*

Flow Rate (cf<Inflow <:Outflow <		
0.01	0%	2%
0.025	20%	6%
0.05	39%	19%
0.1	61%	39%
0.25	82%	96%
0.5	93%	100%
1	100%	100%
3	100%	100%
5	100%	100%
Max. Rate=	0.89	0.26

ax. Flow Meas. Erro	
Inflow	Ouflow
23%	31%

% Overtopping	
Inflow	Ouflow
0%	0%

Site Performance	Ignore
% Capture for Large Event	capture
94%	for Green

Figure E.13 GIFMET Model (Lee 2015)